國立臺灣師範大學生命科學院系

中央研究院生物多樣性國際研究生博士學位學程

博士論文

Department of Life Science, College of Science
Taiwan International Graduate Program on Biodiversity, Academia Sinica
College of Life Science
National Taiwan Normal University
Doctoral Dissertation

微生物在臺灣小毛氈苔的分布及其影響

The role of microbes inside *Drosera spatulata*'s mucilage

孫培峰

Pei-Feng Sun

指導教授： 蔡怡陞 博士

Advisor: Isheng Jason Tsai, Ph.D.

中華民國 **113** 年 **6** 月

June 2024

Acknowledgement

Throughout my Ph.D., I have met many experts whom I would like thank for their guidance and support, which have helped me grow from a novice to a more experienced scholar, and enabled me to tackle various important challenges more easily and quickly.

First of all, I want to thank my advisor, Jason Tsai, who has guided me like a Four-Point Spell. He always points me out what I am missing. Thank you for allowing me to work on the question I was curious about during my Master's degree. Thank you for your guidance in both experimental design and data analysis. Also, for giving me plenty of opportunities to share my ideas with other researchers and understand the results of other scientists on plant-fungus symbiosis at conferences.

Next, I want to thank my lab members. Many of them are like Konami code, always helping me to achieve my goals or solve problems in the fastest way when I run into difficulties. Some of them even have their own catchphrases, and every time they speak those classic lines, I can almost hear a symphony playing the famous music "Passionate Duelist". At that moment, I know everything is going to be alright. Thanks to Tom for carefully guiding me about the microbial community knowledge and data analysis with R. Thanks to A-Mein for advice on experimental design. Thanks to Yi-Chien who always brings new ideas and happiness to the lab. This is important for me to stay in the lab. Thanks to Rubie, Yu-ching, and Cheng-Ping for helping me analyse the data and creating the beautiful result figures. Thanks to A-Guo and Xin-Han for teaching me data analysis. Thanks to Wei-An and Daphne for teaching me about sampling and DNA extraction. Additionally, I would also like to thank the other members of our laboratory for their help and advice.

In addition, I would also like to thank Professor Jimmy Lin and his lab members for their help in extracting plant DNA, RNA, phytohormones, and proteins. I would also like to express my gratitude to Professor Ying Lan Cheng and her lab members for their advice on plant hormone and protein analysis. Without their support, I would not have been able to complete this project. I also want to thank my friends for their assistance. Thank Wei-jun for helping me find ant collecting site and collect lots of ants. Without his assistance, it would be difficult to collect enough ants samples for the predating experiment.

Additionally, I'd like to thank Jason Cheng for helping me practice my English speaking and PowerPoint design. He also alleviated my stress by listening to my frustrations.

Lastly and most importantly, I want to thank myself for persevering. I have successfully prevented my adviser from creating his first Horcrux. A Taiwanese rumour says that the lower you squat, the higher you jump. After seven years of squatting, I had lost all feeling in my feet. Fortunately, I discovered that I could still jump high.

Abstract

Carnivorous plants secrete digestive fluid for nutrient acquisition. Although the fluid provides extreme conditions with low pH value and hydrolytic enzymes, several studies have found that the microbial community inside the mucilage plays an important role for prey digestion. *Drosera spatulata* is a carnivorous plant that secretes mucilage to stick to insects. Its leaves are covered with “tentacles” ending in glandular heads. These heads include glandular cells which produce sticky mucilage. Unlike pitcher plants containing digestive fluid inside modified foliar structures, the mucilage of *D. spatulata* is exposed to the environment. External influences are especially important in determining the distribution and abundance of microorganisms. In this study, we characterised the microbial communities of *D. spatulata* mucilage from northern Taiwan by using amplicon sequencing. To identify the relationship between *D. spatulata* and microorganisms, we inoculated microbes on *D. spatulata* and analyzed their gene expression. As the result, we found that the fungus *Acrodontium crateriforme* is the ecologically dominant species in *D. spatulata* mucilage. Based on the transcriptomes when encountering prey insects, we revealed a high degree of genetic co-option in each species during fungus-plant coexistence and digestion. Expression patterns of the holobiont during digestion further revealed synergistic effects in several gene families including fungal aspartic and sedolisin peptidases, which facilitate the digestion of sundew’s prey, as well as transporters and dose-dependent responses in plant genes involved in the jasmonate signalling pathway. This study shows that botanical carnivory is defined by multidimensional adaptations that correlate with interspecific interactions.

Keywords: *Acrodontium crateriforme*, *Drosera spatulata*, interaction, mucilage, traps

Table of contents

List of Figures

Chapter2

Chapter3

List of Tables

Chapter2

Chapter3

Supplementary Table

Chapter1
Introduction

1.1 Microbe-phyllosphere interaction

Plant-microbe interactions are dynamic and can affect host fitness through a variety of mechanisms. Symbionts can have positive, negative, or neutral effects. Microbes can benefit plants by providing nutrients[1] or regulating phytohormones[2]. Some microbes can inhibit pathogenic microbes[3] and herbivorous pests[4]. In *Arabidopsis thaliana,* phyllosphere microbes can adjust the host to inhibit gray mold[5]. In the pathogenetic relationship, microorganisms gain benefits from the host plant and cause harm or inhibit host development and physiology[6,7]. The phyllosphere is the surface of above-ground organs, that provides a habitat for microorganisms[8,9]. Previous studies have measured the function of single or multiple microorganisms in foliar communities and their influence on the host[10-12]. In *Deschampsia antarctica*, foliar bacteria were found to have the ability to inhibit of ice recrystallisation. Bacteria were also found to have some plant growth promoting traits such as auxin, siderophore, HCN production[13]. Bacteria isolated from the phyllosphere of rice[14] and tomato[15] had the ability to promote plant growth. Although the microbiome is crucial to understanding for the relationship between the microbiota and the phyllosphere, there are still gaps in our knowledge that need to be addressed.

1.2 Carnivorous plants

Carnivorous plants are often characterised by highly modified leaf organs for attracting, capturing, and digesting their preys[16]. These traps can be classified as adhesive traps, snap traps, pitcher traps and bladder traps by their morphology and trapping mechanism. In the plant kingdom, the carnivorous syndrome has independently evolved at least 11 times[17]. Unraveling the evolutionary and molecular basis of predatory capabilities has been an ongoing pursuit for scientists[18,19]. Although the specialised organs of carnivorous plants secrete acidic mucilage with digestive exudates, microorganisms can still be found in these extreme environments[20-22]. The taxonomic composition of phyllosphere microbial communities can be influenced by biotic factors (e.g., host plant species and herbivores) and abiotic factors (e.g., temperature and humidity)[23]. In carnivorous plant traps, studies have found that there are two types of microbial communities inside the digestive fluid - specialist or

generalist strategies. The composition of the microbial communities varies due to abiotic factors. For instance, the study shows that the microbiota in the same species are various even in two samples of the same plant[24]. A specialist strategy means that there is one or few dominant species within the microbiota. For example, the *U. gibba*'s trap microbiome is a unique, and highly diverse bacterial community, with particular species composition even when compared with its surrounding environment[25]. While the significance of microbiota in vertebrate digestion is well established, the symbiotic interplay between carnivorous plants and their associated microbiota is an emerging field of research, and the molecular responses to microorganisms that facilitate or enhance plant carnivory are yet to be fully elucidated.

1.3 *Drosera* spp.

The family Droseraceae comprises three genera – *Aldrovanda*, *Dionaea* and *Drosera*[26]. Both *Aldrovanda* and *Dionaea* are monotypic genera and capture prey by active snap traps. However, *Drosera* stands out as an exception with adhesive traps[27]. *Drosera* plants, also known as sundews, grow in sunny wetlands or moist areas and differ slightly in their habitat preferences. *Drosera* leaves are lined with tentacle-like glandular trichomes with the top of glands usually red. These glands are covered with droplets of acidic mucilage. Due to this reason, *Drosera* plants are also known as sundews. Prey would be attracted by odours and the red color of the leaves[28]. When prey landed on the leaves, prey would get stuck due to the sticky mucilage. *Drosera* leaves would slowly curl up to increase the contact area with the prey and dissolve it through digestive enzymes present in the mucilage. Insects provide about 50% of the nitrogen source in *Drosera* species[29,30]. In the past, microbes have been found residing on the phyllosphere[31] and rhizosphere[32] of *Drosera spatulata* using culture-dependent methods. However, the relationship between *Drosera* plants and the resident microorganisms have not been investigated. *Drosera spatulata*, native to tropical regions including Taiwan, in its genome[19] had been sequenced and microbial presence on its phyllosphere documented[31]. These provide an intriguing model for investigating the potential inter-species interactions between carnivorous plants and their resident microbes. Our research aims to characterise the microbial community of *D. spatulata* mucilage and to assess the symbiotic interactions between carnivorous plants and microbes.

1.4 Objectives

To investigate the potential inter-species interactions, we focus on *Drosera spatulata*[33], a sundew native to tropical regions including Taiwan. The fascinating mechanism of trap movement in sundews, associated with prey digestion, has long attracted scientific curiosity due to its complex operational intricacies[18], but importantly, acts as a tractable response to diverse stimuli[34] in both natural and laboratory settings. This species, with its sequenced genome[19] and documented microbial presence on its phyllosphere — where surface yeast have been shown to promote growth[31] — together represent a model microbial ecosystem to experimentally interrogate the underlying molecular details. We sought to characterise the mucilage microbial community and assess its impact on digestion. By exploring these aspects, our research aims to shed light on the intricate symbiotic interactions between carnivorous plants and their resident microbes.

The main questions of my study are

1. Characterisation the diversity and composition of the mucilage microbiota.
2. Examination of the host plant-microbe interaction.

Chapter2
Persistence of dominant fungus *Acrodontium crateriforme* in mucilage of sundew *Drosera spatulata*

2.1 Introduction

Carnivorous plants attract, capture and digest their prey by using modified leaves known as traps. These traps can be further classified as sticky, snap, pitcher or bladder traps according to their morphology and trapping mechanism[35]. In most carnivorous plants, traps are filled with mucilage containing digestive enzymes and microorganisms[20,21]. As the majority of prey in carnivorous plants are insects, and insect exoskeletons are made of chitin, trap mucilage is acidic to facilitate the digestion process with chitin[36]. Trap mucilage also contains saccharide- or resin-based substances to act as glue[37]. Recently, researchers using metabarcoding have suggested that the digestive mucilage encapsulated by the modified leaves, known as traps, is colonised by diverse communities of microorganisms (**Table 2.1**). In bladderwort, corkscrew and pitcher plants, there were no dominant species present within the traps, but they can be broadly grouped into major bacterial phyla[20-22,24,38]. However, the mucilage of individual plants possesses has microbial communities that were either diverse and little overlap amongst plants[22,24], or the presence of a dominant fungus in carnivorous plants suggests ecological dominance[39]. Besides, some of these microorganisms provide hydrolytic enzymes to promote the degradation of prey carcasses[40,41]. Despite the direct link between plant host nutrient acquisition and associated microbiota, only two trap types have been studied in detail.

An example of an overlooked trap was in the genus of *Drosera,* commonly known as sundew, which belongs to the Droseraceae family, comprising the second largest carnivorous family following the Lentibulariaceae[42]. Members of *Drosera* species have “flypaper” leaves, which are highly modified leaves covered with tentacle-like glandular trichomes[43]. During capture, these trichomes secrete sticky mucilage to attract prey. *D. spatulata* leaves then nearly surround the prey, forming an ‘outer stomach’ during digestion. Once the prey has been captured, the tentacles enwrap the prey, which is then degraded

and mineralised by the secreted digestive enzymes. Previous studies have shown that the pH value of *Drosera* mucilage ranges from 2.5 to 5[44,45]. This acidic environment provided a suitable situation for chitin degradation[36]. Furthermore, acidic mucilage is filled with digestive enzymes such as protease[46,47], chitinase[48,49] and glucanases[50] for prey digestion. The question then arises as to whether the microbiota in the mucilage are changed by the selective pressure of the acidic environment.

D. spatulata, a sundew distributed in tropical and subtropical areas, produces hydrolytic enzymes such as chitinase and protease[46]. Using culture-dependent methods, studies have found that microbes exsist on the phyllosphere[31] and rhizosphere[32] of *Drosera spatulata*. Yeasts present on foliar surfaces were found to promote plant growth[31], while other microbes were not investigated. Mucilage of *D. spatulata* occurs with prolonged exposure in the environments. External influences such as environmental factors might be more evident in sundew mucilage. Therefore, it is a good model to understand whether the structure of the microbiota in sundew mucilage is stable or dynamic.

In this chapter, we chose *D. spatulata* as the target species and aimed to i) characterise the microbial community residing in the digestive mucilage of *D. spatulata*, and ii) determine if there are resident operational taxonomic units (OTUs) in mucilage exist. To figure out if specific species are present in the mucilage of *D. spatulata*, we compared the microbial community of *D. spatulata* mucilage with microbiota from other surrounding plant surfaces. Then, sampling through months and locations to figure out constant residents. Lastly, we observed the morphology of the resident fungus in the mucilage by using scanning electron microscope (SEM).

Table 2.1 References of metabarcoding studies in carnivorous plants

References	year	Species	16S/18S/ITS	bacterial dominant /diverse	eukaryotic dominant /diverse	Presence of dominant bacterial OTU	Presence of dominant eukaryotic OTU	Reanalysis and relative abundance of *Acrodontium*	Metadata
Carnivorous *Nepenthes* Pitchers with Less Acidic Fluid House Nitrogen-Fixing Bacteria	2023	*Nepenthes gracilis, N. rafflesiana, N. ampullaria*	16S	*N. gracilis*: dominant	NA	*N. gracilis*: *Acidocella* (9.5%), *Acidocella* (5.86%)	NA	NA	o
Characterization and comparison of convergence among *Cephalotus follicularis* pitcher plant-associated communities with those of *Nepenthes* and *Sarracenia* found worldwide	2022	*Cephalotus follicularis, N. mirabilis, N. mindanaoensis*	16S/18S	diversity	diversity	NA	NA	0	o

Bacterial Recruitment to Carnivorous Pitcher Plant Communities: Identifying Sources Influencing Plant Microbiome Composition and Function	2022	*Sarracenia purpurea*	16S	diversity	NA	NA	NA	NA	x
Selective Bacterial Community Enrichment between the Pitcher Plants *Sarracenia minor* and *Sarracenia flava*	2021	*S. minor, S. flava*	16S	NA	NA	NA	NA	NA	x
Venus flytrap microbiotas withstand harsh conditions during prey digestion	2019	*Dionaea muscipula*	16S	dominant	NA	*Mycoplasma* (OTU1, 7.96%), *Acidisoma* (OTU3, 13.4%), *Sphingomonas* (OTU13, 8.6%)	NA	NA	o
Diverse microbial communities hosted by the model carnivorous pitcher plant Sarracenia purpurea: analysis of both bacterial and eukaryotic composition across distinct host plant populations	2019	*S. purpurea*	16S/18S	dominant	dominant	16s: *Pseudomonas* (4.9%), *Azospirillum* (9.33%), *Pedobacter* (5.85%), *Duganella* (4.91%)	*Candida palmioleophila* (3.7%, TOP16)	0	o

Superior Dispersal Ability Can Lead to Persistent Ecological Dominance throughout Succession	2019	*S. purpurea*	16S/ITS	diverse	dominant	NA	*Candida pseudoglaebosa* (41%) 9/53	**0.16~1.4% (4/53)***	o
Convergence between the microcosms of Southeast Asian and North American pitcher plants	2018	*N. stenophylla, N. veitchii, N. reinwardtiana, N. tentaculata, N. hirsuta, S. alata, S. flava, S. leucophylla, S. purpurea, S. rosea*	16S/18S	*S. rosea, S. flava & S. leucophylla*: dominant	diverse	*S. rosea*: *Aquitalea* (16.73%), *Rhodopseudomonas palustris* (7.1%); *S. flava*: *Rhodanobacter* sp. (8.4%); *S. leucophylla*: *Serratia* sp. (9.8%)	NA	0	o
Hunters or farmers? Microbiome characteristics help elucidate the diet composition in an aquatic carnivorous plant	2018	*Utricularia vulgaris, U.australis*	16S/ITS	diverse	diverse	NA	NA	0	o

Linking the development and functioning of a carnivorous pitcher plant ' s microbial digestive community	2017	*Darlingtonia californica*	16S	dominant	NA	*Pseudomonas* sp. 22.77%, *Pedobacter* sp. 10.94%	NA	NA	x
Bacterial diversity and composition in the fluid of pitcher plants of the genus *Nepenthes*	2016	*N. albomarginata, N. ampullaria, N. hirsuta, and N. mirabilis*	16S	dominant	NA	*N. albomarginata*: *Acinetobacter* 17.3%; *N. ampullaria: Acinetobacter* 14.44% ; *N. hirsuta*: *Acinetobacter* 12.66%, *N. mirabilis*: *Acinetobacter* 10.39%,	NA	NA	x
The Metagenome of *Utricularia gibba*'s Traps: Into the Microbial Input to a Carnivorous Plant	2016	*N. hemsleyana, N. rafflesiana*	16S	NA	NA	NA	NA	NA	x
Bacterial Diversity and Community Structure in Two Bornean Nepenthes Species with Differences in Nitrogen Acquisition Strategies	2016	*N. rafflesiana, N. hemsleyana*	16S	dominant	NA	*N. hemsleyana*: *Klebsiella* (22%), *N. rafflesiana*: *Acidocella* (25%)	NA	NA	x

The Microbial Phyllogeography of the Carnivorous Plant *Sarracenia alata*	2011	*S. alata*	16S	dominant	NA	Enterobacteriaceae, Comamondaceae, Pseudomonadaceae	NA	NA	x

* indicates *Acrodontium crateriforme* was found in this study

2.2 Methods and Materials

2.2.1 Collection of sundew mucilage and surrounding plants

D. spatulata mucilage samples were collected from five collection sites located in Northern Taiwan (**Supplementary Table 1**). Mucilage from 30 *D. spatulata* leaves was pooled as a sample by using filter paper of size 1 cm x 1.5 cm. To avoid microbial communities being influenced by the same filter paper collection, each filter paper only collected mucilage on one *D. spatulata* plant. The fresh leaves of plants and mosses surrounding *D. spatulata* were also wiped and considered as environmental samples. To understand the microbial dynamics through time, sundew mucilage from Shumei and Shuangxi was sampled monthly from June 2017 to April 2018, except September and October. To determine the spatial distribution of plant-microbe coexistence, 52 mucilage samples were collected from 17 additional sites.

2.2.2 Genomic DNA extraction and metabarcoding of environmental samples

Total genomic DNA was extracted using a modified cetyltrimethylammonium bromide (CTAB) DNA extraction protocol. For cell lysis, 5 ml CTAB buffer (0.1 M Tris, 0.7 M NaCl, 10 mM EDTA, 1% CTAB, 1% beta-mercaptoethanol) was mixed with the sample. After incubation at 65°C for 30 min, an equal volume of chloroform was added. The mixture was centrifuged at 10,000 rpm for 10 minutes. The supernatant was mixed with an equal volume of isopropanol. After centrifugation at 10,000 rpm for 30 minutes at 4°C, the supernatant was discarded and the pellet was washed twice with 70% and once with 90% ethanol. DNA was eluted using 50 µl of elution buffer (Qiagen).

Internal transcribed spacer (ITS) and 16S rRNA amplicons were generated using barcode primer pairs ITS3ngs(mix)/ITS4[51] and V3/V4[52], respectively. Amplicon levels were standardised using the SequalPrep Normalization Plate 96 Kit (Invitrogen Corporation, Carlsbad, CA, USA, Cat. #A10510-01). Concentration of pooled and standardised amplicons was performed using Agencourt AMPure XP beads (Beckman Coulter, Brea, CA, USA, Cat. #A63881). All amplicon libraries were sequenced with Illumina MiSeq PE300

using 2 x 300 bp paired-end chemistry performed by the NGS High Throughput Genomics Core at the Biodiversity Research Center, Academia Sinica, Taiwan.

2.2.3 Amplicon sequencing data processing

Samples were demultiplexed using sabre with one nucleotide mismatch (v1.0; https://github.com/najoshi/sabre) given their respective barcodes. Adaptor and primers sequences were trimmed using USEARCH (v10)[53]. Sequence reads were processed according to the UPARSE pipeline[54]. Forward and reverse reads were merged and filtered using USEARCH. Operational taxonomic units (OTUs) were clustered at 97% sequence identity with a minimum of 8 reads per cluster to denoise the data and remove singletons. The OTU table was generated using the *usearch_global* option and analysed with the *phyloseq* package (v1.28.0)[55]. SINTAX[56] algorithm was used to classify the OTU sequence taxonomy against the RDP[57] training set (v16) and the UNITE[58] database (v7.1).

Prior to data analysis, we compared and confirmed the taxonomic identity of our positive control from the UPARSE pipeline. 16S and ITS datasets were both decontaminated by R package *decontam*[59]. BLAST to curated unclassified ITS and 16S OTU sequences with NCBI nucleotide database. Non-fungal eukaryotic OTUs and non-bacterial 16S OTUs were removed from further analyses. Most analyses were performed with R-Studio. Amplicon data were analyzed with the *phyloseq* package (v1.28.0)[55]. For beta diversity analysis, distances between samples were calculated using Bray-Curtis dissimilarity. Differentially abundant taxa were determined using DESeq2 (v1.24)[60]. For fungal amplicon, OTUs were summarised at the genus and OTU levels. For bacterial amplicon, OTUs were summarised at the family and OTU levels.

Both bacterial and fungal communities from a total of 190 fungal samples and 96 samples were characterised by sequencing the ITS2 region of fungal rRNA and V3-V4 region of 16S rRNA. 15,366,944 fungal sequence reads and 3,623,798 bacterial sequence reads in either community were assigned to 5760 fungal and 3,085 bacterial operational taxonomic units (OTUs), respectively. After rarefaction, each fungal and bacterial sample had 14,000 and 10,000

sequence reads, respectively. In temporal statistical analysis, we removed one sample due to low sequence depth.

2.2.4 Morphology observation of *D. spatulata* stalk gland

The stalk glands of *D. spatulata* were photographed using an Olympus microscope (Olympus CX31) and a digital camera (Nikon D7000). Staining was performed using cotton blue reagent[61]. Scanning electron microscopy (SEM) of the *D. spatulata* stalks were prepared as follows. Leaf tissues were fixed at 4 degrees for 1 hour with P4G5 solution (4% paraformaldehyde and 2.5% glutaraldehyde in 0.1 M phosphate buffer). After three washes with 0.1 M phosphate buffer, secondary fixation was performed in a 1% solution of osmium tetroxide for 2 hours at room temperature. The fixed samples were passed through a series of dehydration steps in 30, 50, 70, 80, 90, 95, 100, 100 and 100% alcohol before drying in a critical point dryer (Hitachi model HCP-2). The dried samples were then coated with a layer of gold using a sputter coater (Cressing-ton model 108). SEM observations of *Drosera* leaves grown under different conditions (laboratory condition, inoculated with *A. crateriforme* and from wild) were performed on a JSM-7401F scanning electron microscope (JEOL) at the Institute of the Plant and Microbial Biology, Academia Sinica, Taiwan.

2.3 Results

2.3.1 Fungal communities in *Drosera* mucilage were distinct from those in surrounding plants

To better understand the microbial diversity and composition of the mucilage found on the sundew *Drosera spatulata*, we employed sterilised filter papers to collect mucilage from sundews (**Fig. 2.1b)** and surrounding plants typically found in cliff habitats of Northern Taiwan (**Fig. 2.2**). A total of 92 samples were subjected to 16S and ITS amplicon metabarcoding (**Supplementary Table 1**). Each sample had an average of 580 and 604 bacterial and fungal operational taxonomic units (OTUs), respectively. Bacterial species diversity was similar between the sundew mucilage and leaf surfaces of co-occurring plants (**Fig. 2.1c**, Wilcoxon rank sum test, P=0.50). In contrast, the fungal communities in the mucilage had a significantly reduced species evenness (**Fig. 2.1c,** Wilcoxon rank sum test, P<0.001). Beta diversity of microbial communities indicated significant differences in bacterial (**Fig. 2.1d**, PERMANOVA, leaf surface: R^2=0.15, P=0.001) and fungal communities (**Fig. 2.1e**, PERMANOVA, leaf surface: R^2=0.27, P=0.001) between leaves of *Drosera* and other plant sources. 89.6% and 95.1% of bacterial and fungal OTUs corresponding to 72.5-100% relative abundance of the mucilage microbiome, respectively, were also found in the co-occurring plant samples (**Supplementary Table 2**), implying that the mucilage microbiota was similar to the microbial composition of co-occurring non-carnivorous plants but these taxa differed in their relative abundance.

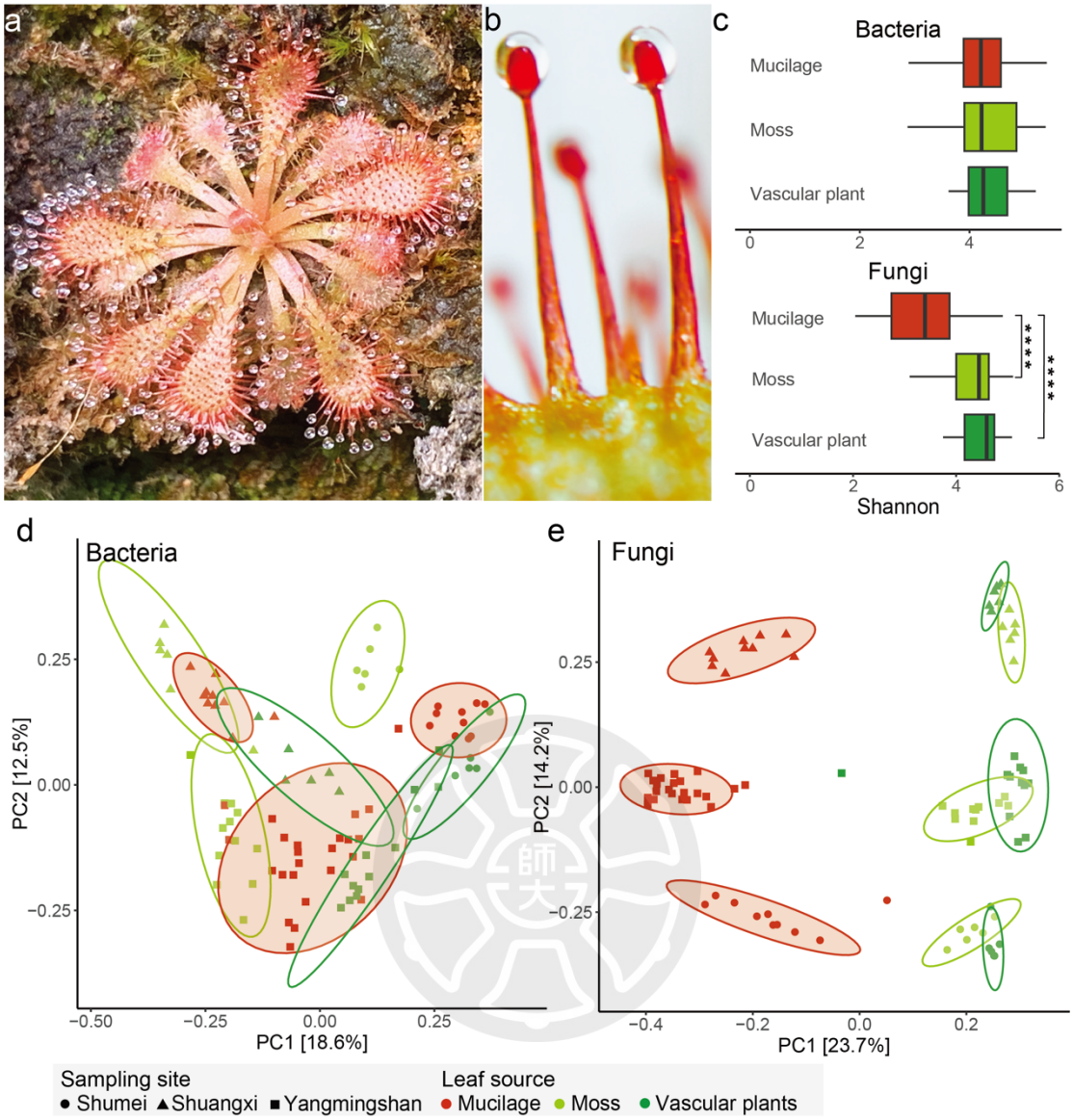

Fig. 2.1 Microbial Communities of *Drosera spatulata* mucilage and surrounding co-occurring plants. a. *Drosera spatulata* and **b.** close up of stalk glands with secreted mucilage. **c.** Evenness of bacterial and fungal species in sundew mucilage versus co-occurring moss and vascular plant leaf plant leaf surfaces. Asterisk denote significant difference from Wilcoxon rank sum test (*** indicates P<0.001). Beta diversity (Bray-Curtis index) of **d.** bacterial and **e.** fungal communities from three sites (**Fig. 2.3)**. Eclipses were drawn at 95% confidence level within samples of the same plant and site.

Fig. 2.2. ***Drosera spatulata* in its natural habitat. a.** *D. spatulata* typically grows on the cliff habitat of northern Taiwan. **b.** Close-up of *D. spatulata* growing surrounded by grasses and moss.

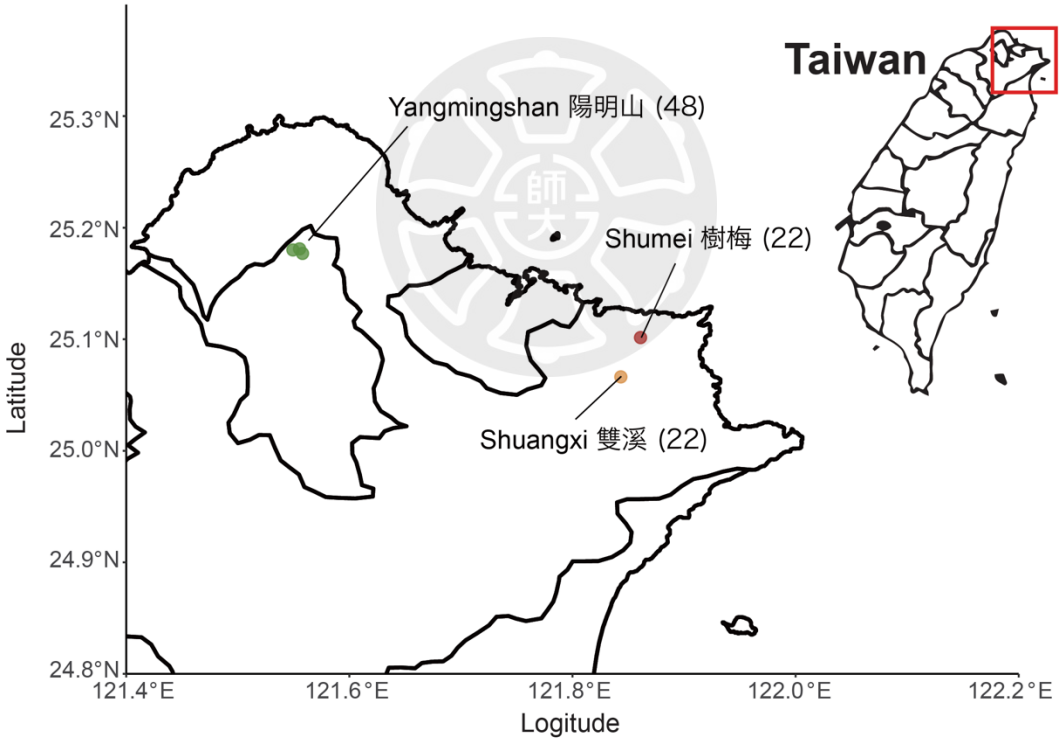

Fig. 2.3. Sampling locations of initial *D. spatulata* mucilage survey. Numbers in bracket denote samples collected in each location. Each dot is a different region separated by at least 3.5 km.

2.3.2 Ecological dominance of *A. crateriforme* in *Drosera* plant

We examined the relative abundances of the five most common bacterial and fungal taxa in the leaf surfaces and revealed a single dominant fungal operational taxonomic unit (OTU) in the mucilage samples averaging 41.8% sequence relative abundance (**Fig. 2.4a**). The dominant fungal OTU belonged to the species *Acrodontium crateriforme*. Continuous sampling of mucilage across two sites for nine months revealed that *Acrodontium crateriforme* maintained its status as the most dominant fungal species, despite lower relative abundance (21.7%) during July and August (**Fig. 2.4b**). To investigate the extent of *Acrodontium* dominance in *D. spatulata*, we carried out ITS sequencing of sundew mucilage and tissue samples collected in Taiwan, UK and USA revealed presence of *A. crateriforme* in all four *Drosera* species across three continents (**Fig 2.4c and Fig. 2.5**). This suggests that the *Drosera*-*A. crateriforme* coexistence is well conserved and may be ancient. *A. crateriforme* remained the most dominant species in 98.1% of the mucilage samples spanning ~44 km of Northern Taiwan, with an average relative abundance of 29.4% (**Fig. 2.4a**). Particularly high *A. crateriforme* dominance (>50% relative abundance) was found in *D. rotundifolia* tissues sampled in both the UK and USA, but was less common in UK samples of *D. anglica* and *D. intermedia* (**Fig. 2.4c**). In addition, re-analysis of 14 published fungal metabarcoding datasets of carnivorous plants also detected the presence of *A. crateriforme* also in *Sarracenia purpurea*, though with low abundance 0.2-1.4% (**Table 1**). Together these results suggest varying symbiotic dynamics of *A. crateriforme* across different carnivorous plant species. The available information from Globalfungi database[62], it was revealed that 1.2% of 57,184 samples harbored *Acrodontium* from forests (77.3%), followed by grasslands (12.2%), with the majority of relative abundances being less than 1% (**Fig. 2.4 and Supplementary Table 3**). *Acrodontium* appeared to be preferentially located in more acidic samples (**Fig. 2.6**), which is considered an ancestral trait as it is phylogenetically closely related to a group of fungi that can thrive at low pH[63].

To investigate the role of fungi in the carnivorous plant host, we isolated the two most dominant OTUs from fresh mucilage of *D. spatulata* and identified them as *A. crateriforme* and *Phoma herbarum* of the families

Teratosphaeriaceae and Didymellaceae, respectively (**Fig. 2.7**). The latter is a plant pathogen causing leaf spots in various crops[64], while *A. crateriforme* is cosmopolitan found in soil[65], plant material[66,67], compost[68], air[69] and rock surfaces[70]. Interestingly, *A. crateriforme* has been isolated in the digestive fluid of the Indian pitcher plant *Nepenthes khasiana*[71] and prefers nitrogen-rich substrates[72]. Like *D. spatulata, A. crateriforme* is well suited for growth under laboratory conditions and can be cultivated using PDA and MS media. *A. crateriforme* grows optimally at pH 4–5, mirroring the acidity of *D. spatulata* mucilage[44,45,73] (**Fig. 2.6a**), suggesting its acidophilic nature. In contrast, *Ph. herbarum* prefers a more neutral pH. The optimal culture temperature for *A. crateriforme* is 25°C (**Fig. 2.6b**), aligning with the growth range (7–32°C) of *D. spatulata* and the average monthly temperature of 22°C at the sampling sites (**Fig. 2.6c**). The summer temperature peaks (29–35°C) at the Taiwanese sites may, combined with biotic factors such as optimal growth of *Ph. herbarum* at this higher temperature range, explain the reduced abundance of *A. crateriforme* at higher temperatures (**Fig. 2.4b**).

Examining the stalk glands of *D. spatulata* growing in a sterilised environment using a scanning electron microscope (SEM) revealed clear surfaces (**Fig. 2.8a and Fig. 2.9a-c**). Inoculating the sundew with *A. crateriforme* revealed hyphae that grew over the glands (**Fig. 2.8b and Fig. 2.9d-f**), while conidiophores and detached conidia were observed in glands collected from the wild (**Fig. 2.8c**). This observation demonstrates that *A. crateriforme* colonises and reproduces on the sundew stalk glands[74], and the mucilage harbours free hyphae or conidiophores. Cultivation of *A. crateriforme* is positively correlated with the amount of *Polyrhachis dives* ant powder added to the medium, suggesting that the fungus can utilise insects as a growth supplement (**Fig. 2.10**).

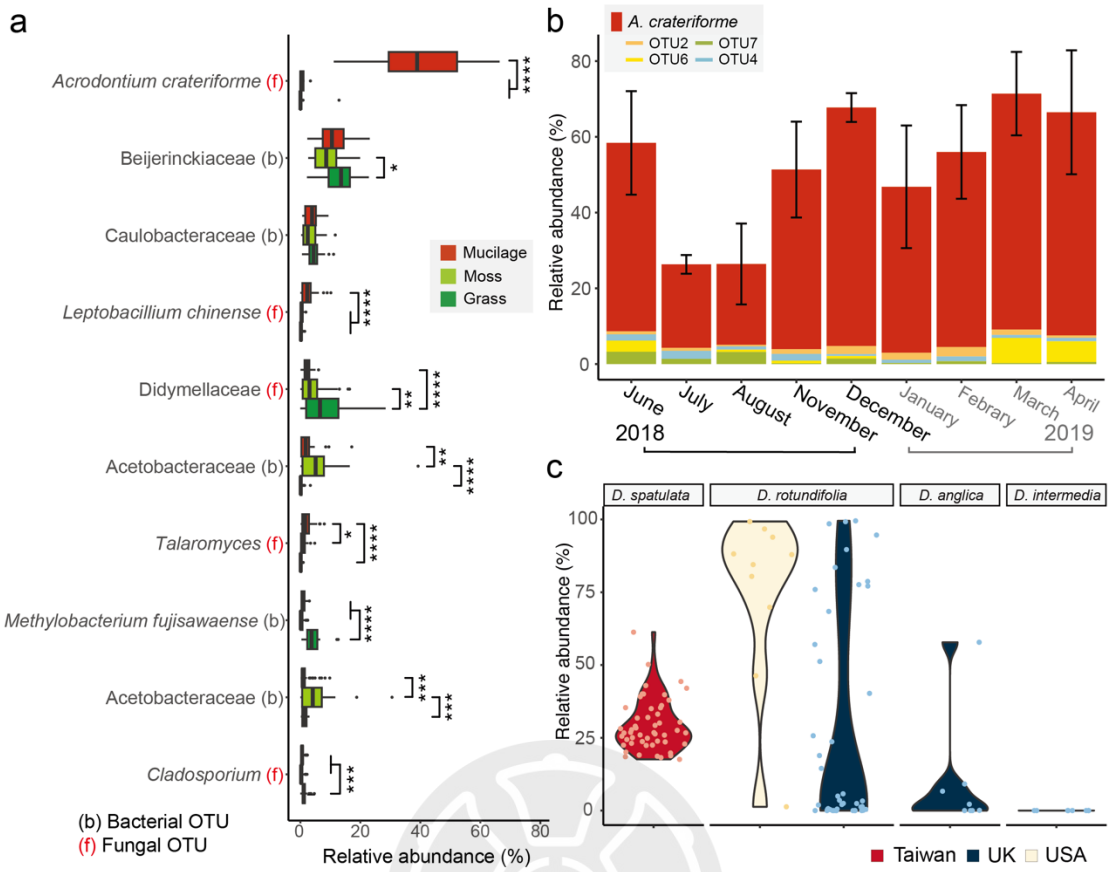

Fig. 2.4 Abundance of *Acrodontium* OTU in *Drosera* mucilage. a. Relative abundances of the ten most abundant bacterial (b) or fungal (f) taxa among mucilage of *D. spatulata*. **b.** Temporal variation of *Acrodontium* and the next four most abundant OTUs shown as relative abundance in mucilage over nine months between 2018-2019 pooled from Shumei and Shuangxi in northern Taiwan (**Fig. 2.3**). **c.** Relative abundance of *A. crateriforme* identified from ITS amplicons from mucilage or tissues of four *Drosera* species sampled across northern Taiwan, North America and the UK.

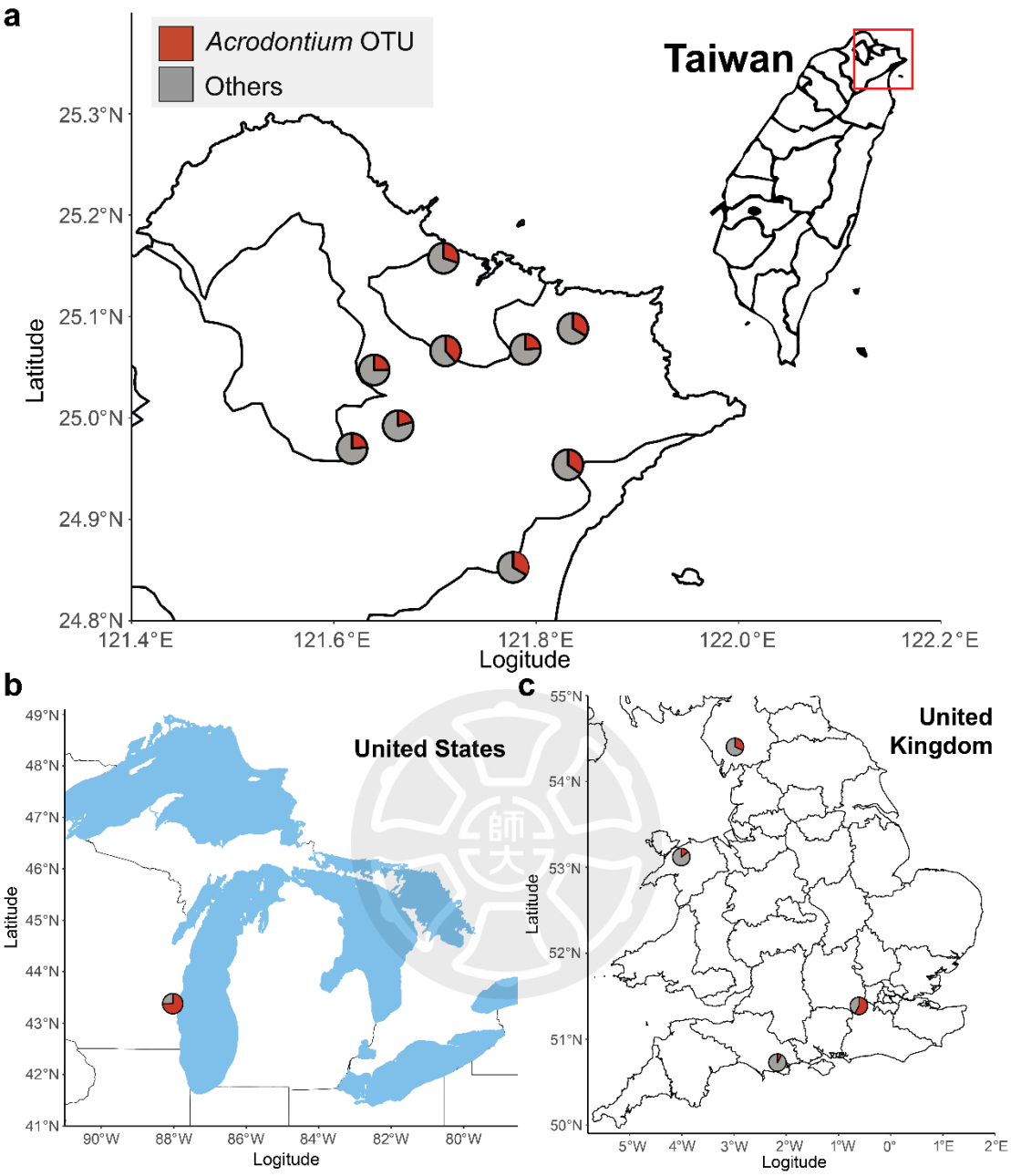

Fig. 2.5 Abundance and spatial distribution of *Acrodontium crateriforme* in a. Taiwan, b. USA and c. UK. Pie chart denote relative abundance of fungal OTUs.

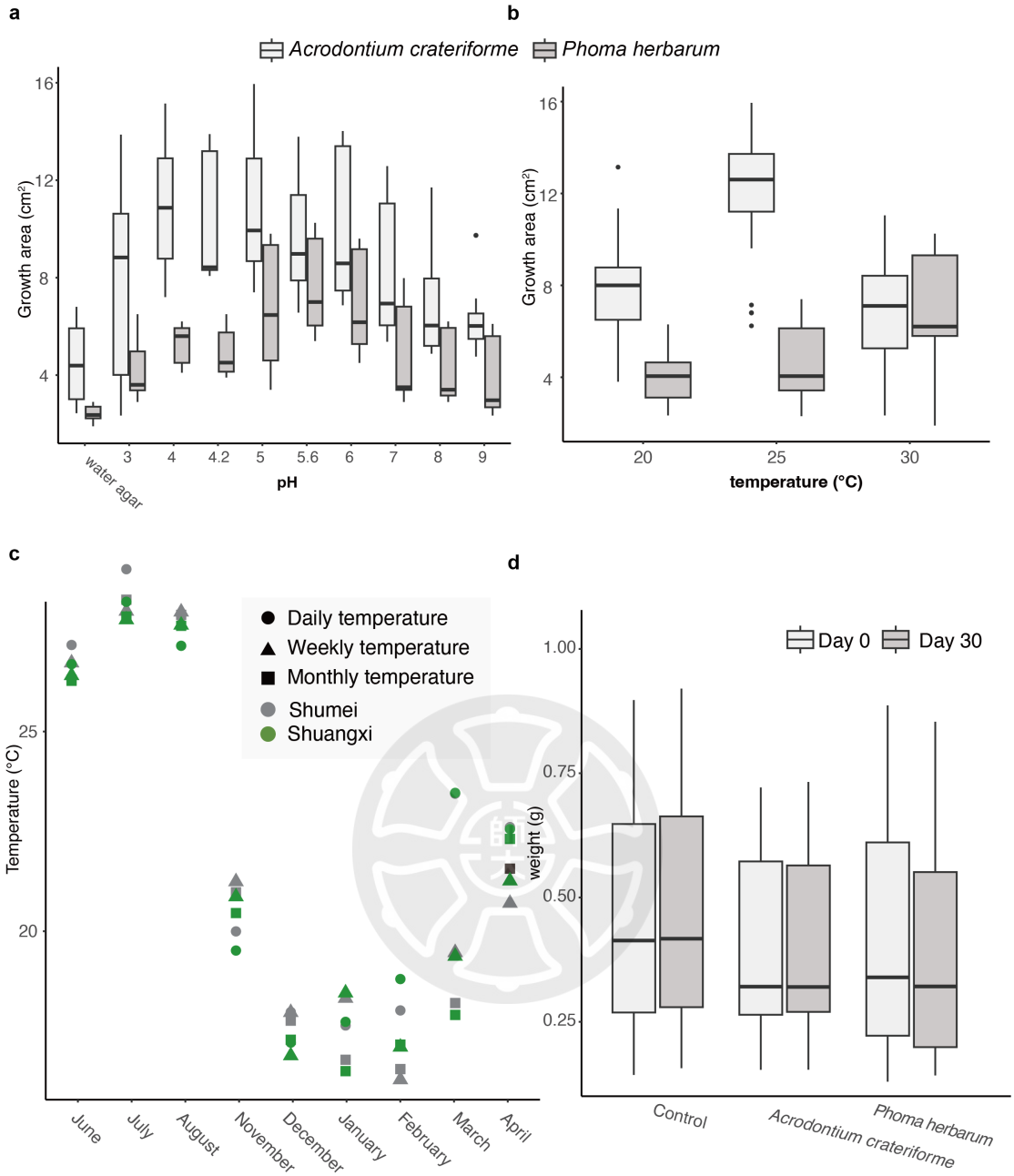

Fig. 2.6. The growth profile of *A. crateriforme* and *P. herbarum* in different a. pH values and b. temperatures. c. Temperature data in Shumei and Shuangxi from Taiwan Central Weather Administration. d. Weight of *D. spatulata* one month after inoculation with different fungi.

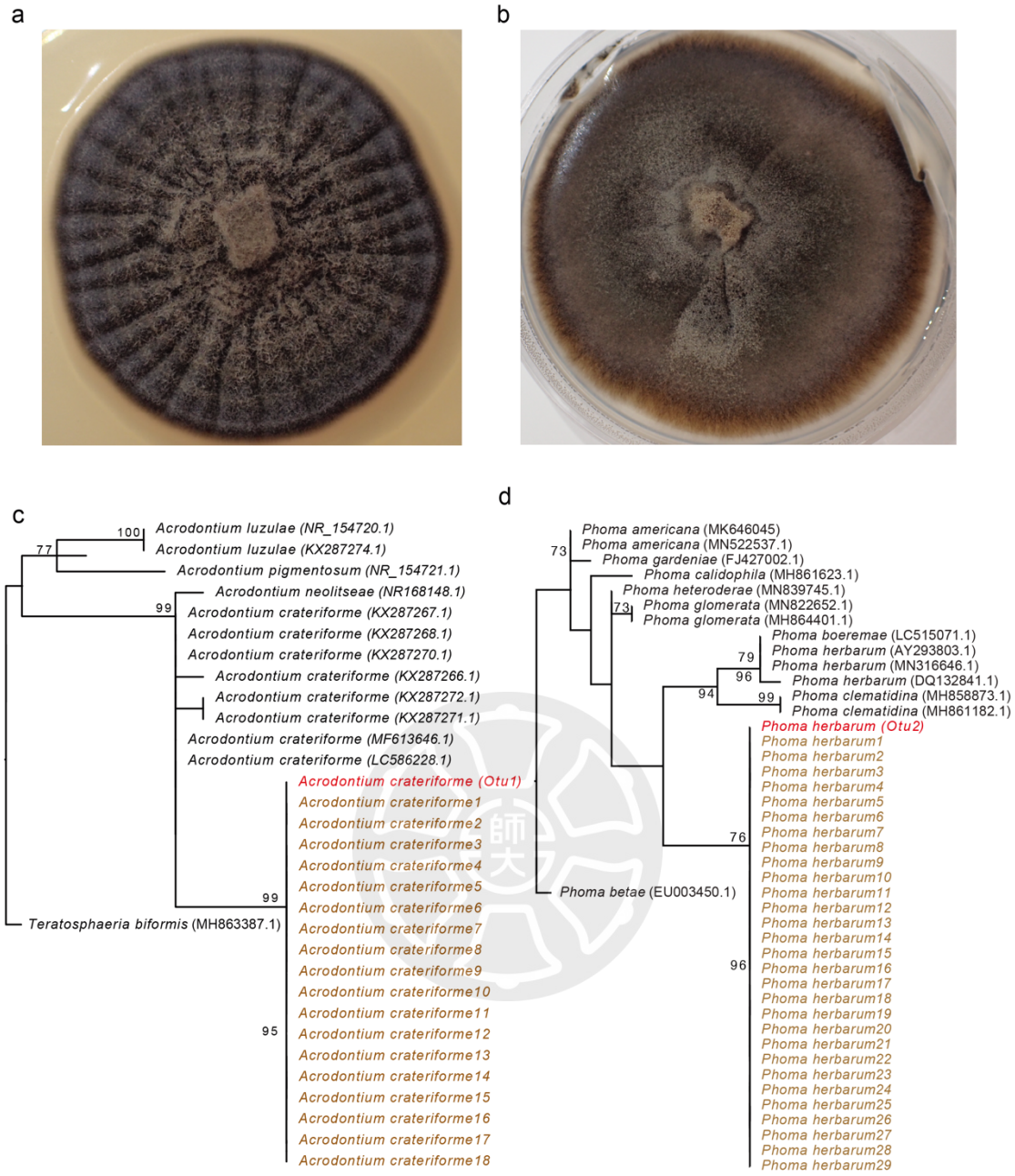

Fig. 2.7 ITS phylogeny of *Acrodontium crateriforme* and *Phoma herbarum*. Photo shows the morphology of **a.** *A. crateriforme* and **b.** *P. herbarum* grown in potato dextrose agar. Red colour represents the consensus sequence of the **c.** *Acrodontium* and *Phoma* OTU from amplicon data. Brown colour represents sequences of strains that were isolated from the mucilage of *Drosera spatulata*.

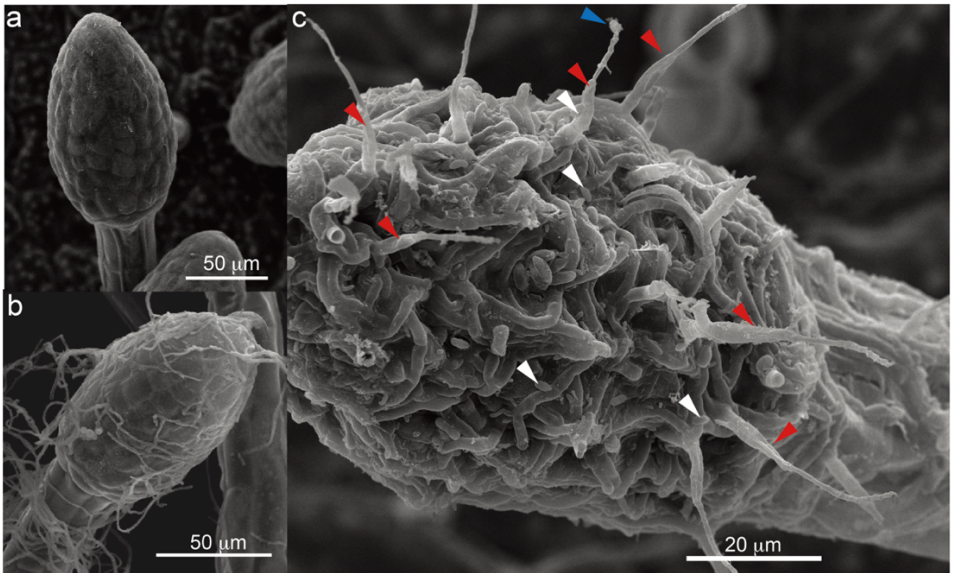

Fig. 2.8. Scanning electron microscope (SEM) images of *D. spatulata* stalk glands. Sundew stalk glands under **a.** sterilised conditions, **b.** inoculated with *A. crateriforme*, and **c.** natural habitat. Different arrow colours denote conidiophores from which conidia were already detached (red), a conidium attached to the tip of a conidiophore (blue), and detached conidia (white).

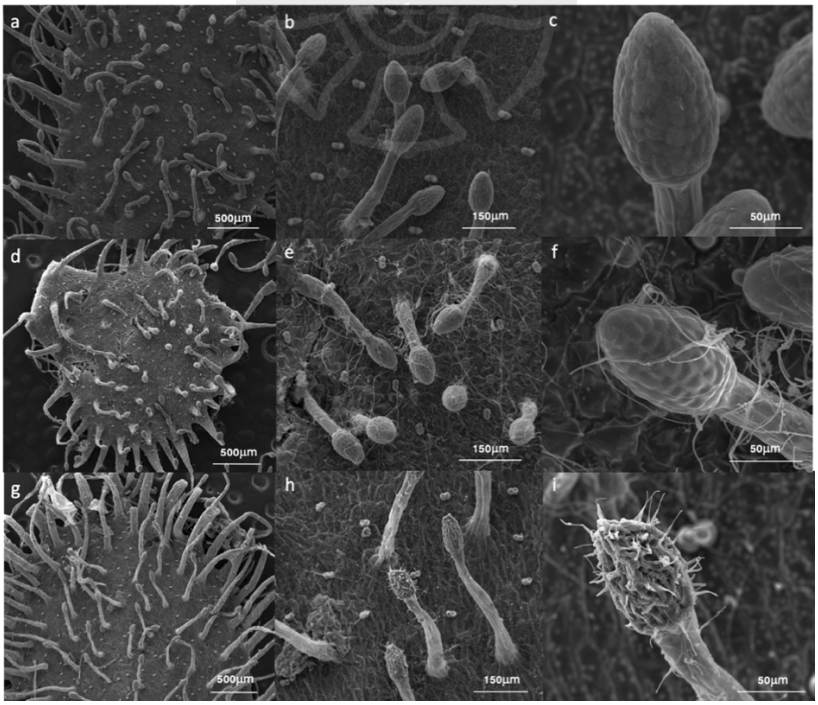

Fig. 2.9 Scanning electron microscope (SEM) image of sundew leaves a-c. under sterilised conditions, **d-f.** inoculated with *A. crateriforme*, and **g-i.** collected from the wild.

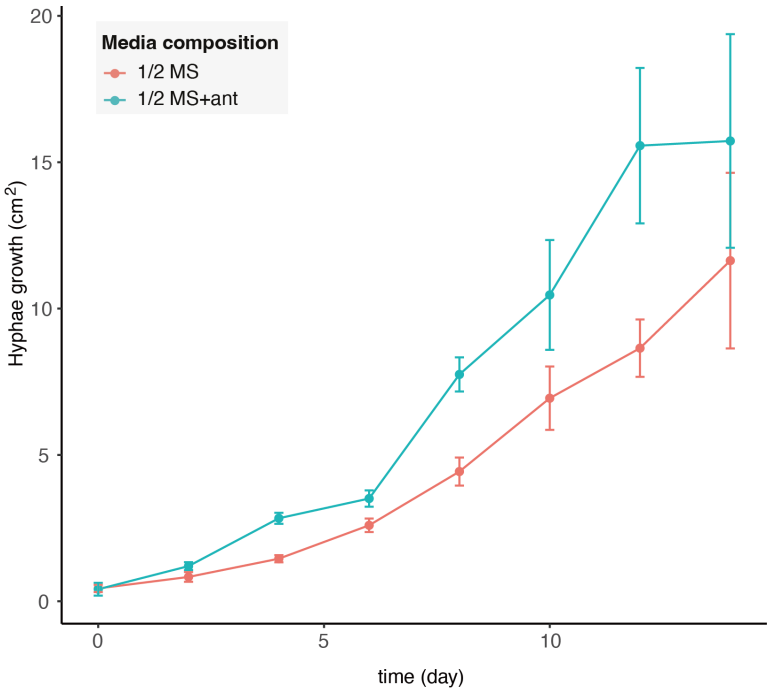

Fig. 2.10 Growth profiling of *A. crateriforme* in 1/2 MS media with and without supplementing ant powder

2.4 Discussion

Plant microbiota is important not only for nutrient supplementation but also for pathogen resistance[1,75] and microbiota have even been found in the digestive liquid in carnivorous plants. However, few types of carnivorous plant' traps have found the composition of the microbiota[20,21,76]. Here, we used the amplicon method on *D. spatulata* mucilage to examine its microbiota. Our result found a dominant fungal species inside the mucilage. Moreover, the scanning electron microscope results suggested that this dominant fungal species had the ability to interact with *D. spatulata*.

The microbial community composition showed a significant correlation with the phylogenetic relatedness of the plants[77]. Our results suggest that all sites of *D. spatulata* mucilage had the dominant fungal species. These results suggest that plant evolutionary speciation and location differ for distinct microbes. Considering plants as a suitable niche for microbial colonisation, there are many factors that influence the foliar microbiota including foliar area, niche variability and the available resources[78,79]. Besides, the harsh acidic conditions of *D. spatulata* mucilage limit the diversity of interactions with

microbial species. Our results are consistent with the description of a selective composition of plant-associated fungal communities under adverse environmental conditions.

Fungal interactions with plants, either beneficial or detrimental, have a major impact on ecosystems. Both beneficial and pathogenic fungi form mycelial colonies on plants. In this study, we found that the mycelium of *A. crateriforme* covers stalk glands of host plants. These results suggest that *A. crateriforme* persisted and interacted with *D. spatulata* through time. Besides, all mucilage samples showed the high relative abundance of *A. crateriforme*. These results suggested that *A. crateriforme* was the most dominant fungal species in the mucilage of all *D. spatulata* populations in Taiwan.

A. crateriforme was previously considered ubiquitous across environments such as soil[65], plant material[66,67], compost[68], air[69] and rock surfaces[70]. It is now acknowledged as part of an integral sundew-fungal holobiont with its presence and frequent dominance in several *Drosera* species globally. This suggests that this fungus is likely to have co-evolved with sundew ancestors. Echoed by observations of selective microbial compositions in adverse environments[79], the chemical restrictions imposed by acidic *D. spatulata* mucilage could may select the spectrum of acid-tolerant microbes possible for digestive collaboration. Establishing a long-term, stable relationship may be a necessary first step for *A. crateriforme* to survive in this extreme environment. The dominance of *A. crateriforme* in the microbiota of *Drosera* species, that was not found in most other carnivorous plants, may also be related with dramatic osmotic stress caused by air exposure of the stalked glands, in contrast to the greater extent liquid medium contained in the traps of carnivorous pitcher plants[24,80,81].

In conclusion, our amplicon analyses suggest that *D. spatulata* had selective pressure on its fungal community. We provide insight into the microbiota between the environment and carnivorous plants. We found the dominance of *A. crateriforme* in the microbiota of several *Drosera* species. Besides, this fungus can survive in acidic environment and its hyphae cover on stalk glands of *D. spatulata*. This provides a model for the interaction between carnivorous plant and its resident and for studying on the function of *A. crateriforme*.

Chapter3
The genomic basis of sundew *Drosera spatulata*'s response to *A. crateriforme* and its prey

3.1 Introduction

Carnivorous plants survive in nutrient-poor environments[82]. For this reason, they use their modified organs to attract, capture, and digest small animal prey with the consequent actively taking up and using of the prey-derived nutrients[16]. Different trap types of carnivorous plants use their own unique mechanisms to capture prey[16]. After capturing prey, the jasmonate (JA) system is activated to stimulate digestive processes of the carnivore[83]. Specialised glands secrete digestive enzymes to digest the prey's chitin-based exoskeleton of prey and degrade the internal soft tissues, converting them into essential nutrients that can readily be absorbed[84]. This process ensures that the carnivorous plant can adapt to nutrient-deficient environments by the utilization of resources. Otherwise, this complex behaviour is mediated by the jasmonate (JA) signaling pathway in non-carnivorous plant ancestors[85]. Recent studies have revealed expansion and clade-specific gene families involved in plant defence, such as JA signaling, peptidases and hydrolases[19,34,83], which are upregulated during the digestion process suggesting that these genes have been co-opted[86] for new roles in carnivory. The extent to which these genes still retain their ancestral functions remains to be elucidated.

In recent years, microbes have been found in several carnivorous plants, providing new insights into the ecology of plant carnivory. In pitcher plants, bacteria were found to be capable of degrading carbohydrates and chitin[20]. In the pitcher plant *Darlingtonia californica,* bacterial diversity and biomass were found to improve prey decomposition rates by increasing nitrogen uptake efficiency[81]. Meta-transcriptomic profiling of *Genlisea* species revealed that non-host transcripts of the host leaves were dominated by metazoan hydrolases, suggesting a role in phosphate supplementation[41]. In addition, the composition of the microbiota appears to be highly time-dependent and influenced by factors such as the host[81], the surrounding environment[76], prey-associated bacteria[76] and enhanced species dispersal capabilities[38], highlighting the complex interplay of factors that shape these microbial

communities. Although studies have begun to focus on the relationship between carnivorous plants and microbes, the role of microbes in sundew mucilage has not been investigated.

In this chapter, we hypothesise that *A. crateriforme* which positively enhances their digestive process, The digestion process therefore involves a sundew-fungal holobiont[87]. To test this hypothesis, we sequenced the fungal genome (*A. crateriforme*) genome and compared it with closely related fungal genomes. Besides, we designed greenhouse experiments to analyse the interaction between *A. crateriforme* and *D. spatulata.* We sought to assess the impact of *A. crateriforme* on digestion. By exploring these aspects, our research aims to shed light on the intricate symbiotic interactions between carnivorous plants and their resident microbes.

3.2 Methods and Materials

3.2.1 Isolation and identification of fungal species from sundew mucilage

Mucilage-soaked filter papers were placed in potato dextrose broth (PDB) containing chloramphenicol (50 ug/ml) and incubated for at 30°C for 24 hours. The broth culture was then serially diluted (10^{-2}, 10^{-3}, 10^{-4}) and 200 µl of the diluted culture was transferred to potato dextrose agar (PDA). The plate was spread on sterilised glass until the medium was dry and incubated at 30°C for 24 hours. Single colonies were transferred to fresh PDA using sterilised toothpicks and morphology was examined by using light microscopy. Genomic DNA was extracted from the fungal pure cultures corresponding to the morphological description of *Acrodontium*, followed by amplification and sequencing of the fungal ITS region as previously described[71,88]. To construct a phylogenetic tree, ITS sequences of the sequenced 18 isolates, 15 *Acrodontium, Teratosphaeria biformis* and *Aureobasidium pullulans* ITS sequences from NCBI were first aligned using MAFFT[89] (v.7.4) and trimmed using trimAl[90] (v.1.2). A maximum likelihood phylogenetic tree with 100 bootstraps was constructed from the alignment using IQtree[91] (v.1.6.1). All 18 isolates were classified as *A. crateriforme* based on morphological description and grouped with the *A. crateriforme* ITS sequence.

3.2.2 Preparation of sterilised *Drosera spatulata*

D. spatulata seeds were collected from the sampling sites and sterilised by washing with 70% ethanol for 10 seconds, 3% (w/v) calcium hypochlorite ($CaCl_2O_2$) for 30 seconds and finally rinsed 3 times with ddH_2O. Surface sterilised seeds were pregerminated on 0.5% water agar and incubated in the dark at 20°C for 6-8 weeks. Shoots were then transferred to 1/2 MS agar with pH adjusted to 5.7. Shoots were grown under white fluorescent light at 20°C with a 16h:8h, light:dark photoperiod for 90 days as recommended[92].

3.2.3 Preparation of different substrates for feeding experiment

Ant individuals (*Polyrhachis dives)* were collected from the National Taiwan University campus. The collected ants were washed with distilled water (ddH_2O) and subsequently dried for two days. The ants were then frozen in liquid nitrogen and crushed into powder. Wood (*Populus tristis*) was provided by the laboratory of Prof. Ying-Chung Jimmy Lin at National Taiwan University. We used dissecting scissors to cut the wood into 0.4 cm x 0.4 cm x 0.1 cm pieces. Shrimp shells (*Litopenaeus vannamei*) were collected from commercial shrimp (Kirkland Signature Frozen Raw Tail-On Shrimp, #7777000). Shrimp tissues were removed, and the shells were washed with sterile distilled water for 20 minutes. Subsequently, shrimp shells were cut into pieces measuring 0.4 cm x 0.3 cm pieces using dissecting scissors(D8NH-76000). Prepared substrates were autoclaved at 121 °C for 40 minutes and drying at 60 °C in Forced Air Flow Oven (DV-092) for two days. 1 gram of ant powder was mixed with 1 liter of ddH_2O to be used in subsequent experiment.

3.2.4 *A. crateriforme* growth conditions in different condition

A. crateriforme was inoculated in nutrient-rich medium agar plate in different temperatures (20, 25, 30 degrees) and pH values (pH 3-pH 9) for two weeks. To test the growth conditions of *A. crateriforme* in different ants, we supplemented ant powder in nutrient-rich or nutrient-poor medium agar plate. Then, *A. crateriforme* was inoculated into these medium with or without ant powder for two weeks. The fungal growth area was photographed every two days using Nikon digital camera. The growth area was then measrued by using ImageJ[93].

3.2.5 Genome sequencing, assembly and annotation of *A. crateriforme*

Genomic DNA was subjected to Oxford Nanopore library preparation according to the manufacturer's instructions (SQK-LSK109), and sequenced on a GridION instrument. Basecalling was using Guppy (ver. 3.0.3). For Illumina sequencing, genomic DNA was used for NEB Next Ultra library preparation and 150bp paired-end reads were generated on a Novaseq 6000 sequencer. Nanopore reads were first corrected from the initial assembly of the canu[94] assembler (ver. 1.9), which were then assembled using the flye assembler (ver. 2.5). The initial assembly was polished by Racon[95] (four iterations; ver. 1.4.11), followed by Medaka (ver. 0.11.0; https://github.com/nanoporetech/medaka) using nanopore reads and Pilon[96] with Illumina reads. The mitochondrial genome was assembled separately using NOVOPlasty[97] (ver. NOVOPlasty2.7.0.pl).

3.2.6 Greenhouse experiment for plant-microbe interaction

Six treatments (tissue culture of *D. spatulata* w/o predation, *A. crateriforme* only w/o predation and co-culture of *D. spatulata* and *A. crateriforme* w/o predation) are used for the analysis of plant-fungal interaction. For the tissue culture samples, we transferred the tissue-cultured *D. spatulata* from the 1/2 MS medium to vermiculite with ddH2O and incubate them for 3 weeks. For fungal inoculation, conidia were removed from 14-day fungal colonies by washing with sterile distilled water. Then, adjusted the suspension to 10^6 spores/ml. After that, we used a pipette to inoculate microbe into stalk gland. After 1 month following inoculation, the sundew is able for the experiment. We added insect substrate to five leaves on an individual plant and harvested them after 72 hours as predation samples. In addition to the plants already inoculated with *A. crateriforme,* we also inoculated *D. spatulata* with dead *A. crateriforme* spores and chitin.

3.2.7 RNA extraction

We pooled 80 leaves as one replicate and each treatment had five replicates. At each harvest, leaf tissue was cut from the plant and washed immediately in de-ionised water to remove prey residue. The leaf was then flash-frozen in liquid nitrogen (−196 °C). The time from cutting to freezing was always <30 s. Plant and fungal RNA was extracted by modified CTAB method. 2ml CTAB buffer (0.1 M Tris, 2 M NaCl, 25 mM EDTA, 2% CTAB, 1% PVP-40, 2% beta-mercaptoethanol) was added to 2 ml tube containing leaf samples. Samples were frozen in liquid nitrogen and grinding by Precellys 24 tissue

homogenizer. After incubation at 65°C for 20 min, an equal volume of chloroform: isomylalcohol (24:1) was added. The mixture was centrifuged twice at 12,000 rpm for 10 minutes. The supernatant was mixed with 1/3 volume of LiCl and put in 4 °C overnight for RNA precipitate. After centrifugation at 10,000 rpm for 30 minutes at 4°C, the supernatant was discarded and the pellet was washed twice with 70% ethanol. RNA was eluted with 30 µl of DEPC water. RNA samples were sequenced by using Novaseq 6000.

3.2.8 Gene prediction of *A. crateriforme*

Transcriptome reads were mapped to the *A. crateriforme* genome assembly using STAR[98] (ver. 2.7.7a) and assembled using Trinity[99] (ver. 2.13.2; guided approach), Stringtie[100] (ver. 2.1.7) and Cufflinks[101] (ver. 2.2.1). Transcripts generated by Trinity were mapped to the assembly using Minimap2[102] (ver. 2.1, options: -ax splice), and splice junctions were quantified using Portcullis[102] (ver. 1.2.3). The gene predictor Augustus (ver. 3.4.0) and gmhmm[103] were trained using BRAKER2[98,104] (ver. 2.1.6) and SNAP[105] with proteomes and RNAseq mappings as evidence hints to generate an initial set of annotations. Assembled transcripts selected by MIKADO[106] (ver 2.3.3), proteome downloaded from Uniprot Fungi (version October 2019) as homology, and BRAKER2 annotations were combined as evidence hints for input into the MAKER2 annotation pipeline[107] to produce a final annotation for each species. Repetitive elements were identified based on the protocol by Berriman *et al*.[108], and masked using Repeatmasker[109] (ver 4.1.2).

Functional domains within the proteomes were identified using pfam_scan[110] (ver. 1.6) against the downloaded Pfam database[111] (ver. 36). Diamond[112] (ver. 2.1.6) was utilised to identify transporters, blasting proteomes against TransportDB[113] (ver. 2.0). Proteomes were functionally annotated to identify carbohydrate-active enzymes (CAZy) and peptidases using dbCAN[114] (ver. 2.0.11), and MEROPS[115] (ver. 12.4), respectively. Annotations of biosynthetic gene cluster (BGC) regions and Gene Ontology (GO) terms were performed using antiSMASH[116] (fungi ver. 7.0.1) and eggNOG[117] (ver. 2.1.12), respectively. Analysis and visualisations were conducted under R[118] environment (ver. 4.3.1). Various packages were utilised to enhance the analysis: topGO[119] (ver. 2.52.0) for GO enrichment analysis, pheatmap[120] (ver. 1.0.12) and ggplot2[121] (ver. 3.4.4) for gene expression visualisation.

3.2.9 Inoculation experiment

We used *D. spatulata* plants derived from tissue culture in vermiculite with ddH_2O as our control samples. We inoculated *A. crateriforme* and *Ph. herbarum* on *D. spatulata* leaves and incubated the plants at 25 degrees for 30 days. Photographs of *D. spatulata* in different treatments, including control plants, were taken daily and the area of the leaf displaying symptoms of infection was quantified every two days using ImageJ[93]. Whole *D. spatulata* plants were dried with tissue paper and weighted on the first and 30th day of the experiment.

3.2.10 Western blot

We mixed 10 µl of protein sample with 10 µl of 2X loading dye in a 0.2 µl PCR tube. The samples were then incubated for 10 minutes at 99 degrees in the PCR machine. After incubation, the protein samples were loaded onto the SDS-PAGE. Electrophoresis was performed at 90 V for 20 minutes in the stacking gel and then at 120 V for 120 minutes in the running gel. After electrophoresis, we transfer the SDS-PAGE into a 1X transfer buffer for 10 minutes. Subsequently, we put soaked filter papers, membrane, and SDS-PAGE together. The machine parameters for transferring were set to 0.8 mA/cm² for 1 hour. We washed the membrane in 1x PBST for 5 minutes twice. Then, soaked the membrane in blocking buffer at room temperature for 1 hour. Then, washed membrane in 1x PBST for 5 minutes twice. To proceed, we add the secondary antibody solution and shake it for 30 minutes at room temperature. After that, we washed the membrane with 1X PBST for 8 minutes at room temperature three times. Finally, we prepare the Luminol substrate and peroxidase in a 1:1 ratio (750 µl + 750 µl). The membrane is placed into the detecting chamber for signal detection and the detection is performed by Bioanalytical Instruments.

3.2.11 Feeding experiment of *D. spatulata*

10^{-5} g of sterilised ant powder was added to a single leaf of an individual *D. spatulata* plant with or without *A. crateriforme* inoculation. The capture time (from the time ant substrate was added until the tentacles fully covered the prey) and digestion time (from the time tentacles fully covered the prey until the trap reopened) of five replicates were recorded. The same set of experiments were repeated with additional application of Protease Inhibitor Cocktail (#P9599, Sigma). To compare the effect of protein digestion in mucilage from *D. spatulata*

with and without *Acrodontium*, mucilage from 30 plants in each treatment were collected prior to the experiment. The mucilage was mixed with HSP-biotin-labelled BSA at both 25 degrees for 16 hours and 24 hours. Western blot was performed and the amount of protein digestion was quantified using ImageJ[93].

3.2.12 Comparative genomics and phylogenomics

The assembly and annotation of *A. crateriforme* is detailed in the methods above. A total of 32 genomes from representative fungi and plants were downloaded from JGI and NCBI databases (**Table 3.1**). For each gene, only the longest isoforms were selected for subsequent analysis. Orthogroups (OGs) were identified using Orthofinder[122] (ver. 2.5.5). For each orthogroup, an alignment of the amino acid sequences each gene was produced using mafft[89] (version 7.741). A maximum likelihood orthogroup tree was made from the alignment using IQtree[91] (version 2.2.2.6). A species phylogeny was constructed from all orthogroup trees using ASTRAL-III[123] (version 5.7.1). OG gains and losses at each node of the species phylogeny were inferred using DOLLOP[124] (ver. 3.69.650).

3.2.13 Transcriptome analysis

Total RNA of was extracted from *D. spatulata* and underwent transcriptome sequencing. RNA-Seq raw reads were trimmed using fastp[125] (v0.23.2) to remove the adaptor and low-quality sequences. The trimmed reads were mapped to the corresponding genome using STAR[98] (ver. 2.7.10b) and assigned to genes using featureCounts[126] (ver. 2.0.3). Notably, the reads from coexistence treatment, with or without ant powder, were mapped to both the *A. crateriforme* and *D. spatulata* genomes[19]. To prevent the false positive of gene expressions, sequences mapped to both genomes and had low mapping qualities were excluded from further analyses. The samples of *D. spatulata* exposed to ant powder which obtained in two different time points were grouped as a digestion sample. The differentially expressed genes (DEGs) of different conditions comparing to control, were inferred by DESeq2[60] (ver. 1.38.3; padj < 0.05 & $|\log2FD| > 1$). The gene ontology enrichment of comparisons was identified using topGO[119] (ver. 2.50.0). We also performed weighted gene co-expression network analysis (WGCNA) to further categorise the expression patterns of peptidases respectively in *A. crateriforme* and *D. spatulata*. Due to the presence of peptidase without any expressions across conditions in *D. spatulata*, we removed the 30% lowest-expressed genes in each transcriptome using the sum of samples.

3.2.14 Phytohormone analysis

Different treatments (1g/L of BSA, chitin, BSA+chitin, and ants, 10^6 spores/ml of *A. crateriforme*, and 10^5 spores/ml of *A. crateriforme*) were applied to *D. spatulata* leaves for 2 hours. The leaves were cut and washed in de-ionized water to remove residues. Then, leaves were rapidly frozen in liquid nitrogen. The time from cutting to freezing was consistently under 30 seconds. The prepared samples were then ready for the metabolite extraction.

For metabolite extraction, 1 mL $CHCl_3$:MeOH (2:1) was used as the extraction solvent with Dihydrojasmonic acid (H_2JA) (7.5 ng for 0.3 g of leaf tissue) added as an internal standard. Equal volumes of the supernatant were stored at −80 °C. Samples were reconstituted in 50 µL of 20 % aqueous methanol each. The samples were analysed by the Vanquish UHPLC system coupled with a Dual-Pressure Ion Trap Mass Spectrometer (Velos Pro, Thermo Fisher Scientific). Jasmonoyl-L-isoleucine (JA-Ile) and its standard H_2JA were separated by an HSS T3 column (Waters ACQUITY HSS T3 100Å, 1.8 µm, 100 × 2.1 mm) at 40°C using the mobile buffer consisted of 2% ACN/0.1% FA (Buffer A) with an eluting buffer of 100% ACN/0.1% FA (Buffer B) with a 11 mins gradient of 0.5-30% Buffer B at 0-6 min, 30-50% Buffer B at 6-7 min, 50-99.5% Buffer B at 7-7.5 min, 99.5- 0.1% Buffer B at 9.5-10 min and then equilibrated with 0.1% Buffer B at 10-11 min. The selected m/z 322.20 to 130.09 for JA-Ile and 211.13 to 59.01 for H_2JA[127].

Table 3.1. Representative 25 species used for comparative genomics analyses in this study

Species	Genome size	n	N50	L50	N90	L90	Total gene number	Busco (%)	Busco single	Busco duplication	nonoverlapping gene number	gene length	intergene length	exon number	exon length	intron length
Acrodontium crateriforme	**23,104,782**	**15**	**1,746,009**	**5**	**1,214,626**	**12**	**8,030**	**98.94**	**98.94**	**0**	**8,018**	**13,325,656**	**9,779,126**	**17,963**	**12,412,599**	**913,057**
Sphaerulina musiva	29,352,103	729	2,040,975	5	1,517,083	11	8,815	99	99	0	7,397	17,058,853	12,293,250	19,706	12,077,080	4,981,773
Cercospora zeae-maydis	46,606,380	1723	720,376	19	90,530	68	11,684	99.12	99.12	0	11,348	17,223,241	29,383,139	26,930	14,716,479	2,506,762
Cercospora beticola	37,057,033	52	4,173,231	4	2,174,017	9	11,397	99.18	99.12	0.06	10,523	21,089,550	15,967,483	25,544	16,456,086	4,633,464
Pseudocercospora fijiensis	74,141,167	564	5,901,819	5	1,006,785	41	12,113	99.12	99.12	0	11,119	21,504,266	52,636,901	42,862	15,451,266	6,053,000
Passalora fulva	61,113,266	65	56,512	50	5,928	56	14,127	96.54	96.25	0.29	14,127	19,998,515	41,114,751	30,740	18,300,722	1,697,793

Dothistroma septosporum	30,209,431	202	2,595,548	5	1,558,309	11	10,432	98.77	98.77	0	8,284	19,016,357	11,193,074	21,860	13,055,111	5,961,246
Zasmidium cellare	38,247,703	67	675,253	19	175,257	56	15,988	98.89	98.83	0.06	15,961	23,589,686	14,658,017	40,004	21,570,712	2,018,974
Zymoseptoria tritici	39,686,251	21	2,674,951	6	773,098	14	10,851	99.06	99.06	0	10,769	17,359,488	22,326,763	28,056	14,150,583	3,208,905
Dissoconium aciculare	26,537,235	541	1,777,118	6	395,542	16	9,378	98.48	98.48	0	8,457	15,261,761	11,275,474	20,049	12,275,199	2,986,562
Piedraia hortae	16,946,159	3231	260,314	221	67,429	7110	6,541	94.9	94.78	0.12	5,510	9,404,552	7,541,607	11,684	8,022,289	1,382,263
Acidomyces richmondensis	29,883,570	642	41,652	91	4,206	861	10,614	98.13	98.07	0.06	10,026	15,735,470	14,148,100	23,575	12,974,378	2,761,092
Teratosphaeria nubilosa	28,443,146	731	239,765	34	65,854	20	9,912	98.83	98.83	0	8,826	16,043,241	12,399,905	21,113	12,649,357	3,393,884
Salinomyces thailandica	23,885,016	63	331,982	23	109,811	70	8,778	98.65	98.65	0	8,778	14,996,653	8,888,363	20,381	13,604,113	1,392,540

		6		1		3										
Hortaea	49,94	5	153,	0	39,5	3		99.1				25,98	23,962,	35,68	24,03	1,946
werneckii	2,992	1	735	0	43	7	15,723	8	13.66	85.52	15,698	0,944	048	5	4,698	,246
		2				1										
		9		3		4										
Friedmanniomy	37,79	8	30,1	4	5,87	7		96.8				21,21	16,574,	33,90	18,46	2,748
ces simplex	0,643	8	39	6	2	5	13,766	3	83.29	13.54	13,766	5,993	650	2	7,530	,463
Friedmanniomy		9														
ces	23,49	0	669,	1	76,2	4		98.4				14,81	8,685,0	20,94	13,88	930,5
endolithicus	7,870	2	536	2	49	5	9,242	7	98.24	0.23	9,242	2,846	24	3	2,251	95
			1,30		1,09											
Baudoinia	21,87	1	0,63		3,22	1		98.9				15,33	6,544,1	20,77	12,40	2,925
panamericana	6,451	9	7	7	3	4	10,007	4	98.94	0	9,501	2,259	92	6	6,900	,359
			1,94		1,02											
Hortaea	20,43	3	3,56		0,33	1		98.6				14,82	5,603,6	20,70	12,40	2,427
acidophila	2,448	9	9	5	9	1	9,040	5	98.65	0	8,249	8,767	81	1	1,239	,528
		4				1										
Polychaeton	27,20	1	280,	3	73,0	0		98.6				15,83	11,370,	20,20	12,89	2,938
citri	7,581	6	913	0	26	2	9,677	5	98.59	0.06	8,772	7,071	510	0	8,076	,995
			1,07													
Aureobasidium	25,42	4	4,98		338,	2						15,24	10,186,	26,57	13,92	1,319
namibiae	8,601	7	2	9	807	3	10,253	99	99	0	10,240	1,653	948	2	2,499	,154
		1	1,53													
Elsinoe	28,27	6	3,95		178,	1		99.1				15,52	12,743,	21,41	12,44	3,080
ampelina	0,677	1	5	7	698	9	9,264	8	99.12	0.06	8,319	7,303	374	8	6,635	,668

		2														
Elsinoe	26,01	8	694,	1	116,	4		98.4				16,05	9,958,8	23,97	15,02	1,025
fawcettii	1,141	6	004	2	278	2	10,170	8	98.42	0.06	10,170	2,256	85	1	7,063	,193
			1,86		1,27											
Myriangium	25,68	1	2,75		5,22	1		98.7				16,32	9,357,0	23,32	13,65	2,676
duriaei	5,045	6	7	5	3	2	9,946	7	98.77	0	9,207	7,974	71	9	1,694	,280
Parastagonosp	37,21	1	1,04	1	320,	3	15,649	98.3	98.36	0	15,308	20,67	16,539,	40,04	17,84	2,826
ora nodorum	3,987	0 8	5,36 3	3	110	7		6				4,897	090	4	8,640	,257

3.3. Result

3.3.1 *A. crateriforme* enhance prey digestion in *D. spatulata*

To establish the potential contribution of *A. crateriforme* to the sundew host, *A. crateriforme* was first inoculated onto the leaves of *D. spatulata* and there were no significant differences in the plant morphology and net weight after one month (**Fig. 2.6d & Fig. 3.1a**). Conversely, inoculation with *Ph. herbarum* at the same concentration resulted in plant wilt (**Fig. 3.1b**), suggesting a stable plant-fungus coexistence between *A. crateriforme* and *D. spatulata*. When the leaves were supplemented with ant powder, the recorded times required for the stalk glands to fully cover the prey, and return to their original position were recorded in averaged 92 hours (**Fig. 3.2a**). Mechanical stimulation or supplementing on sundew leaves with shrimp and wood powder resulted in much quicker re-opening of the traps (~23 hours), suggesting *D. spatulata* was able to distinguish between prey and non-prey. Inoculating the sterile sundew leaves with three different microbial communities resembling: i) *A. crateriforme* only, ii) sundew natural microbiota and iii) leaf surface microbiota from sundew co-occurring plants revealed significantly reduced re-opening time of traps compared to sterile sundew ($P<0.001$, Wilcoxon rank sum test; **Fig 3.2a**). This suggests that the presence of the microbial community enhanced the sundews' responses against substrates. Significantly faster trap re-opening was observed between sundews inoculated with *A. crateriforme* only than those with microbiota of the surrounding environment from co-occurring plants (median 73 h vs. 81 h; Wilcoxon rank sum test, Adjusted $P < 0.01$; **Fig. 3.2a**), demonstrating positive involvement of *A. crateriforme* in digestion on sundew leaves. The addition of protease inhibitor significantly enhanced the reopening time in all treatments (averaging 182.8 h; **Fig. 3.3**), corroborating previous findings that the peptidases were involved in digestion[46,128,129]. To establish whether microbes facilitate prey digestion by increasing protein degradation capability, we analysed the digestion rates of the applied biotinylated BSA, which showed that mucilage from inoculated plants. Application of biotinylated bovine serum albumin to the collected mucilage showed a declining trend during digestion and was significantly reduced after 24 hours from the *A. crateriforme* inoculated samples (85.9% vs others: 92.4–94.1%, adjusted $P=0.01$, Wilcoxon rank sum exact test, **Fig. 3.2b;** with repeated experiments also displaying the same trend

in **Fig. 3.4**). This result emphasises that more proteins were digested in the presence of *A. crateriforme* and that *A. crateriforme* is a functional part of the sundew holobiont for digestion.

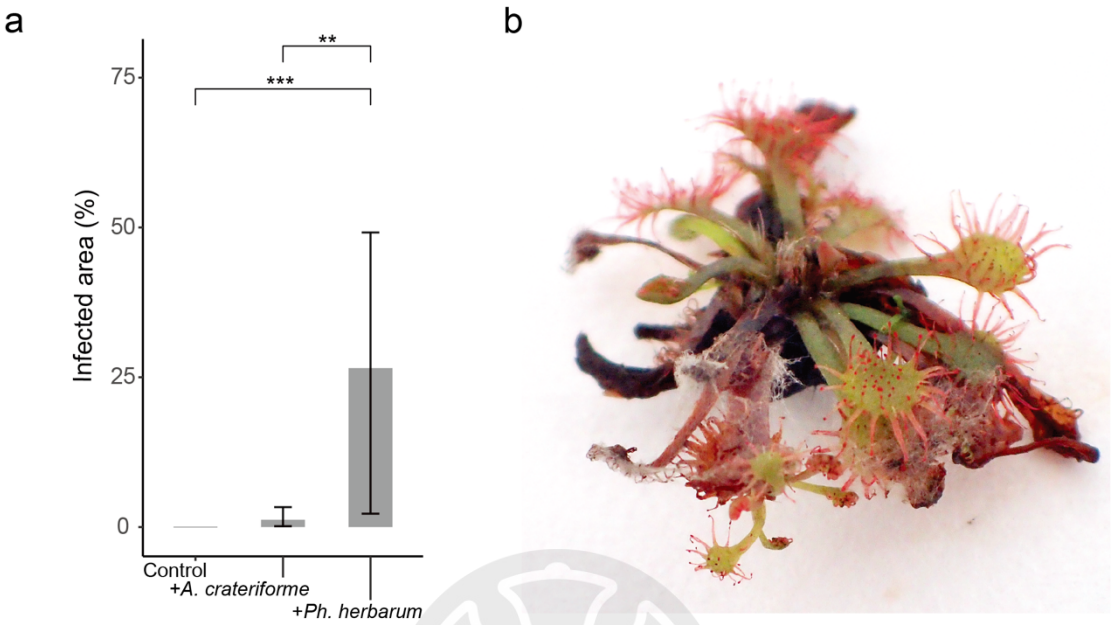

Fig. 3.1 The result of inoculated *D. spatulata*. a. Infected areas of *D. spatulata* one month after post-inoculation with *A. crateriforme* and *Ph. herbarum*. b. A photo showing wilt of *D. spatulata* as a result of inoculating *Ph. herbarum*.

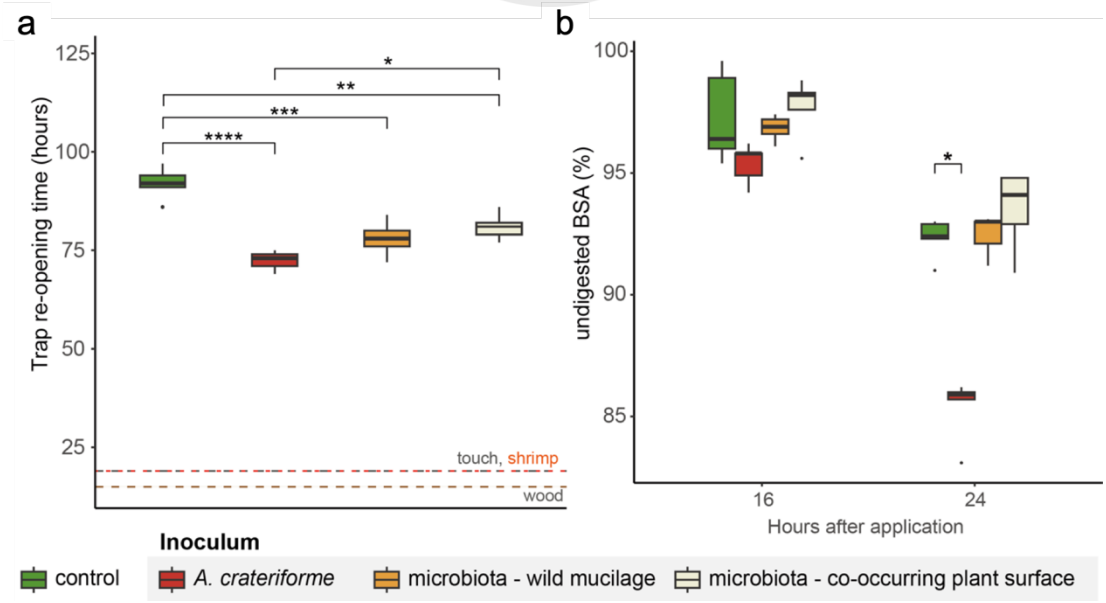

Fig. 3.2. The *A. crateriforme-Drosera spatulata* holobiont. a. Re-opening time of sundew traps supplemented with different substrates and without (control) or with different microbiota inoculation. Median re-opening time for

touch, shrimp and wood in sundews with different microbiota are plotted as dashed lines. **b.** Application of biotin-labelled BSA as a protein substrate during 16 and 24 h of sundew digestion showing decline in BSA with digestion using collected mucilage from sundews inoculated with different inoculum.

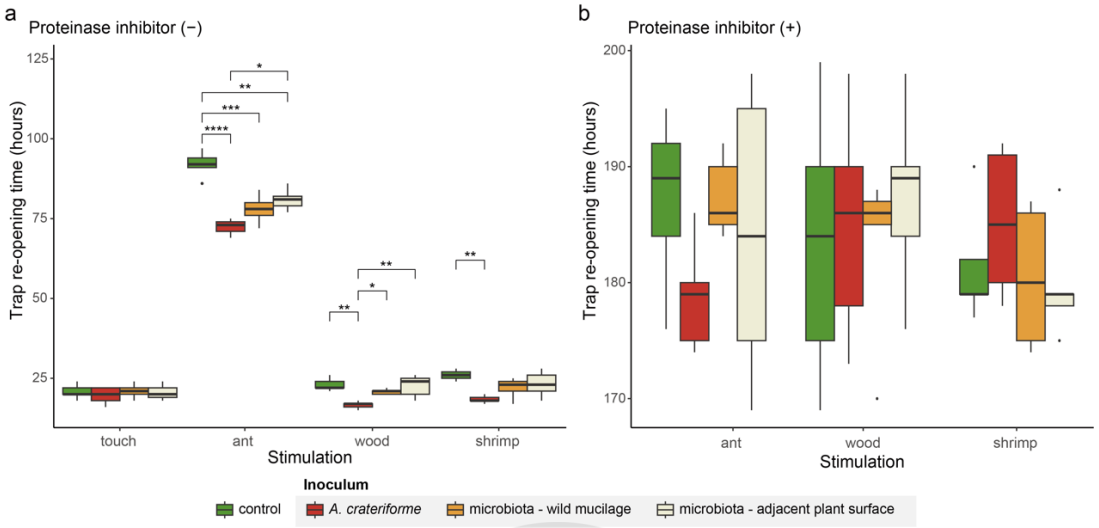

Fig. 3.3. Re-opening time of sundew traps grown one month after different inoculum and fed with different substrates/stimulation.
a. Treatment without proteinase inhibitor. **b.** Treatment with proteinase inhibitor. Asterisk denote P values from Wilcoxon-rank sum test (* P<0.05, ** P<0.01, *** P<0.001). + and – denote presence and absence of treatment, respectively.

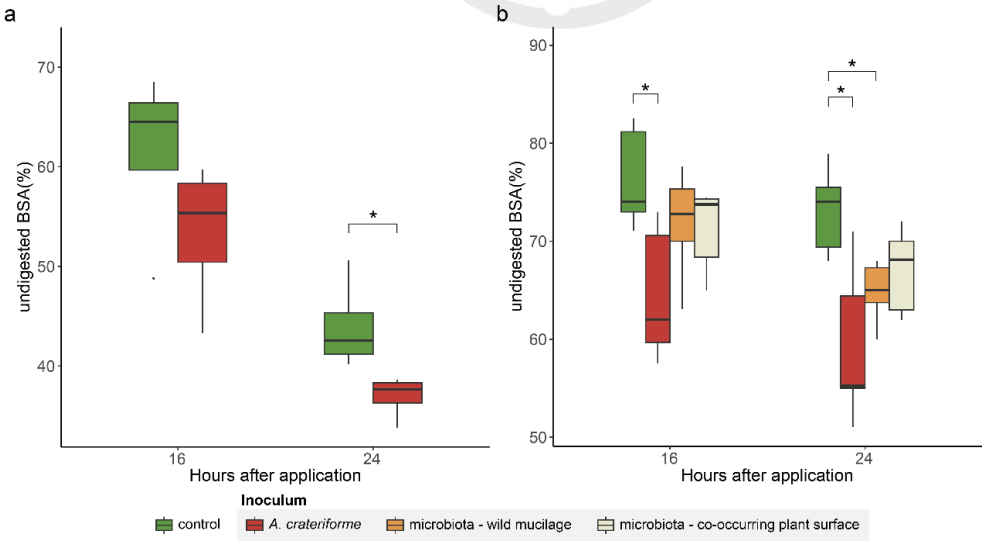

Fig. 3.4. Another two batches from Fig. 3.3. experiment showing the application of biotin-labelled BSA as a protein substrate during 16 and 24 h of sundew digestion using collected mucilage from sundews inoculated with different inoculum.

3.3.2 Genome of *A. crateriforme* as an extremophilic fungus

To examine the genetic potential for digestive functions, we sequenced and assembled the *A. crateriforme* genome using 10.5Gb of Oxford Nanopore long reads and polished the consensus sequences with Illumina reads. The final assembly resulted in 14 contigs, with 13 containing TTAGGG copies at both ends corresponding to gapless chromosomes (**Table 3.2**). The assembly size of 23.1 Mb represented the first genome from the genus *Acrodontium*. We predicted 8,030 gene models using MAKER pipeline[130] with RNAseq as hints. Of these, 97.3% of the predicted gene models were found to be orthologous to at least one of the 25 representative species in the order Capnodiales (**Table 3.1**), suggesting a conserved core genome with potentially unique adaptations. A species phylogeny was constructed by coalescencing 9,757 orthogroup trees, which placed *A. crateriforme* within a group of extremophilic species (**Fig. 3.5a**) including well-known acidophiles such as *Acidomyces richnondensis* and *Neohortaea acidophila*[131]. We determined the mating locus and its adjacent orthologs of *A. crateriforme* and we found that this was in syntenic with sister species (**Fig. 3.6**). The result suggests that this fungus is likely to be heterothallic, similar to the ancestral Mycosphaerellales[132].

To identify genes and gene families associated with its ecology and metabolism, we functionally annotated the *A. crateriforme* proteome (**Fig. 3.5b**). PCA of protein family domain numbers from each species first differentiated the extremophiles *Friedmanniomyces simplex* and *Hortaea werneckii* from others with their partial[133] or whole[134] duplicated genomes (**Fig. 3.7a**). *A. crateriforme* was positioned between its extremophile relatives and the outgroup plant pathogens (**Fig. 3.7b**). Among the extremophiles, inference of gene family dynamics indicated a relatively high number of losses in *A. crateriforme* compared to the human dermatophyte *Piedraia hortae* (**Fig. 3.5a**). *A. crateriforme* has lost members of glycoside hydrolase 6, 11, 28, and 43 which degrade the plant cell wall and their losses have been implicated as signatures of symbiotic[135] fungi such as ectomycorrhizal fungi[136] (**Fig. 3.8 and Table 3.1**). Further specialisations of *A. crateriforme* include a higher number of polyketide synthase clusters within this group of species (**Fig. 3.5b**). Most of the identified BGCs in *A. crateriforme* were unique and not shared with other representative species, implying its distinct profile of secondary metabolites, particularly the polyketides (**Fig. 3.9**). Interestingly, *A. crateriforme* encodes two Neprosin domain-containing genes (**Fig. 3.10**), which were absent in all representative species and rare in fungi (149 versus 8,118 in Viridiplantae; InterPro, last assessed October 2023). Neprosin was first discovered in Raffles' pitcher plant

Nepenthes rafflesiana as a novel peptidase capable of digesting proteins at low concentrations without substrate size restriction[137], hinting at its potential involvement in prey digestion.

The role of genomic rearrangements, especially in subtelomeric regions, in fungal evolution has been well-documented, particularly in pathogenic species[138,139]. We sought to characterise the mode of genome evolution in this group of extremophilic fungi, and identified on an average of 4,747 pairwise single copy orthologs between *A. crateriforme* and sister extremophiles. Clustering of these orthologs with corresponding *A. crateriforme* chromosomes identified only one one-to-one linkage groups of chromosome 13 (**Fig. 3.5c**), suggesting frequent chromosomal fusions and fissions since their last common ancestor. Gene order within linkage groups has been lost (**Fig. 3.11**), suggesting extensive intra-chromosomal rearrangements, which appear to be a hallmark of genome evolution in the Capnodiales[140]. Such high genomic plasticity often led to the high turnover of gene family dynamics or the emergence of biosynthetic gene clusters (BGCs) capable of producing novel secondary metabolites[141]. In the case of *A. crateriforme*, BGCs were enriched at subtelomeres (12/26 in subtelomeres with Observed to Expected ratio of 4.7; **Fig. 3.12**). We identified a case of one polyketide cluster located on the end of chromosome six, which is shared with the plant pathogens *Elsinoe ampelina* and *Parastagonospora nodorum* (**Fig. 3.5d**), presumably as a result of *A. crateriforme* constantly encountering a plant-associated environment.

Table 3.2 Distribution of telomere repeat TTAGGG in *A. crateriforme*

Contig name	Contig length	Repeat designation	Repeat start	Repeat end	Number of copies
Acrcra.chr01	2,837,075	5'	1	104	17.3
Acrcra.chr01	2,837,075	3'	2836972	2837075	17.3
Acrcra.chr02	2,596,228	5'	1	94	15.7
Acrcra.chr02	2,596,228	3'	2596127	2596228	17
Acrcra.chr03	2,270,476	5'	1	106	17.5
Acrcra.chr03	2,270,476	3'	2270369	2270476	18.2
Acrcra.chr04	2,208,761	5'	1	104	17.3
Acrcra.chr04	2,208,761	3'	2208662	2208761	16.7
Acrcra.chr05	1,746,009	5'	1	110	18.7
Acrcra.chr05	1,746,009	3'	1745910	1746009	16.7
Acrcra.chr06	1,680,911	5'	1	102	17
Acrcra.chr06	1,680,911	3'	1680814	1680911	16.5
Acrcra.chr07	1,281,409	5'	1	101	16.8
Acrcra.chr07	1,281,409	3'	1281295	1281409	18.8
Acrcra.chr08	1,278,406	5'	1	103	17.2
Acrcra.chr08	1,278,406	3'	1278306	1278406	16.8
Acrcra.chr09	1,251,688	5'	1	101	16.8

Acrcra.chr09	1,251,688	3'	1251591	1251688	16.3
Acrcra.chr10	1,249,817	5'	1	105	17.5
Acrcra.chr10	1,249,817	3'	1249726	1249817	15.3
Acrcra.chr11	1,227,428	5'	1	99	16.5
Acrcra.chr11	1,227,428	3'	1227334	1227428	15.8
Acrcra.chr12	1,214,626	5'	1	115	18.8
Acrcra.chr12	1,214,626	3'	1214529	1214626	16.3
Acrcra.chr13	1,169,335	5'	1	104	17.3
Acrcra.chr13	1,169,335	3'	1169238	1169335	16.3
Acrcra.chr14	1,038,175	5'	1	95	15.8

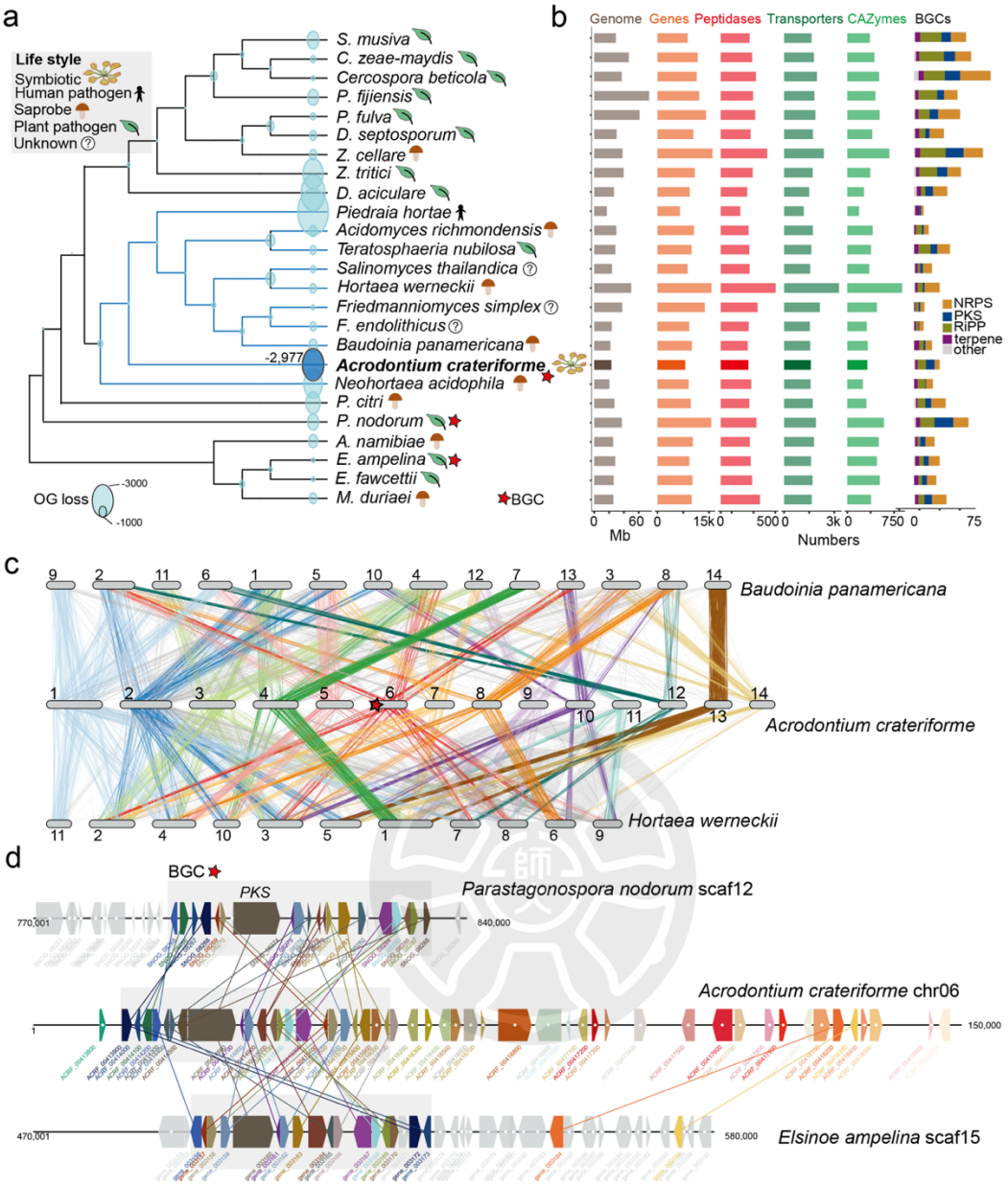

Fig. 3.5 Genomic features of *A. crateriforme*

a. Phylogenetic placement of *A. crateriforme* among extremophilic fungi denoted in blue branches, highlighting its association with known acidophiles. All nodes have a 100% bootstrap support. Number next to *A. crateriforme* denote the number of lost OGs inferred by DOLLOP. **b.** Genome description and functional annotations of the *A. crateriforme* proteome. **c.** Chromosomal rearrangements amongst extremophile fungi *A. crateriforme, Baudoinia panamericana, Hortaea werneckii* through clustering of single copy ortholog pairs. Line colour designate corresponding *A. crateriforme* chromosomes **d.** Synteny between a subtelomeric polyketide cluster on *A. crateriforme* chromosome six and the plant pathogens *E. ampelina* and *P. nodorum*. *A. crateriforme* genes and orthologs are coloured sequentially.

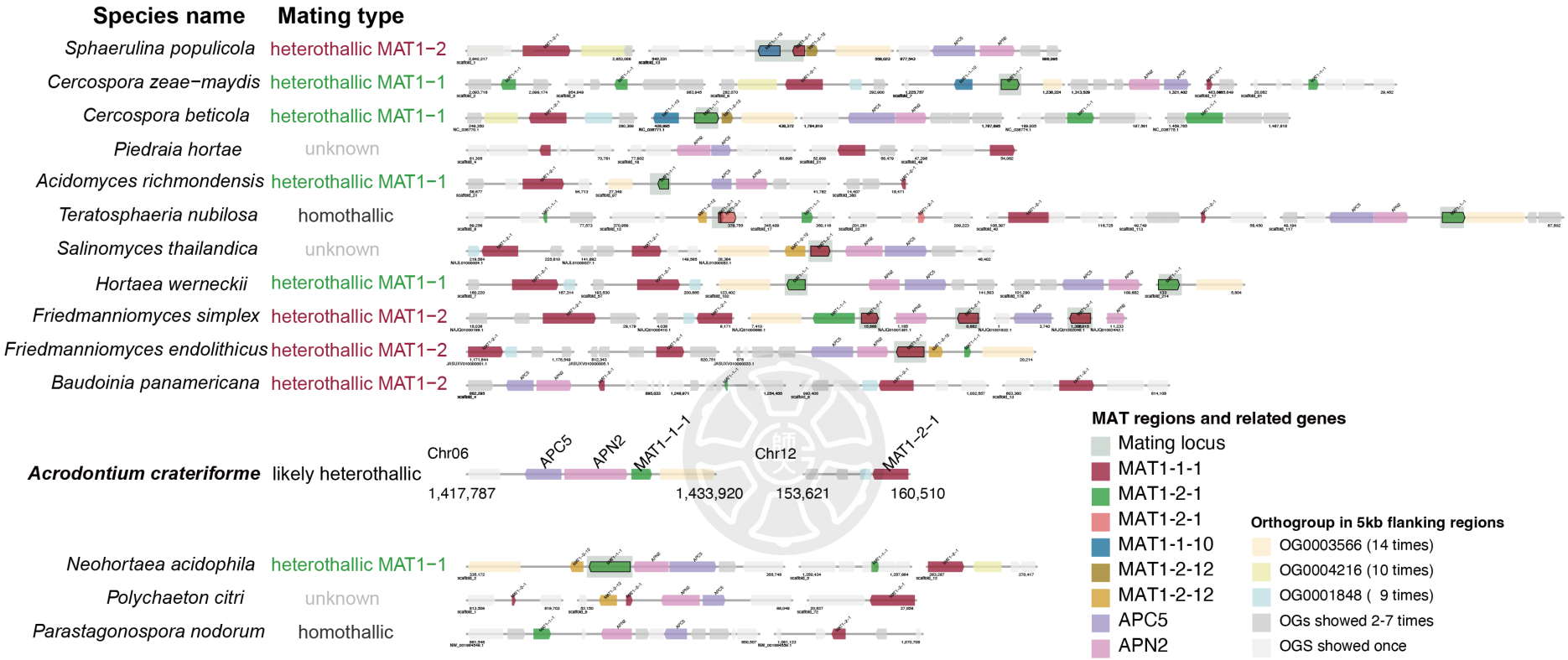

Fig. 3.6 The gene distributions around mating type (MAT) related genes.

The mating locus and related orthologs were identified by BLAST the mating related gene sequences retrieved from *Aylward* et al [132] against the *A. crateriforme* gene predictions. Within the *A. crateriforme* assembly, were located adjacent to each other and inferred as putative mating locus. We identified the orthologs of MAT genes and related APC5 and APN2 genes which are adjacent to each other and displayed in synteny with sister species. This region was inferred as putative mating locus and the gene distributions around MAT, APC5, and APN2 genes (including 5kb up- and down-stream flanking regions) are drawn

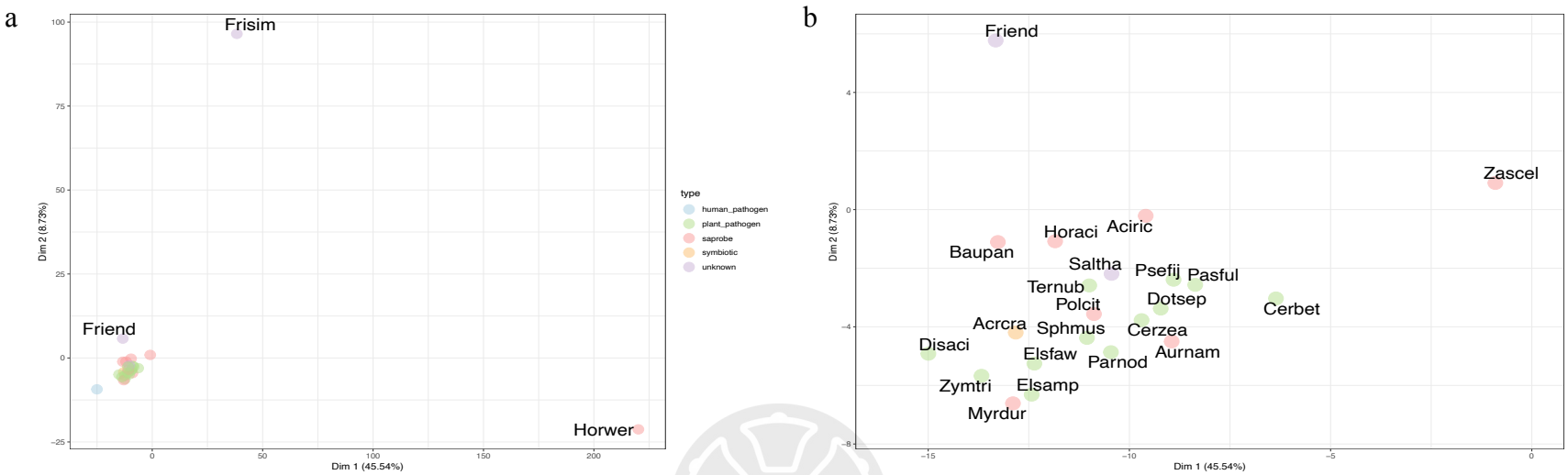

Fig. 3.7 PCA of protein family domain numbers from 25 fungal species a. PCA of all species, **b.** zoomed in plot. Species full names corresponding to abbreviations are available in **Table 3.1**

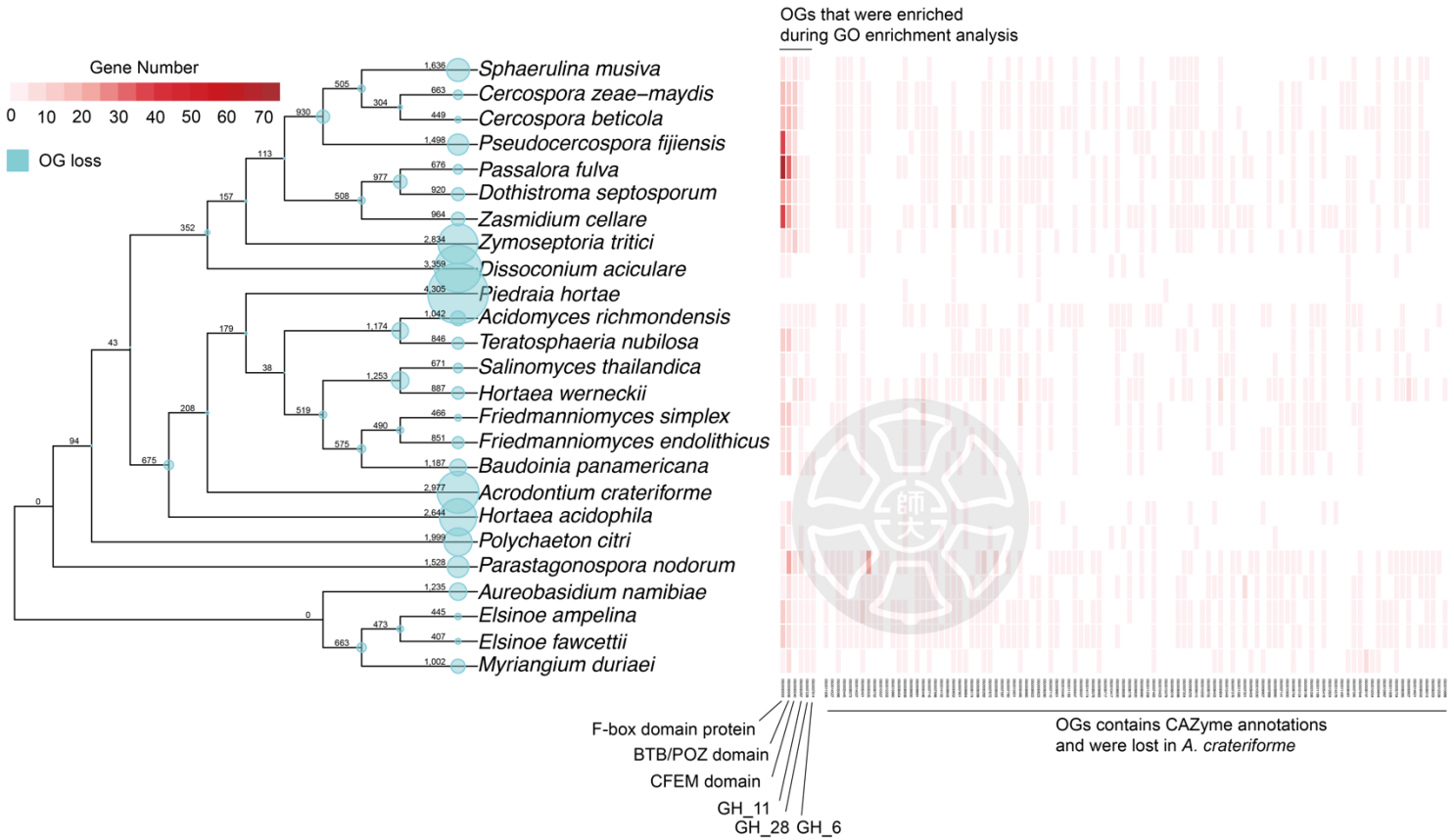

Fig. 3.8 *Acrodontium* phylogeny with OG losses and gene number. The blue circles on phylogeny described the loss OG number at each node. The heatmaps showed gene numbers of OGs in representative species. *A. crateriforme* was inferred to loss these OGs.

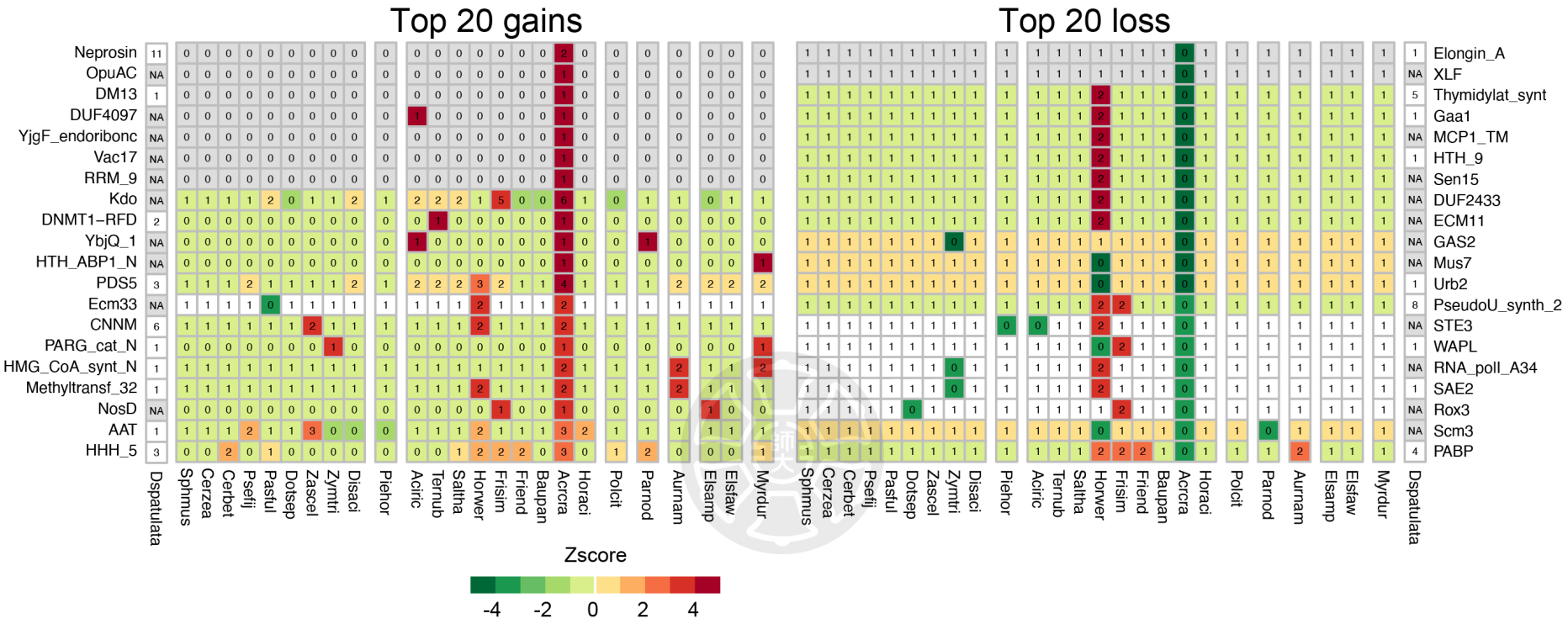

Fig. 3.9 Top 20 Pfam gain and loss of *A. crateriforme.*

Gains and losses were ranked by domain frequencies. A z-score was calculated for the corresponding abundance of every domain in each species.

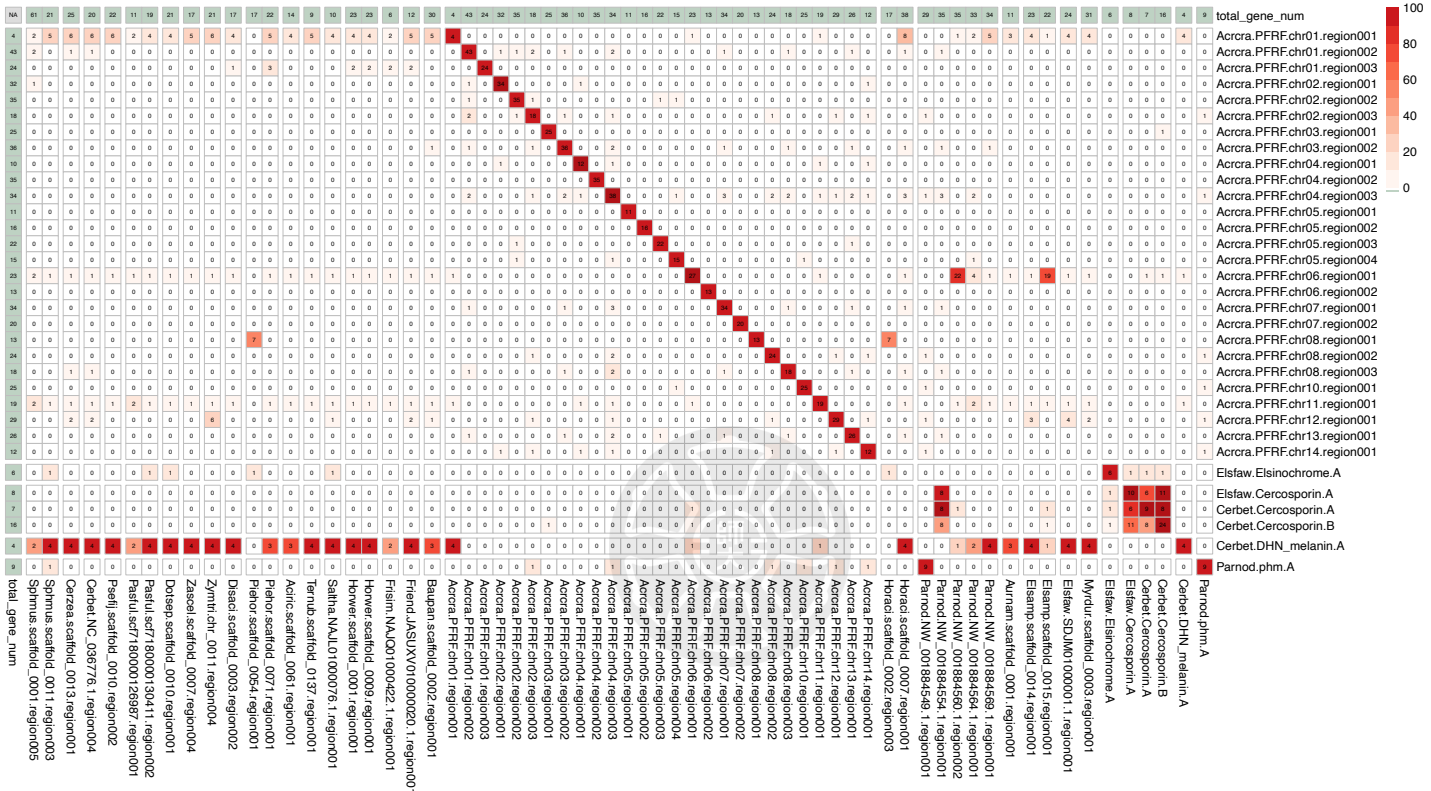

Figure 3.10. Heatmap of biosynthetic gene clusters (BGC) in 25 fungal species. Figure only showed regions with more than 50% orthology to at least one another region

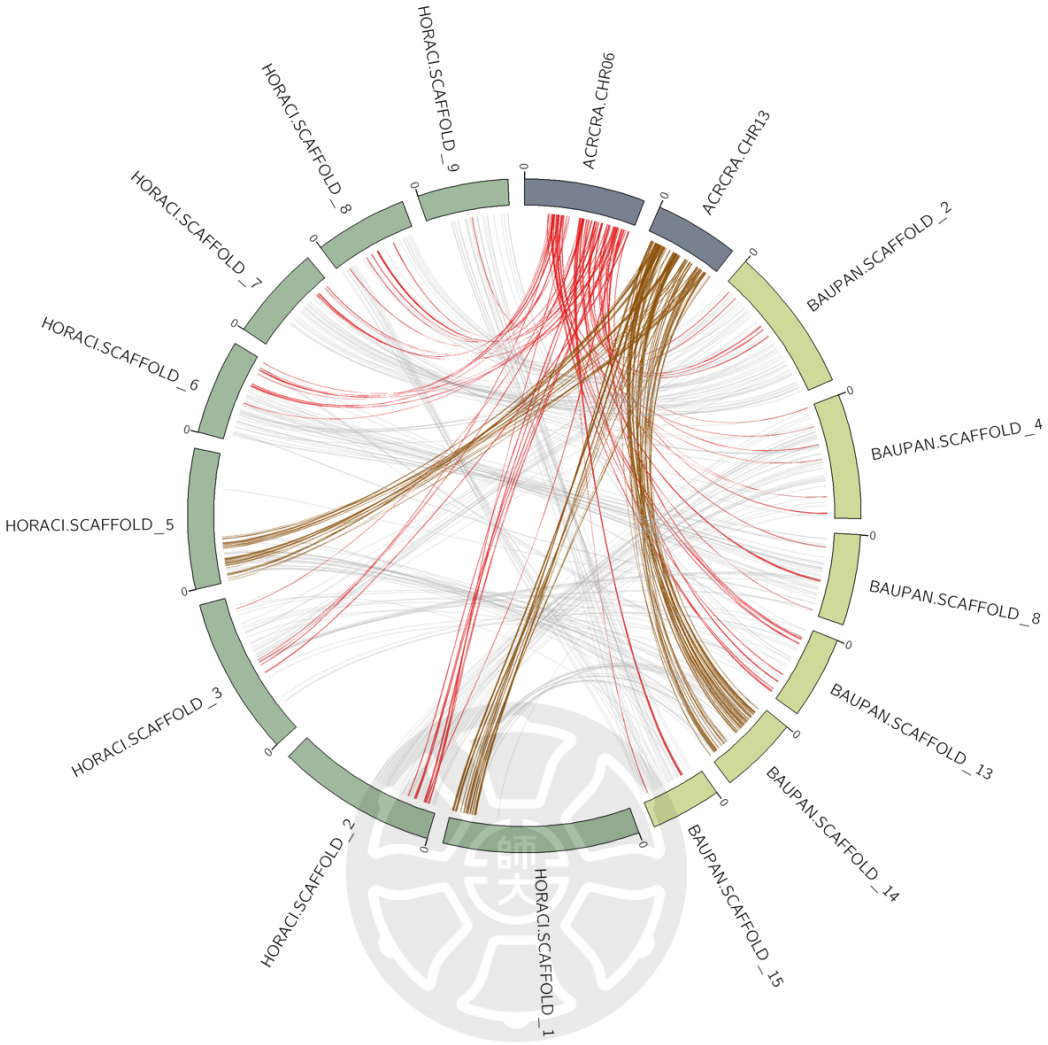

Fig. 3.11 Gene order within linkage groups has been lost

Synteny blocks were determined with DAGchainer[142] (ver. r120920) and visualized via CIRCOS[143] (ver. 0.69.9).

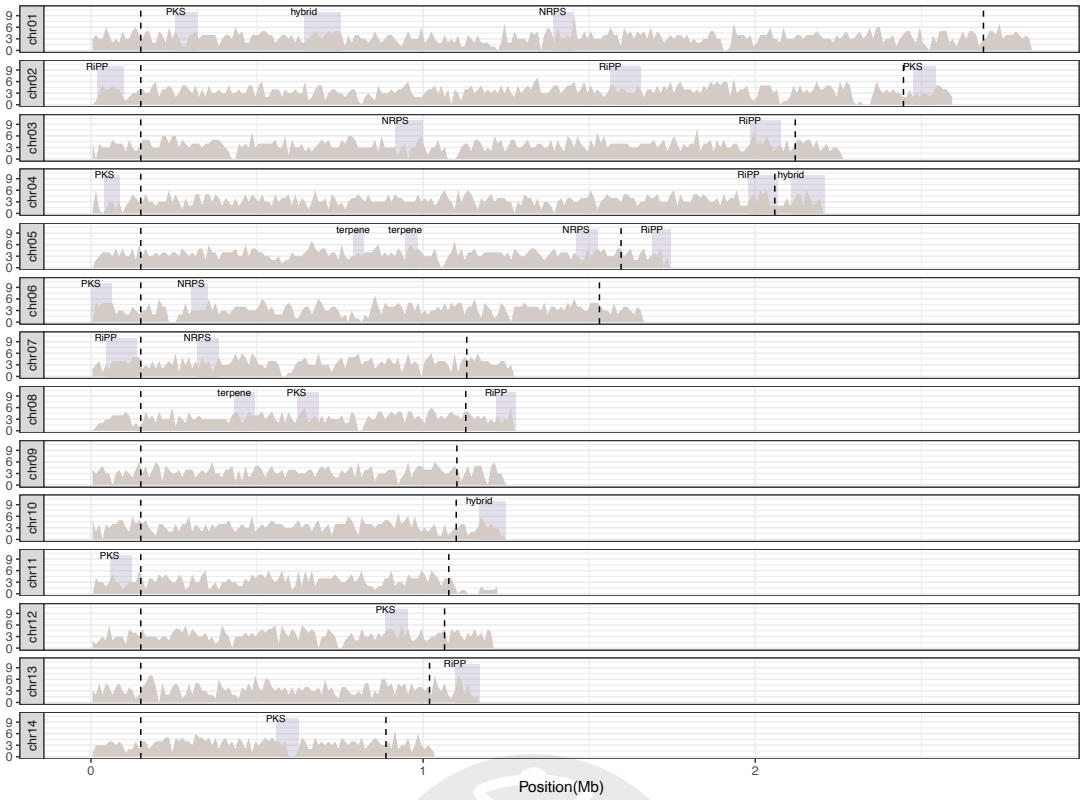

Fig. 3.12 BGCs were enriched in subtelomere regions. Purple areas are BGC regions, light brown areas show gene density in 10kb sliding windows, and dashed lines show the boundaries of 150kb subtelomere regions.

3.3.3 Digestion genes were co-opted and retained ancestral expression trends from plant-microbial coexistence

To dissect how sundew and *A. crateriforme* respond to each other or encountering insects at the transcriptome level, we first generated gene expression data from both species cultured under minimal nutrient conditions. This baseline data was then compared to two experimental conditions: application to ant powder indicative of insect digestion and fungal inoculation onto sundew leaves denoting coexistence (**Fig. 3.11**). Remarkably, 58.6–63.8% of the differentially expressed genes (DEGs) identified between the baseline and digestion phases for each species were co-expressed in the coexistence phase (**Fig. 3.13a**), suggesting an intrinsic regulatory synergy between the two processes. Gene ontology (GO) analysis revealed that more than half of the GO term enrichment of the up-regulated genes overlapped between the two conditions in *D. spatulata,* with the most significant terms including secondary metabolic process, response to chemical and other organisms (**Fig. 3.14 and Table 3.3**). This suggests that the majority of plant genes that were involved in defence mechanisms[83,144] have been co-opted into

the digestion process but still retained their ancestral functions. An example includes members of the plant chitinase (GH18 and GH19) (**Fig. 3.15**), which have roles in insect digestion and original functions in defence against phytopathogens[145,146]. The coexistence phase yielded more DEGs compared to the digestion phase, consistent with that the former process being ancestral[147]. For nutrient acquisition related genes, ammonium transporters, nitrate transporter and nitrate reductase in *D. spatulata* showed increased transcript abundance in both digestion and coexistence phases, and are central to nitrogen uptake and assimilation[148] but were more highly expressed in coexistence than in digestion phase (determined by DESeq2[60]; $|\log_2$ fold change$| > 1$ and adjusted $P < 0.05$; **Fig. 3.16**), suggesting that active nitrogen exchange and use already taking place within the plant-fungus holobiont.

Table 3.3 GO enrichment of differentially upregulated *D. spatulata* genes in either coexistence or digestion processes

For each category, the top 20 most significant terms are reported

DEG type	GO.ID	Term	Annotated	is DEG	Expected	P value	Present in two phases
Upregulated in coexistence	GO:0019748	secondary metabolic process	226	55	15.33	1.60E-17	yes
Upregulated in coexistence	GO:0050896	response to stimulus	3707	327	251.45	2.50E-11	yes
Upregulated in coexistence	GO:0044550	secondary metabolite biosynthetic proces...	157	36	10.65	4.80E-11	yes
Upregulated in coexistence	GO:0011101	response to acid chemical	825	105	55.96	4.80E-11	yes
Upregulated in coexistence	GO:1901700	response to oxygen-containing compound	1203	138	81.66	4.80E-11	yes
Upregulated in coexistence	GO:0042221	response to chemical	2088	207	141.63	1.60E-10	yes
Upregulated in coexistence	GO:0006950	response to stress	2116	207	143.53	5.80E-10	
Upregulated in coexistence	GO:0009611	response to wounding	178	35	12.07	7.20E-09	yes
Upregulated in coexistence	GO:0080167	response to karrikin	97	24	6.58	1.80E-08	
Upregulated in coexistence	GO:0098660	inorganic ion transmembrane transport	275	45	18.65	2.10E-08	yes

Upregulated in coexistence	GO:0006811	ion transport	553	71	37.51	7.40E-08	
Upregulated in coexistence	GO:0102403	response to organonitrogen compound	222	38	15.06	8.30E-08	
Upregulated in coexistence	GO:0043207	response to external biotic stimulus	736	87	49.92	1.00E-07	yes
Upregulated in coexistence	GO:0100035	response to inorganic substance	716	85	48.57	1.20E-07	yes
Upregulated in coexistence	GO:0009607	response to biotic stimulus	740	87	50.2	1.30E-07	yes
Upregulated in coexistence	GO:0009404	toxin metabolic process	29	12	1.97	1.50E-07	yes
Upregulated in coexistence	GO:0051707	response to other organism	733	86	49.72	1.80E-07	yes
Upregulated in coexistence	GO:0009605	response to external stimulus	1027	111	69.66	1.80E-07	
Upregulated in coexistence	GO:0044419	biological process involved in interspec...	764	88	51.82	2.80E-07	yes
Upregulated in coexistence	GO:0009407	toxin catabolic process	14	8	0.95	8.90E-07	
Upregulated in digestion	GO:0019748	secondary metabolic process	226	40	12.58	4.00E-11	yes
Upregulated in digestion	GO:0042221	response to chemical	2088	174	116.22	6.40E-10	yes

	GO:0					9.00	
Upregulated	05170	response to other org				E-	
in digestion	7	anism	733	78	40.8	09	yes
	GO:0					1.10	
Upregulated	04320	response to external			40.9	E-	
in digestion	7	biotic stimulus	736	78	7	08	yes
	GO:0					1.40	
Upregulated	00960	response to biotic sti			41.1	E-	
in digestion	7	mulus	740	78	9	08	yes
	GO:0					1.80	
Upregulated	05083	defense response to f			11.2	E-	
in digestion	2	ungus	202	33	4	08	
	GO:0					5.60	
Upregulated	04441	biological process inv			42.5	E-	
in digestion	9	olved in interspec...	764	78	3	08	yes
	GO:0					6.20	
Upregulated	01062	programmed cell deat				E-	
in digestion	3	h involved in cell d...	32	12	1.78	08	
	GO:0					7.90	
Upregulated	00110	response to acid che			45.9	E-	
in digestion	1	mical	825	82	2	08	yes
	GO:0					1.00	
Upregulated	00960	response to external			57.1	E-	
in digestion	5	stimulus	1027	96	7	07	yes
	GO:1					1.10	
Upregulated	90170	response to oxygen-		10	66.9	E-	
in digestion	0	containing compound	1203	8	6	07	yes
	GO:0					1.40	
Upregulated	00961					E-	
in digestion	1	response to wounding	178	29	9.91	07	yes
	GO:0					1.40	
Upregulated	04865					E-	
in digestion	3	anther development	69	17	3.84	07	
	GO:0					1.50	
Upregulated	00962				14.0	E-	
in digestion	0	response to fungus	253	36	8	07	

Upregulated in digestion	GO:0050896	response to stimulus	3707	259	206.34	2.80E-07	yes
Upregulated in digestion	GO:0051702	biological process involved in interacti...	74	17	4.12	4.20E-07	
Upregulated in digestion	GO:0098660	inorganic ion transmembrane transport	275	36	15.31	1.20E-06	yes
Upregulated in digestion	GO:0010035	response to inorganic substance	716	70	39.85	1.60E-06	yes
Upregulated in digestion	GO:0044550	secondary metabolite biosynthetic proces...	157	25	8.74	1.60E-06	yes
Upregulated in digestion	GO:0009404	toxin metabolic process	29	10	1.61	2.00E-06	yes

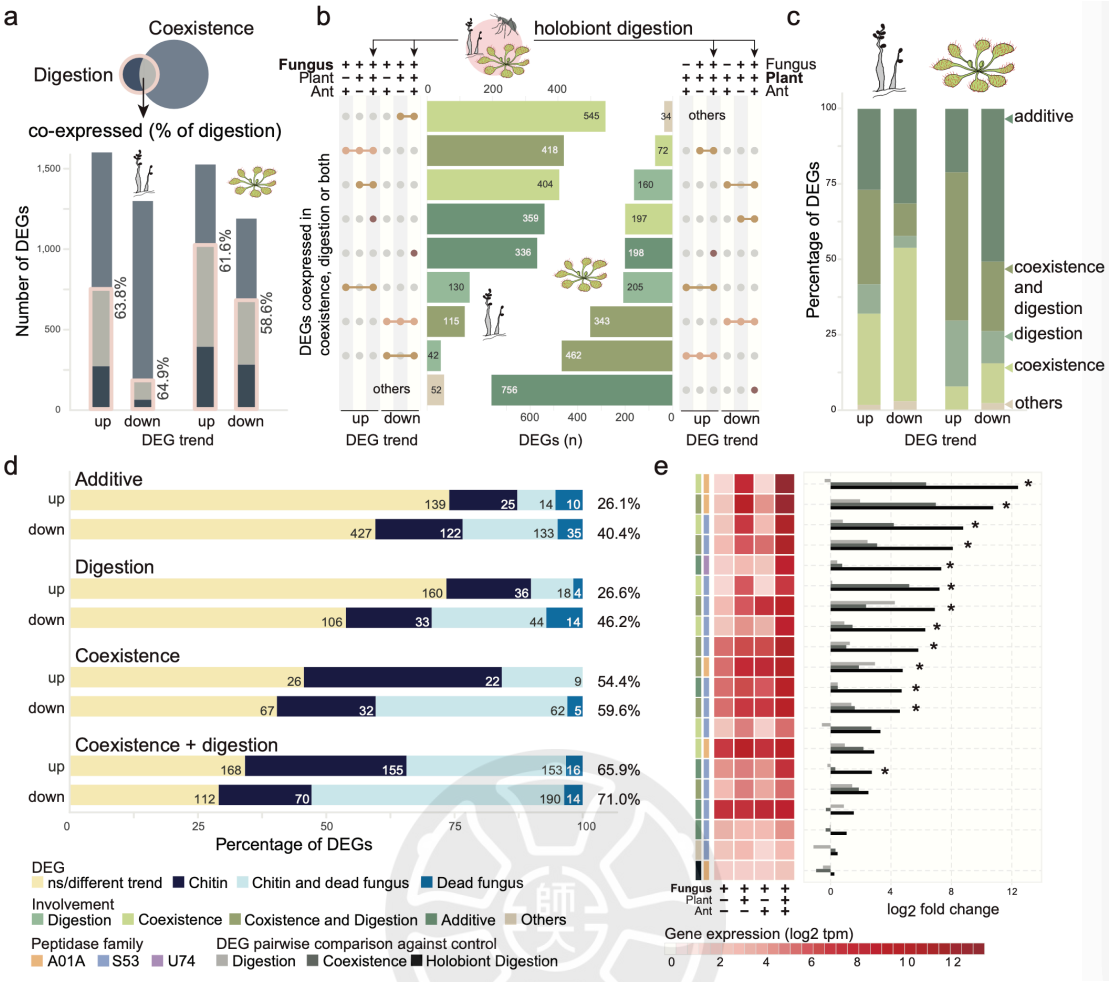

Fig 3.13. Transcriptome of the *D. spatulata-A. crateriforme* holobiont during digestion.

a. Overlap of upregulated (up) or downregulated (down) DEGs during digestion and coexistence for both species in comparison to baseline controls (determined by DESeq2; $|\log_2$ fold change$| > 1$ and adjusted $P < 0.05$). Percentages indicate the proportion of differentially expressed genes in the digestion phase that were also expressed in the same trend in the coexistence phase. **b.** Transcriptome profiling of the plant-fungus holobiont during digestion with fungus on right and plant on left. DEGs were compared whether the same trends were observed in either digestion or coexistence process. **c.** Schematic representation of the role of the DEGs involved in the holobiont digestion. **d.** Schematic representation of designated categories of DEGs in **Fig 5c**. when compared to transcriptome changes in plant treated with chitin or dead fungus. Numbers in rectangles denote number of genes. ns denote the not significant, i.e., DEGs that did not exhibit expression changes in response to elicitors. Numbers in brackets denote proportion of DEGs that were also expressed in the same trend when plant was treated with different elicitors. **e.** Expression of

representative fungal peptidases in a co-expression module (module 2 in **Fig. 3.21**) showing synergistic effects when both plant and insect prey are present. Asterisks indicate significantly upregulated expression between holobiont digestion and either digestion or coexistence phase. Tpm denote transcript per million.

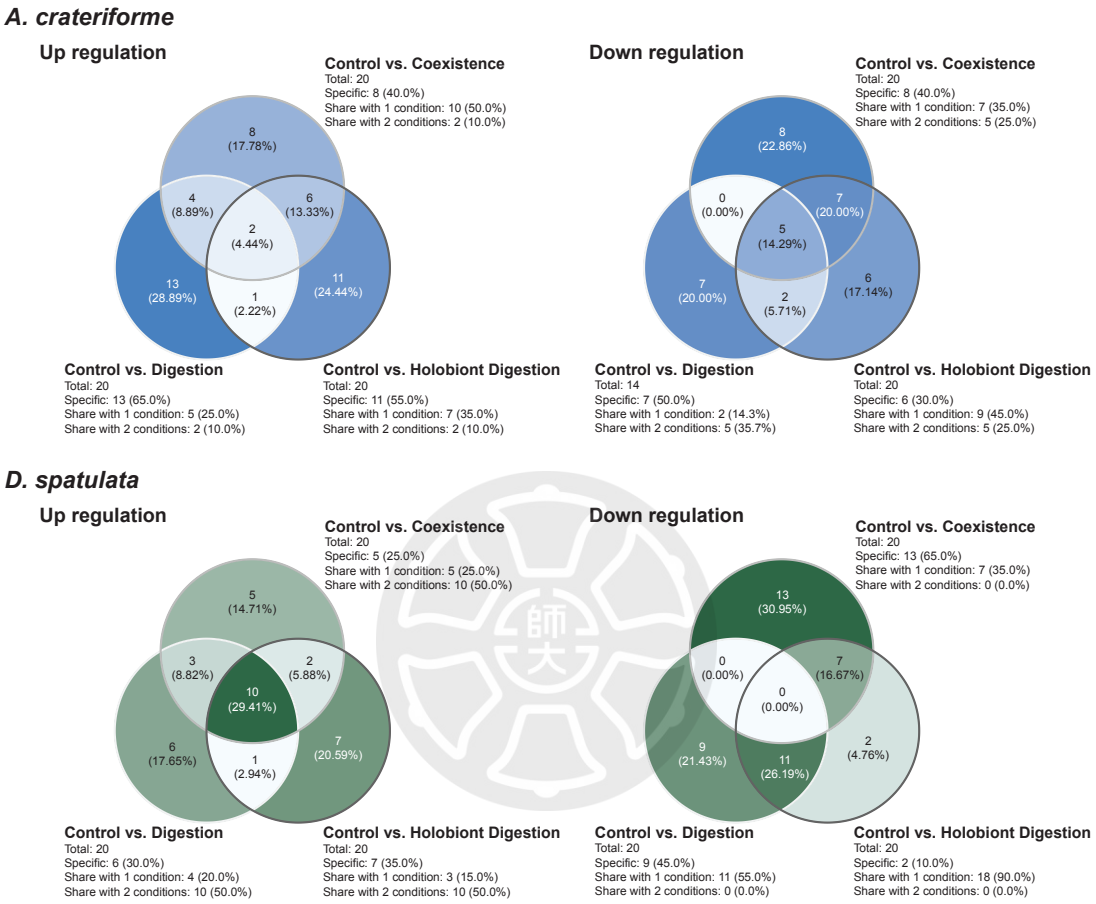

Fig. 3.14. Overlap of top 20 enriched GO terms in *A. crateriforme* and *D. spatulata* under different conditions.

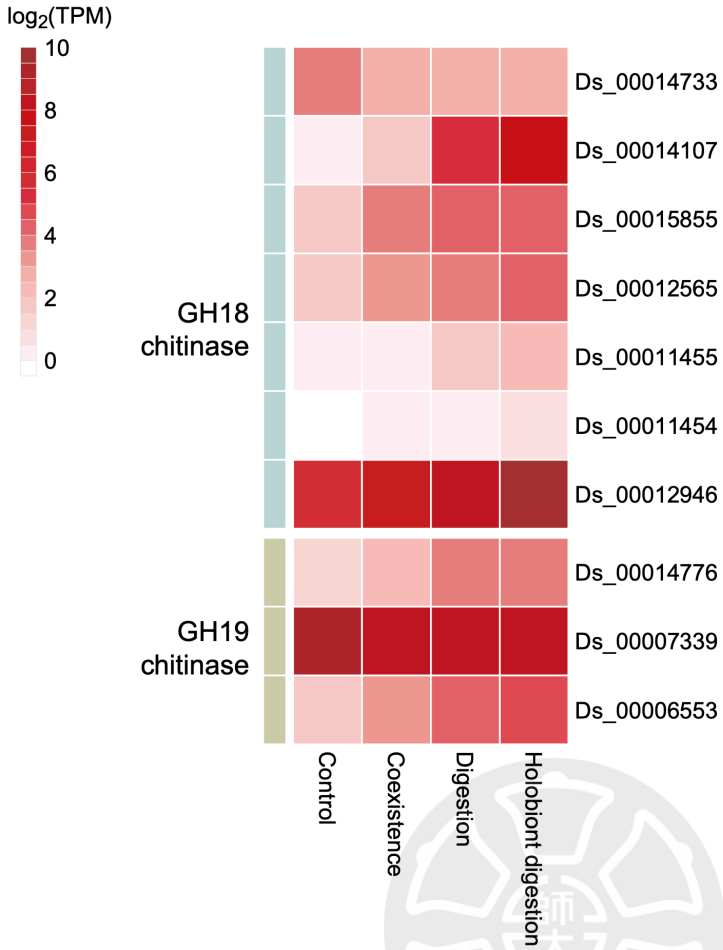

Fig. 3.15. Expression of sundew chitinase in different treatments

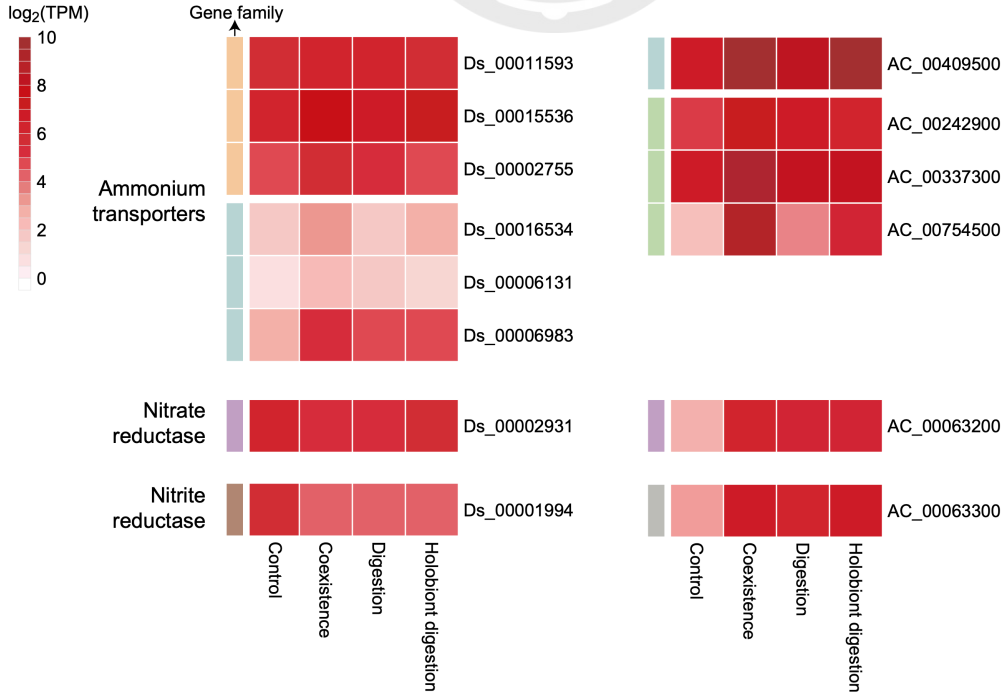

Fig. 3.16. Expression of ammonium transporters in different treatments

3.3.4 Transcriptome dynamic of holobiont digestion in nature

In nature, the digestion of insects takes place in the mucilage of *D. spatulata*, with arthropod remains to adhere to the stalk glands, where *A. crateriforme* can be observed growing over the insect surface (**Fig. 3.17**). To elucidate the mechanisms of carnivorous holobiont digestion, we further characterised the holobiont transcriptome when supplemented with ant powder (**Fig. 3.18**). We identified 2,401 and 2,427 DEGs in *A. crateriforme* and *D. spatulata*, respectively. We desigated the majority of these genes into three categories (**Fig. 3.13b**): differentially expressed in single (co-existence or digestion) or similar expression trends in both processes (co-existence and digestion). We also defined a fourth 'additive' category, in which the genes were only significantly differentially expressed when stimuli from both the interacting partner and the insect prey nutrient source were present (**Fig. 3.13c**). More than half of upregulated DEGs in both species were designated in the both or additive categories, suggesting co-evolution and optimisation of the plant holobiont transcriptome as a result of constantly encountering each other and ant nutrient[87].

In *A. crateriforme*, the highest number of DEGs were classified as involved in coexistence, suggesting its primary role in species interaction. Only 22.2% of the fungal DEGs were differentially expressed in both processes. A BGC on chromosome six (**Fig. 3.5d**), showed a consistent upregulation in the co-existence and digestion phases (**Fig. 3.19**), highlighting the need to effectively respond to multiple stimuli in natural environments. Interestingly, GO term enrichment of condition-specific genes revealed an opposite trend of up- and down-regulation of genes involved in the fungal and plant cell cycle, respectively (**Table 3.4**), suggesting divergent responses in both species when faced with similar environments. To investigate the nature of sundew DEGs in these categories, we conducted leaf transcriptomes inoculated with dead *A. crateriforme* or chitins (**Fig. 3.18**) and compared them with the baseline transcriptome of sterile leaves. Between 54.4% and 71.0% of the previously mentioned DEGs, identified in either the co-existence phase or both the co-existence and digestion phases, were also differentially expressed in the same manner, respectively, upon exposure to chitin or dead fungal material (**Fig. 3.13d**). This suggests that these two categories of DEGs are primarily triggered by the presence of chitin, paralleling findings in the Venus' flytrap *Dionaea muscipula* that demonstrated chitin as a crucial cue for gene expression to set the trap towards a "posed to capture" mode[149]. Conversely, 26.1–46.2% of the DEGs within the digestion or additive category showed similar expression

patterns upon elicitor application, respectively (**Fig. 3.14d**). For example, asparagine synthetase, a key enzyme in plant amino acid assimilation[150], was designated in the up-regulated additive category (**Fig. 3.20**). Gene Ontology (GO) enrichment analysis of the upregulated genes in these categories, which were unaffected by the presence of elicitors, revealed genes involved in the auxin-activated signaling pathway and cation transmembrane transport (**Table 3.5**), suggesting the optimization of the genes repurposed for prey digestion[19] or in response to available nutrients towards the end of the digestion process.

Table 3.4 – GO enrichment of differentially *A. crateriforme* genes in either coexistence or digestion processes

For each category, the top 20 most significant terms are reported

DEG type	GO.ID	Term	Annotated	isDEG	Expected	P value
Upregulated in digestion	GO:0016999	antibiotic metabolic process	61	14	1.83	1.40E-09
Upregulated in digestion	GO:0017001	antibiotic catabolic process	21	9	0.63	3.00E-09
Upregulated in digestion	GO:0000272	polysaccharide catabolic process	26	9	0.78	2.80E-08
Upregulated in digestion	GO:0016052	carbohydrate catabolic process	71	13	2.13	1.00E-07
Upregulated in digestion	GO:0032787	monocarboxylic acid metabolic process	135	17	4.04	3.00E-07
Upregulated in digestion	GO:0005975	carbohydrate metabolic process	188	20	5.63	4.10E-07
Upregulated in digestion	GO:1901615	organic hydroxy compound metabolic proce...	125	16	3.74	5.60E-07
Upregulated in digestion	GO:0072329	monocarboxylic acid catabolic process	36	9	1.08	6.60E-07
Upregulated in digestion	GO:0055085	transmembrane transport	331	27	9.91	6.90E-07
Upregulated in digestion	GO:0006066	alcohol metabolic process	98	14	2.93	7.90E-07
Upregulated in digestion	GO:0044550	secondary metabolite biosynthetic proces...	38	9	1.14	1.10E-06
Upregulated in digestion	GO:0034220	ion transmembrane transport	203	20	6.08	1.40E-06
Upregulated in digestion	GO:0044281	small molecule metabolic process	633	39	18.96	2.00E-06
Upregulated in digestion	GO:0044275	cellular carbohydrate catabolic process	31	8	0.93	2.20E-06
Upregulated in digestion	GO:0006811	ion transport	272	23	8.15	3.10E-06
Upregulated in digestion	GO:0019748	secondary metabolic process	44	9	1.32	4.10E-06

Upregulated in digestion	GO:00 06812	cation transport	165	17	4.94	5.30 E-06
Upregulated in digestion	GO:00 16054	organic acid catabolic proc ess	74	11	2.22	8.90 E-06
Upregulated in digestion	GO:00 46395	carboxylic acid catabolic p rocess	74	11	2.22	8.90 E-06
Upregulated in digestion	GO:00 44282	small molecule catabolic p rocess	120	14	3.59	9.30 E-06
Upregulated in coexistence	GO:00 50000	chromosome localization	53	15	4.26	1.00 E-05
Upregulated in coexistence	GO:00 06811	ion transport	272	41	21.88	3.70 E-05
Upregulated in coexistence	GO:00 16054	organic acid catabolic proc ess	74	17	5.95	5.20 E-05
Upregulated in coexistence	GO:00 46395	carboxylic acid catabolic p rocess	74	17	5.95	5.20 E-05
Upregulated in coexistence	GO:00 51303	establishment of chromos ome localization	42	12	3.38	7.10 E-05
Upregulated in coexistence	GO:00 19748	secondary metabolic proc ess	44	12	3.54	0.00 012
Upregulated in coexistence	GO:00 07020	microtubule nucleation	16	7	1.29	0.00 012
Upregulated in coexistence	GO:00 19740	nitrogen utilization	21	8	1.69	0.00 013
Upregulated in coexistence	GO:00 51455	monopolar spindle attach ment to meiosis ...	21	8	1.69	0.00 013
Upregulated in coexistence	GO:00 51316	attachment of spindle micr otubules to ki...	22	8	1.77	0.00 019
Upregulated in coexistence	GO:00 55085	transmembrane transport	331	45	26.62	0.00 02
Upregulated in coexistence	GO:00 45143	homologous chromosome segregation	47	12	3.78	0.00 023
Upregulated in coexistence	GO:19 03508	positive regulation of nucle ic acid-temp...	220	33	17.7	0.00 025
Upregulated in coexistence	GO:19 02680	positive regulation of RNA biosynthetic ...	221	33	17.78	0.00 027
Upregulated in coexistence	GO:00 34220	ion transmembrane transp ort	203	31	16.33	0.00 028

Upregulated in coexistence	GO:00 90033	positive regulation of filam entous growt...	35	10	2.82	0.00 029
Upregulated in coexistence	GO:19 00430	positive regulation of filam entous growt...	35	10	2.82	0.00 029
Upregulated in coexistence	GO:00 45893	positive regulation of DNA-templated tra...	213	32	17.13	0.00 03
Upregulated in coexistence	GO:00 06109	regulation of carbohydrate metabolic pro...	42	11	3.38	0.00 033
Upregulated in coexistence	GO:00 45927	positive regulation of growt h	42	11	3.38	0.00 033
Downregulated in coexistence	GO:00 07005	mitochondrion organizatio n	211	14	3.01	7.20 E-07
Downregulated in coexistence	GO:19 90542	mitochondrial transmembr ane transport	82	8	1.17	1.50 E-05
Downregulated in coexistence	GO:00 06839	mitochondrial transport	107	8	1.53	0.00 011
Downregulated in coexistence	GO:00 06879	cellular iron ion homeostas is	40	5	0.57	0.00 022
Downregulated in coexistence	GO:00 55072	iron ion homeostasis	41	5	0.58	0.00 024
Downregulated in coexistence	GO:00 06811	ion transport	272	12	3.88	0.00 031
Downregulated in coexistence	GO:00 00963	mitochondrial RNA proces sing	11	3	0.16	0.00 042
Downregulated in coexistence	GO:00 06812	cation transport	165	9	2.35	0.00 043
Downregulated in coexistence	GO:00 00959	mitochondrial RNA metab olic process	26	4	0.37	0.00 043
Downregulated in coexistence	GO:00 55085	transmembrane transport	331	13	4.72	0.00 052
Downregulated in coexistence	GO:00 07006	mitochondrial membrane o rganization	49	5	0.7	0.00 057
Downregulated in coexistence	GO:00 44743	protein transmembrane im port into intrac...	51	5	0.73	0.00 069
Downregulated in coexistence	GO:00 33108	mitochondrial respiratory c hain complex ...	30	4	0.43	0.00 076
Downregulated in coexistence	GO:00 06626	protein targeting to mitoch ondrion	54	5	0.77	0.00 09

Downregulated in coexistence	GO:0070585	protein localization to mitochondrion	56	5	0.8	0.00106
Downregulated in coexistence	GO:0072655	establishment of protein localization to...	56	5	0.8	0.00106
Downregulated in coexistence	GO:0045332	phospholipid translocation	15	3	0.21	0.0011
Downregulated in coexistence	GO:0034599	cellular response to oxidative stress	116	7	1.65	0.00111
Downregulated in coexistence	GO:0008535	respiratory chain complex IV assembly	16	3	0.23	0.00134
Downregulated in coexistence	GO:0033617	mitochondrial cytochrome c oxidase assem...	16	3	0.23	0.00134
Downregulated in digestion	GO:1901566	organonitrogen compound biosynthetic pro...	805	258	149.47	8.90E-27
Downregulated in digestion	GO:0006412	translation	348	144	64.62	7.10E-26
Downregulated in digestion	GO:0043043	peptide biosynthetic process	358	144	66.47	2.40E-24
Downregulated in digestion	GO:0032543	mitochondrial translation	91	60	16.9	8.50E-24
Downregulated in digestion	GO:0140053	mitochondrial gene expression	106	65	19.68	4.20E-23
Downregulated in digestion	GO:0043604	amide biosynthetic process	421	157	78.17	1.70E-22
Downregulated in digestion	GO:0006518	peptide metabolic process	387	148	71.86	2.10E-22
Downregulated in digestion	GO:0043603	cellular amide metabolic process	485	171	90.06	1.70E-21
Downregulated in digestion	GO:1990542	mitochondrial transmembrane transport	82	53	15.23	1.60E-20
Downregulated in digestion	GO:0006839	mitochondrial transport	107	61	19.87	2.00E-19
Downregulated in digestion	GO:0007005	mitochondrion organization	211	92	39.18	3.40E-18
Downregulated in digestion	GO:0006119	oxidative phosphorylation	31	27	5.76	1.70E-16
Downregulated in digestion	GO:0070585	protein localization to mitochondrion	56	36	10.4	3.80E-14

Downregulated in digestion	GO:00 72655	establishment of protein lo calization to...	56	36	10.4	3.80 E-14
Downregulated in digestion	GO:00 09060	aerobic respiration	67	40	12.44	5.20 E-14
Downregulated in digestion	GO:00 06626	protein targeting to mitoch ondrion	54	35	10.03	6.00 E-14
Downregulated in digestion	GO:00 02181	cytoplasmic translation	194	78	36.02	3.60 E-13
Downregulated in digestion	GO:00 07006	mitochondrial membrane o rganization	49	32	9.1	5.50 E-13
Downregulated in digestion	GO:00 09161	ribonucleoside monophos phate metabolic p...	72	40	13.37	1.40 E-12
Downregulated in digestion	GO:00 19646	aerobic electron transport chain	21	19	3.9	1.50 E-12

Table 3.5 GO enrichment of additive/synergistic genes in holobiont digestion

DEG type	GO.ID	Term	Annotated	isDEG	Expected	P value
Fungus additive/synergistic upregulated	**GO:19 03047**	**mitotic cell cycle proc ess**	**419**	**44**	**12.43**	**1.70 E-15**
Fungus additive/synergistic upregulated	GO:00 00278	mitotic cell cycle	435	44	12.9	7.20 E-15
Fungus additive/synergistic upregulated	GO:01 40014	mitotic nuclear division	196	29	5.81	7.80 E-14
Fungus additive/synergistic upregulated	GO:00 00070	mitotic sister chromatid segregation	165	25	4.89	3.40 E-12
Fungus additive/synergistic upregulated	**GO:00 22402**	**cell cycle process**	**573**	**46**	**17**	**8.90 E-12**
Fungus additive/synergistic upregulated	GO:00 00819	sister chromatid segreg ation	177	25	5.25	1.70 E-11

Fungus additive/synergistic upregulated	GO:00 07076	mitotic chromosome co ndensation	20	10	0.59	4.90 E-11
Fungus additive/synergistic upregulated	**GO:00 07049**	**cell cycle**	**611**	**46**	**2**	**18.1 9.10 E-11**
Fungus additive/synergistic upregulated	GO:00 30261	chromosome condensa tion	21	10	0.62	9.20 E-11
Fungus additive/synergistic upregulated	GO:00 51307	meiotic chromosome se paration	16	9	0.47	1.20 E-10
Fungus additive/synergistic upregulated	GO:00 98813	nuclear chromosome s egregation	195	25	5.78	1.50 E-10
Fungus additive/synergistic upregulated	GO:00 00280	nuclear division	263	29	7.8	1.60 E-10
Fungus additive/synergistic upregulated	GO:00 00281	mitotic cytokinesis	113	19	3.35	3.10 E-10
Fungus additive/synergistic upregulated	GO:00 48285	organelle fission	271	29	8.04	3.30 E-10
Fungus additive/synergistic upregulated	GO:00 61640	cytoskeleton-dependent cytokinesis	114	19	3.38	3.70 E-10
Fungus additive/synergistic upregulated	GO:00 07059	chromosome segregati on	208	25	6.17	6.20 E-10
Fungus additive/synergistic upregulated	GO:00 00910	cytokinesis	119	19	3.53	7.90 E-10
Fungus additive/synergistic upregulated	GO:19 02412	regulation of mitotic cyt okinesis	41	12	1.22	9.50 E-10

Fungus additive/synergistic upregulated	GO:00 90529	cell septum assembly	43	12	1.28	1.70 E-09
Fungus additive/synergistic upregulated	GO:19 02410	mitotic cytokinetic proc ess	74	15	2.2	1.90 E-09
Fungus additive/synergistic downregulated	GO:00 09119	ribonucleoside metaboli c process	32	8	1.2	1.50 E-05
Fungus additive/synergistic downregulated	GO:19 01657	glycosyl compound met abolic process	43	9	1.61	2.10 E-05
Fungus additive/synergistic downregulated	GO:00 09116	nucleoside metabolic pr ocess	37	8	1.38	4.70 E-05
Fungus additive/synergistic downregulated	GO:00 46128	purine ribonucleoside metabolic process	15	5	0.56	0.00 015
Fungus additive/synergistic downregulated	GO:19 01659	glycosyl compound bio synthetic process	25	6	0.93	0.00 024
Fungus additive/synergistic downregulated	GO:00 42278	purine nucleoside meta bolic process	18	5	0.67	0.00 039
Fungus additive/synergistic downregulated	GO:00 42455	ribonucleoside biosynth etic process	20	5	0.75	0.00 067
Fungus additive/synergistic downregulated	GO:00 09163	nucleoside biosynthetic process	21	5	0.78	0.00 085
Fungus additive/synergistic downregulated	GO:00 08033	tRNA processing	101	11	3.77	0.00 117
Fungus additive/synergistic downregulated	GO:00 06399	tRNA metabolic proces s	161	14	6.02	0.00 237

Fungus additive/synergistic downregulated	GO:0044272	sulfur compound biosynthetic process	71	8	2.65	0.00449
Fungus additive/synergistic downregulated	GO:0044283	small molecule biosynthetic process	316	21	11.81	0.00593
Fungus additive/synergistic downregulated	GO:0006085	acetyl-CoA biosynthetic process	11	3	0.41	0.00675
Fungus additive/synergistic downregulated	GO:0006400	tRNA modification	76	8	2.84	0.0068
Fungus additive/synergistic downregulated	GO:0034470	ncRNA processing	322	21	12.03	0.00735
Fungus additive/synergistic downregulated	GO:0035384	thioester biosynthetic process	12	3	0.45	0.00876
Fungus additive/synergistic downregulated	GO:0071616	acyl-CoA biosynthetic process	12	3	0.45	0.00876
Fungus additive/synergistic downregulated	GO:0009086	methionine biosynthetic process	23	4	0.86	0.00949
Fungus additive/synergistic downregulated	GO:0055086	nucleobase-containing small molecule met...	214	15	8	0.01252
Fungus additive/synergistic downregulated	GO:0006555	methionine metabolic process	25	4	0.93	0.01279
Plant additive/synergistic upregulated	GO:0032544	plastid translation	10	3	0.11	0.00016
Plant additive/synergistic upregulated	GO:0090332	stomatal closure	25	3	0.28	0.0027

Plant additive/synergistic upregulated	GO:0010102	lateral root morphogenesis	55	4	0.62	0.00338
Plant additive/synergistic upregulated	GO:0010101	post-embryonic root morphogenesis	56	4	0.63	0.00361
Plant additive/synergistic upregulated	GO:0045727	positive regulation of translation	28	3	0.32	0.00375
Plant additive/synergistic upregulated	GO:0034250	positive regulation of cellular amide me...	29	3	0.33	0.00415
Plant additive/synergistic upregulated	GO:0034219	carbohydrate transmembrane transport	61	4	0.69	0.00492
Plant additive/synergistic upregulated	GO:0010118	stomatal movement	100	5	1.13	0.00541
Plant additive/synergistic upregulated	GO:0008645	hexose transmembrane transport	32	3	0.36	0.0055
Plant additive/synergistic upregulated	GO:0010623	programmed cell death involved in cell d...	32	3	0.36	0.0055
Plant additive/synergistic upregulated	GO:0046323	glucose import	32	3	0.36	0.0055
Plant additive/synergistic upregulated	GO:1904659	glucose transmembrane transport	32	3	0.36	0.0055
Plant additive/synergistic upregulated	GO:0008643	carbohydrate transport	64	4	0.72	0.00584
Plant additive/synergistic upregulated	GO:0015749	monosaccharide transmembrane transport	33	3	0.37	0.006

Plant additive/synergistic upregulated	GO:1990069	stomatal opening	11	2	0.12	0.00653
Plant additive/synergistic upregulated	GO:0010206	photosystem II repair	13	2	0.15	0.00913
Plant additive/synergistic upregulated	GO:0030091	protein repair	14	2	0.16	0.01057
Plant additive/synergistic upregulated	GO:0006767	water-soluble vitamin metabolic process	41	3	0.46	0.01099
Plant additive/synergistic upregulated	GO:0006417	regulation of translation	119	5	1.35	0.0111
Plant additive/synergistic upregulated	GO:0034248	regulation of cellular amide metabolic p...	122	5	1.38	0.01227
Plant additive/synergistic downregulated	**GO:0007049**	**cell cycle**	**436**	**55**	**19.07**	**4.60E-13**
Plant additive/synergistic downregulated	**GO:0022402**	**cell cycle process**	**338**	**45**	**14.78**	**1.20E-11**
Plant additive/synergistic downregulated	GO:0032502	developmental process	2392	157	104.61	1.50E-09
Plant additive/synergistic downregulated	GO:0006260	DNA replication	126	23	5.51	4.10E-09
Plant additive/synergistic downregulated	GO:0007275	multicellular organism development	1915	131	83.75	6.90E-09
Plant additive/synergistic downregulated	GO:0048856	anatomical structure development	2240	146	97.97	1.50E-08

Plant additive/synergistic downregulated	GO:0006261	DNA-templated DNA replication	100	19	4.37 E-08	4.80
Plant additive/synergistic downregulated	GO:0032501	multicellular organismal process	2119	13 8	92.6 7 E-08	5.60
Plant additive/synergistic downregulated	GO:0019438	aromatic compound biosynthetic process	1696	11 6	74.1 7 E-08	8.70
Plant additive/synergistic downregulated	GO:0010374	stomatal complex development	41	12	1.79 E-07	1.00
Plant additive/synergistic downregulated	GO:0009059	macromolecule biosynthetic process	1961	12 9	85.7 6 E-07	1.10
Plant additive/synergistic downregulated	GO:0000278	mitotic cell cycle	238	30	10.4 1 E-07	1.40
Plant additive/synergistic downregulated	GO:0006355	regulation of DNA-templated transcriptio...	1221	90	53.4 E-07	1.60
Plant additive/synergistic downregulated	**GO:1903047**	**mitotic cell cycle process**	**189**	**26**	**8.27 E-07**	**1.70**
Plant additive/synergistic downregulated	GO:0010564	regulation of cell cycle process	120	20	5.25 E-07	2.10
Plant additive/synergistic downregulated	GO:1901362	organic cyclic compound biosynthetic pro...	1785	11 9	78.0 7 E-07	2.30
Plant additive/synergistic downregulated	GO:0032774	RNA biosynthetic process	1313	94	57.4 2 E-07	3.10
Plant additive/synergistic downregulated	GO:0007017	microtubule-based process	146	22	6.39 E-07	3.20

Plant additive/synergistic downregulated	GO:19 03506	regulation of nucleic aci d-templated tra...	1242	90	54.3 2	3.60 E-07
Plant additive/synergistic downregulated	GO:20 01141	regulation of RNA biosy nthetic process	1242	90	54.3 2	3.60 E-07

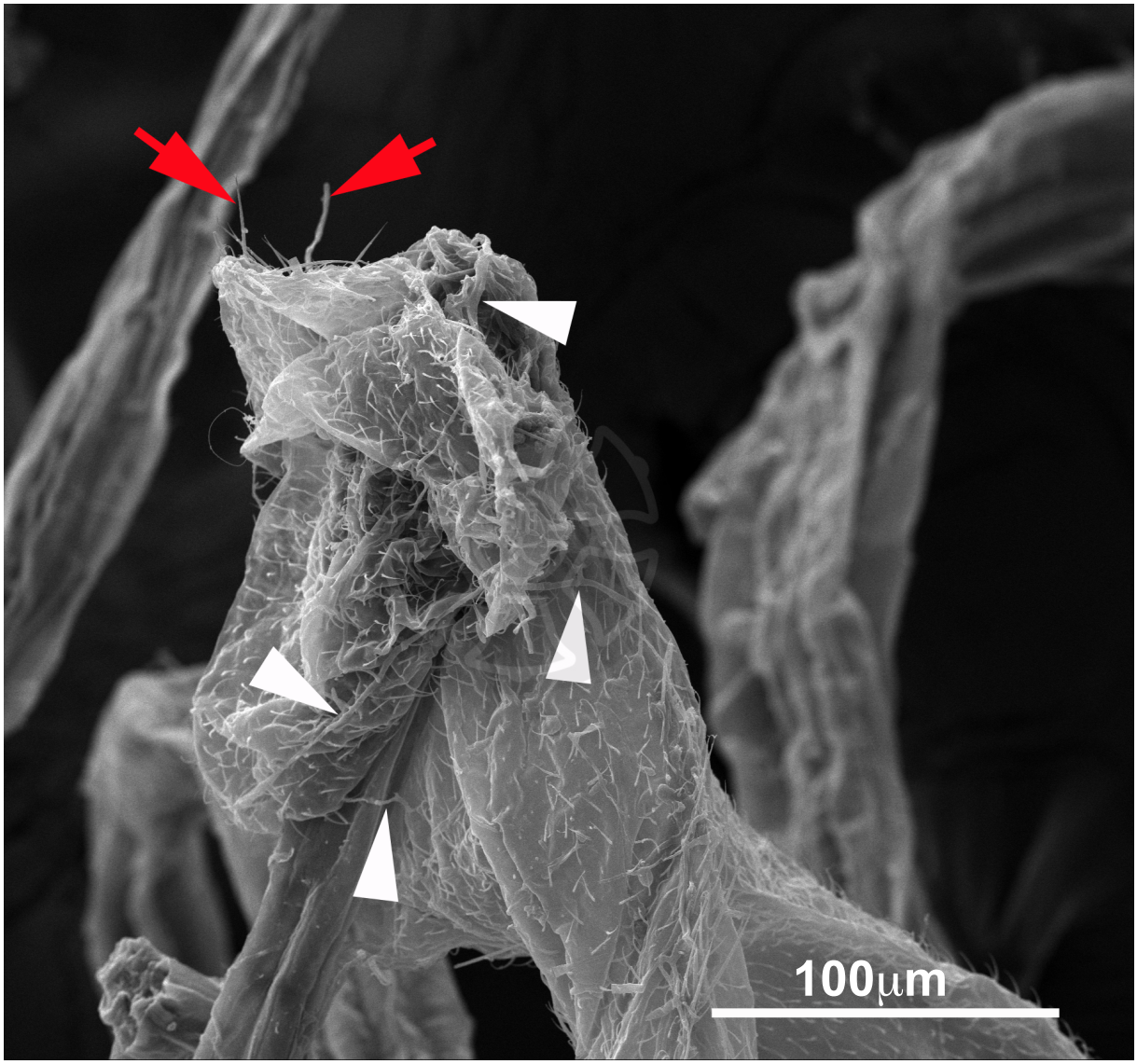

Fig. 3.17 – Fungal growth on remains of dead arthropod (covered by evenly spread hairs) on wild *Drosera spatulata*. Fungal growth on remains of dead arthropod (covered by evenly spread hairs) on wild *Drosera spatulata*. Fungal hyphae indicated by white arrowheads, two conidiophores of *Acrodontium crateriforme* by red arrows.

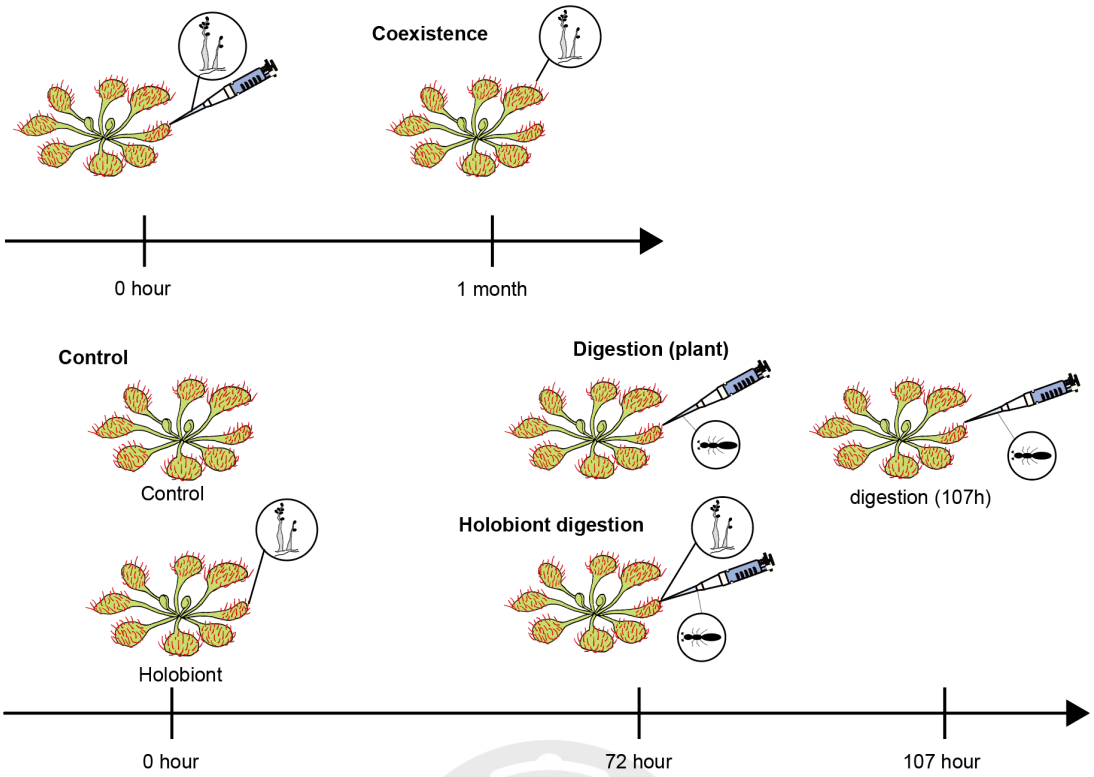

Fig. 3.18. Schematic diagram of different treatment in experiment for RNAseq. Coexistence samples mean *Acrodontium crateriforme* was inoculated on *Drosera spatulata* for one month. Digestion samples show ant powder add on *Drosera spatulata* for 3 days. Coexistence digestion samples show ant powder add on inoculated *Drosera spatulata* for 3 days. To make sure the impact of RNA expression in late stage, we add ant powder add on *Drosera spatulata* for 107 hours.

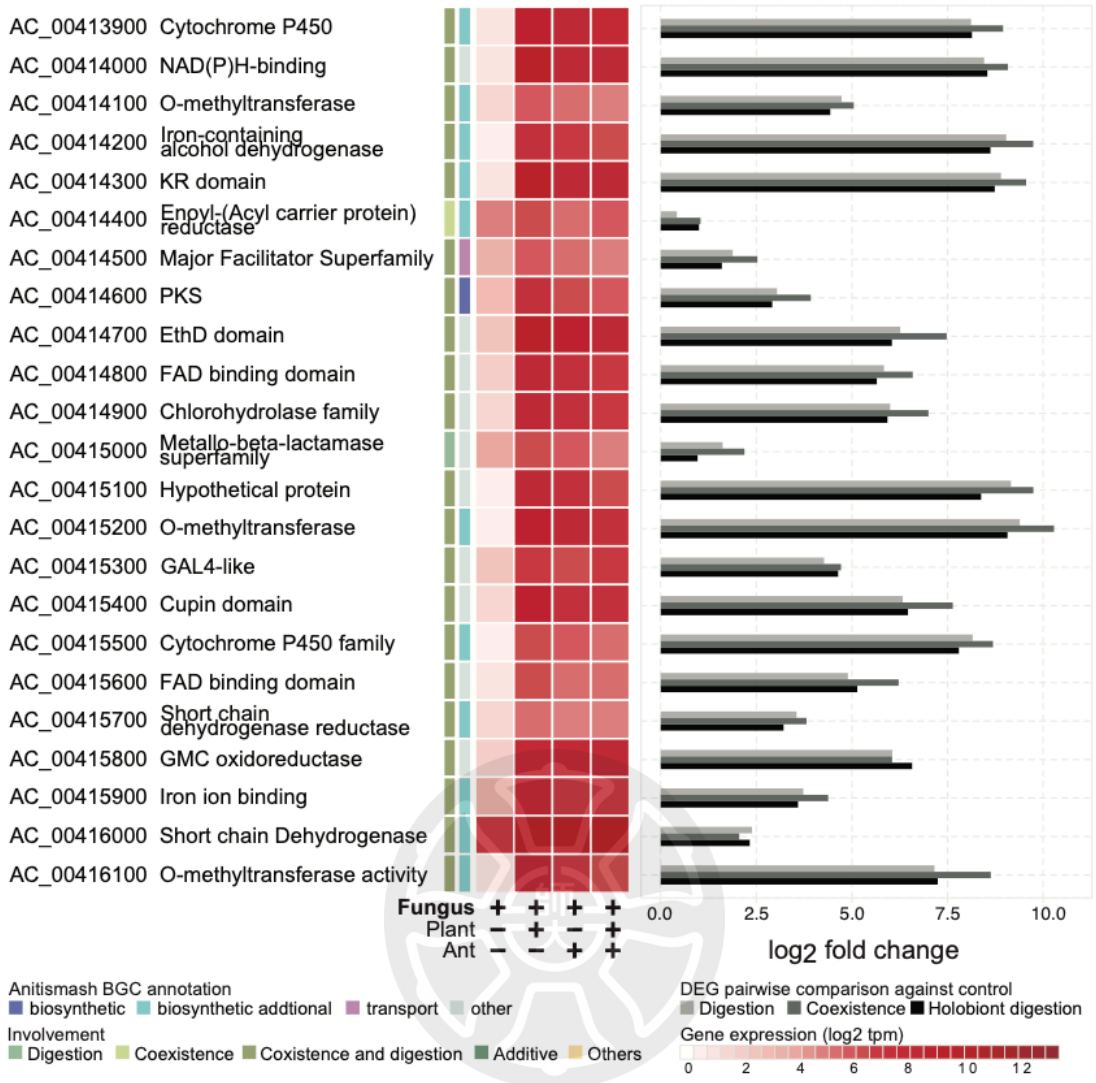

Fig. 3.19. Upregulation of a BGC on chromosome six in *A. crateriforme*.

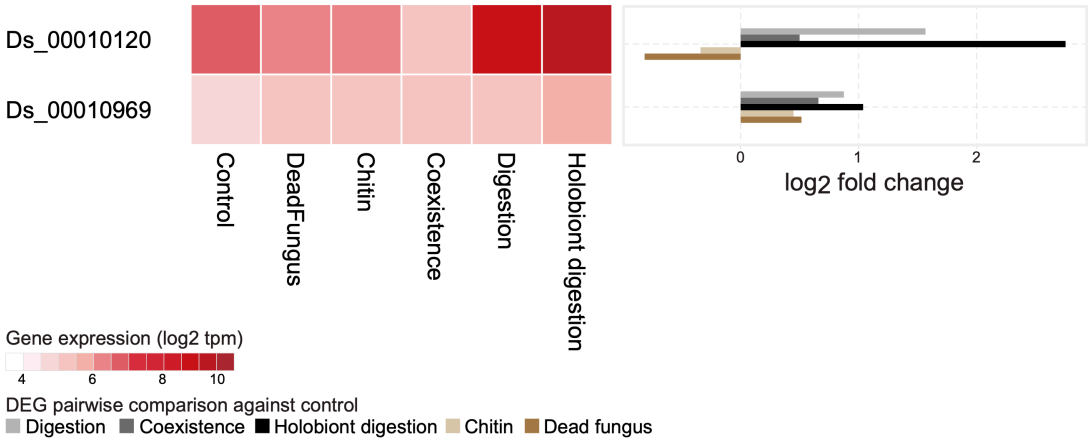

Fig. 3.20. Expression of asparagine synthetase in different treatment

3.3.5 Synergistic expression in fungal peptidases and transporters

Insect digestion in carnivorous plants is a well-coordinated process, involving first the synthesis and secretion of digestive enzymes to break down nutrients, followed by the assimilation of nutrients with specialised transporters[148,151]. To investigate the role of digestion in these gene families, additional transcriptome sequencing was performed in *D. spatulata* towards the end of the digestion process (**Fig. 3.18**). Weighted correlation network analysis (WGCNA)[152] was used to determine the regulation of peptidases during the different digestion or co-existence phases. We identified five and nine co-expression modules in *A. crateriforme* and *D. spatulata*, respectively (**Fig. 3.21 and 3.22**). The most dominant secreted peptidases in *D. spatulata* belonged to the cysteine (MEROPS[115]: C1) and aspartic families (MEROPS: A1). Droserasin, which has been implicated in digestion[34,128], was contained in two co-expression modules (**Fig. 3.22**). The two modules differed in that one module included genes that were constitutively up-regulated across conditions, whereas the other module contained genes that were only up-regulated during digestion on its own. In contrast, most of the highly expressed peptidases in *A. crateriforme* belonged to a co-expression module harbouring two copies of aspartic peptidase (AC_00151800 and AC_00417900), the entire sedolisin[153] family (14/14 copies; MEROPS: S53) associated with increasing acidity and plant-associated lifestyle[154], and a fungal copy with the aforementioned Neprosin domain (**Fig. 3.23**). These genes demonstrated a synergistic effect in expression in prey digestion during co-existence, for instance, the aspartic peptidases emerged as the dominant and third dominant entities across the entire transcriptome, with their expression levels increasing up to six-fold compared to either condition (**Fig. 3.13e**). The same trend was also observed in potassium, amino acid, oligopeptide and sugar transporters (**Fig. 3.23**). Taken together, the results suggest a potential role for *A. crateriforme*'s in facilitating and benefiting from digestion in response to the combined signal of host and nutrient.

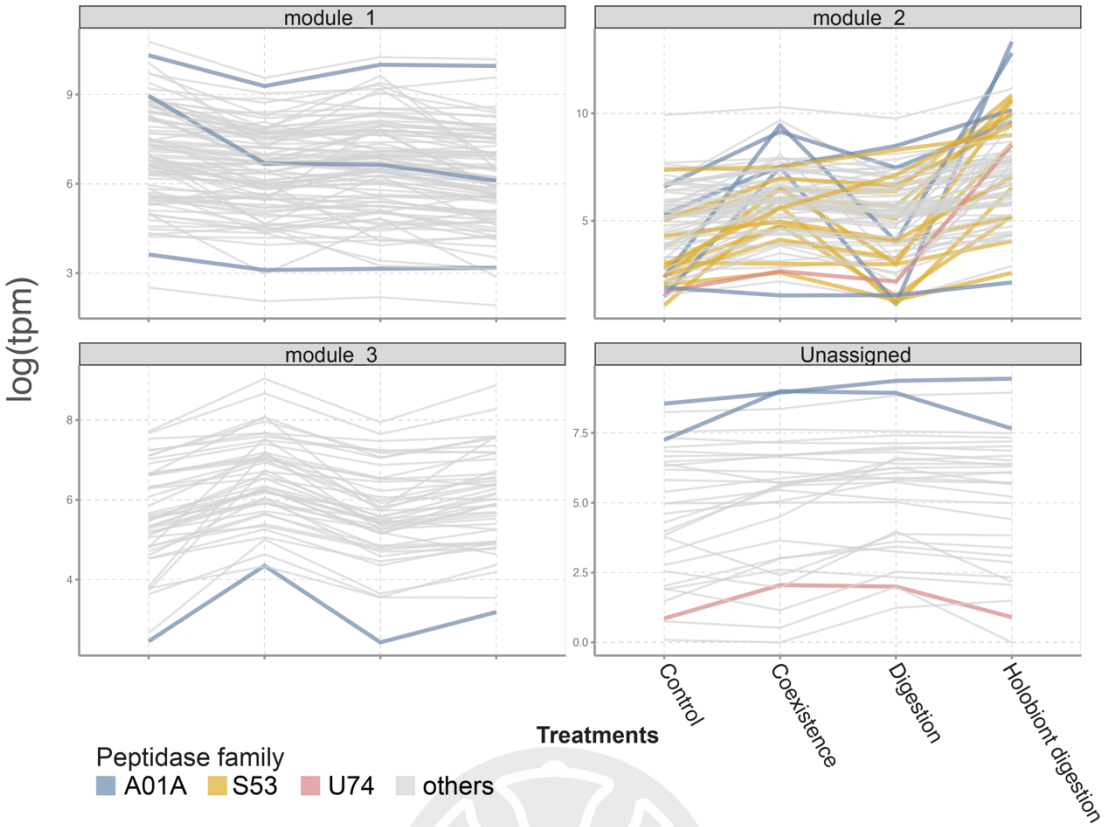

Fig. 3.21 Co-expression gene modules in *A. crateriforme* across digestion and coexistence conditions using the weighted correlation network analysis (WGCNA)

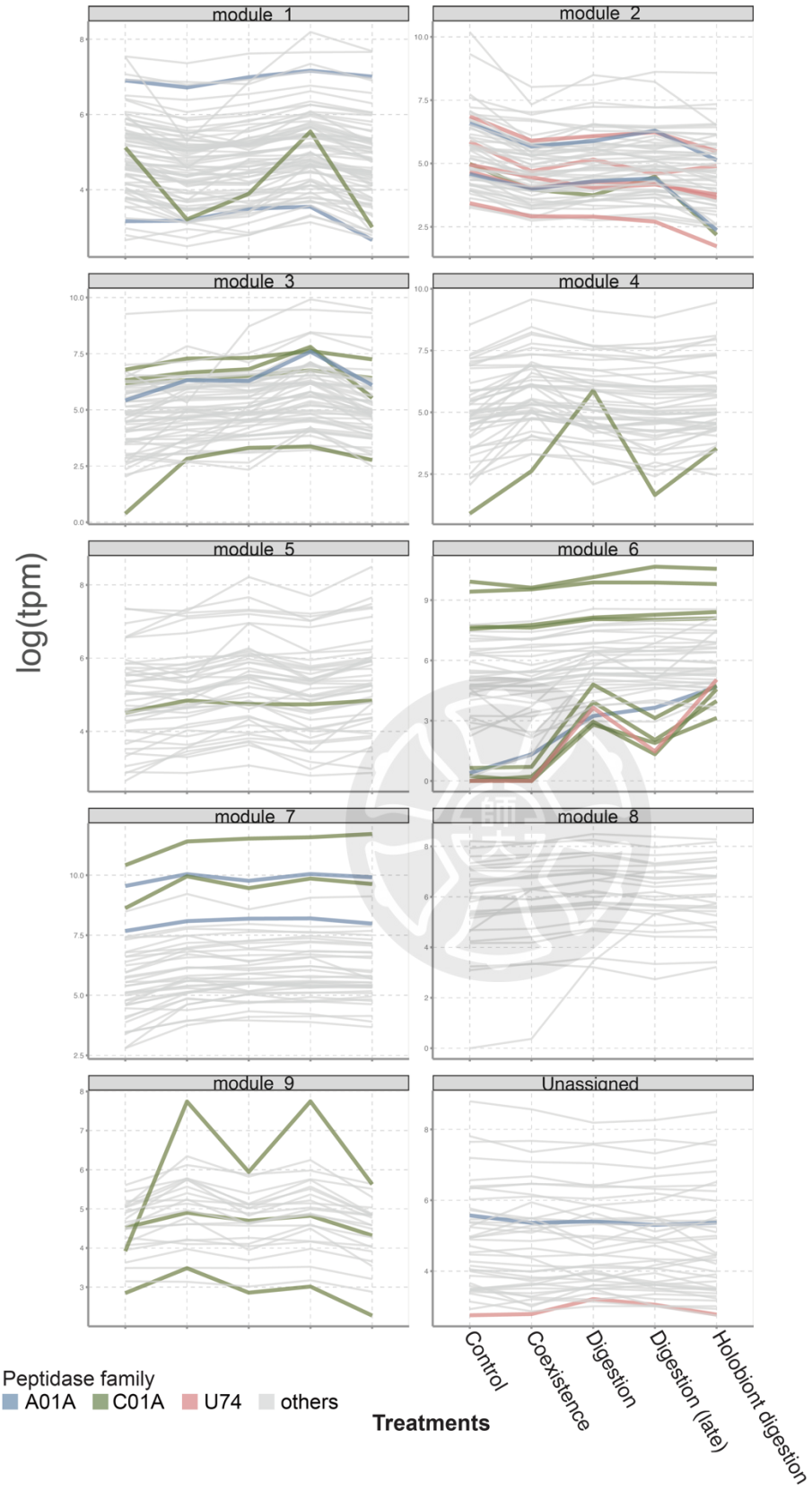

Fig. 3.22. Co-expression gene modules in *D. spatulata* across digestion and coexistence conditions using the weighted correlation network analysis (WGCNA)

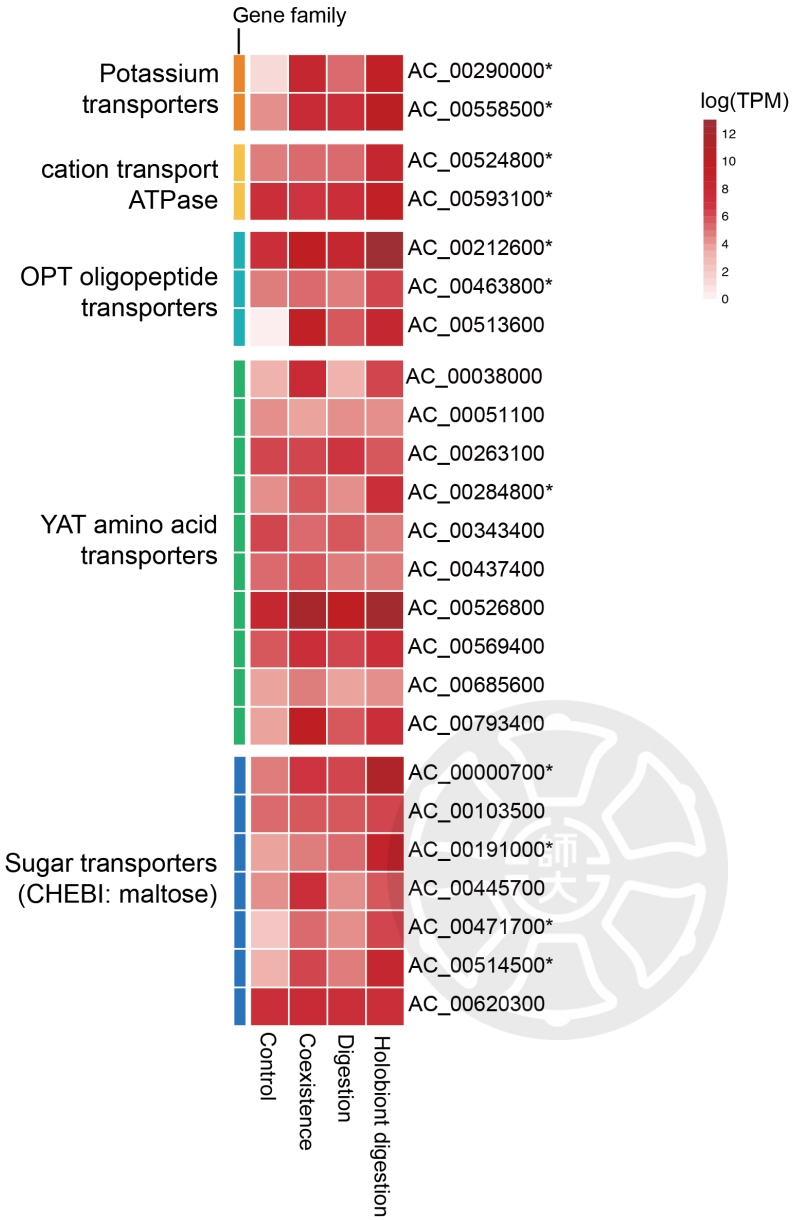

Fig. 3.23 Expression of fungal transporters in different treatments. Star denote significant upregulation in the holobiont digestion phase compared to either digestion or coexistence process.

3.3.6 Sundew priming via jasmonate (JA) signaling pathway

How carnivorous plants respond specifically to either symbiotic microbes or prey can be challenging, as the phytohormones are accumulate to elicit pathogen resistance in plants that induce genes that were also involved in digestion to prey stimuli[34,83]. We quantified the changes in *D. spatulata* phytohormone levels after treatment with insects or different fungi. Application of both ant powder and different fungi to the leaves significantly increased the amount of Jasmonoyl-L-isoleucine (JA-Ile), a bioactive molecule of JA, after two hours (**Fig. 3.24 & 3.25**) indicative of a potential priming effect. When plants inoculated with *A. crateriforme* were supplemented with ant powder, we found that JA levels displayed an increasing trend. This result has been correlated with the activation of JA-related priming in plants[155,156]. In contrast, no differences in salicylic acid were observed between control and treatments (**Fig. 3.26**). The observed acceleration in trap re-opening when plants were inoculated with microbes (**Fig. 3.2a**) further emphasises the role of *A. crateriforme*-induced JA biosynthesis and signaling in enhancing prey digestion.

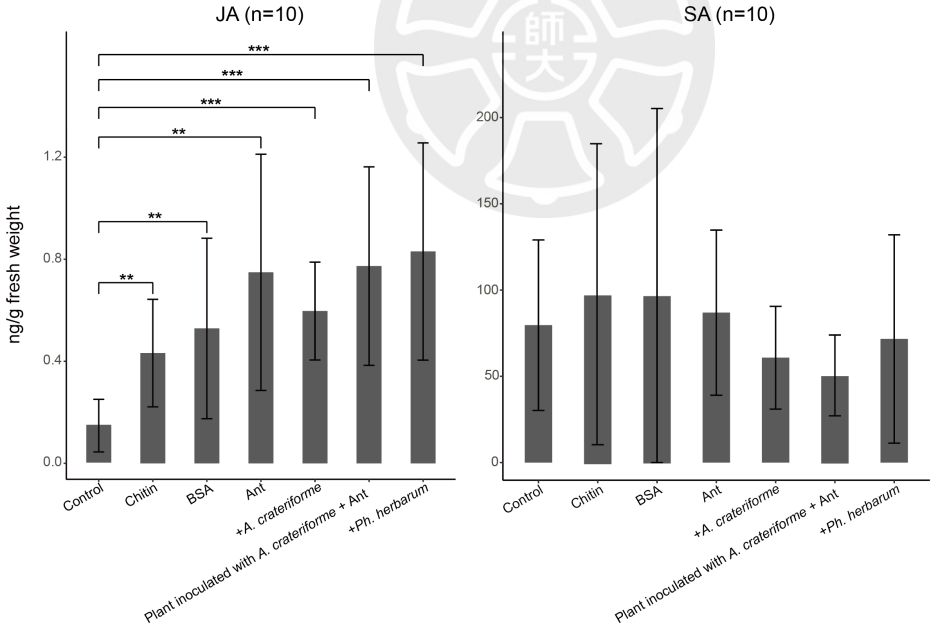

Fig. 3.24 Quantification of jasmonic acid (JA) and salicyclic acid (SA) levels in *D. spatulata* following treatments with added chitin, BSA protein, ant insect prey, and inoculated with *A crateriforme* or the pathogenic *Ph. herbarum*. (Wilcoxon rank sum test; * P<0.05. ** P<0.01, *** P<0.001).

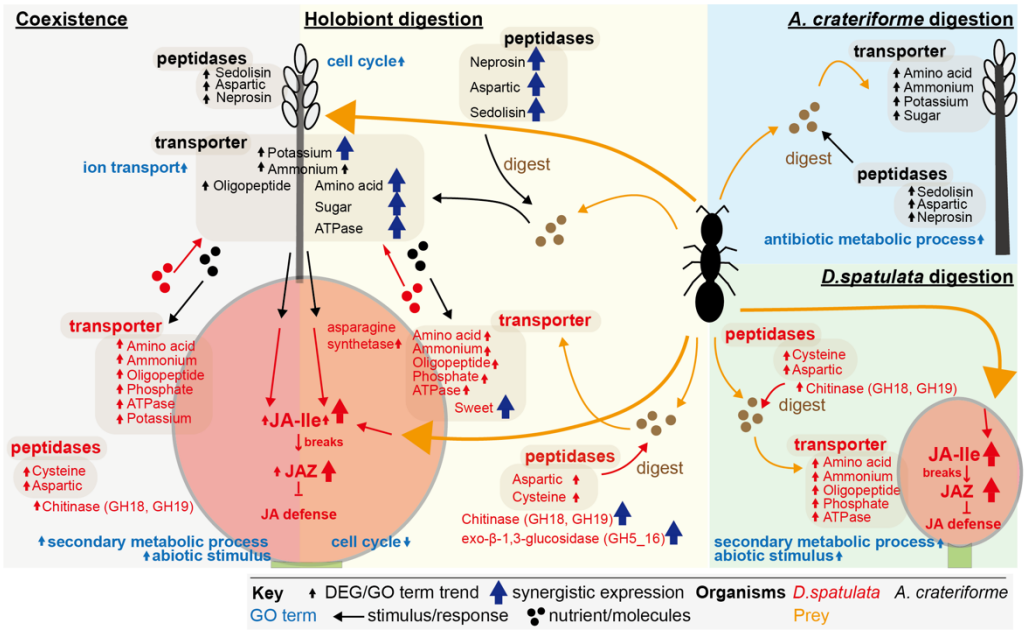

Figure 3.25 Phytohormone responses and the *D. spatulata-A. crateriforme* holobiont. a. Accumulation of Jasmonoyl-L-isoleucine (JA-Ile) levels in *D. spatulata* following various treatments. (Wilcoxon rank sum test; * P<0.05. ** P<0.01, *** P<0.001) **b.** Expression of genes involved in the JA signalling pathway during different phases. Asterisk indicate genes that exhibited highest expression in the digestion phase. **c.** Schematic representation of the holobiont response to each other and during digestion. A summary of gene expression changes in this study are shown. Genes that are co-expressed in different phases are shown multiple times.

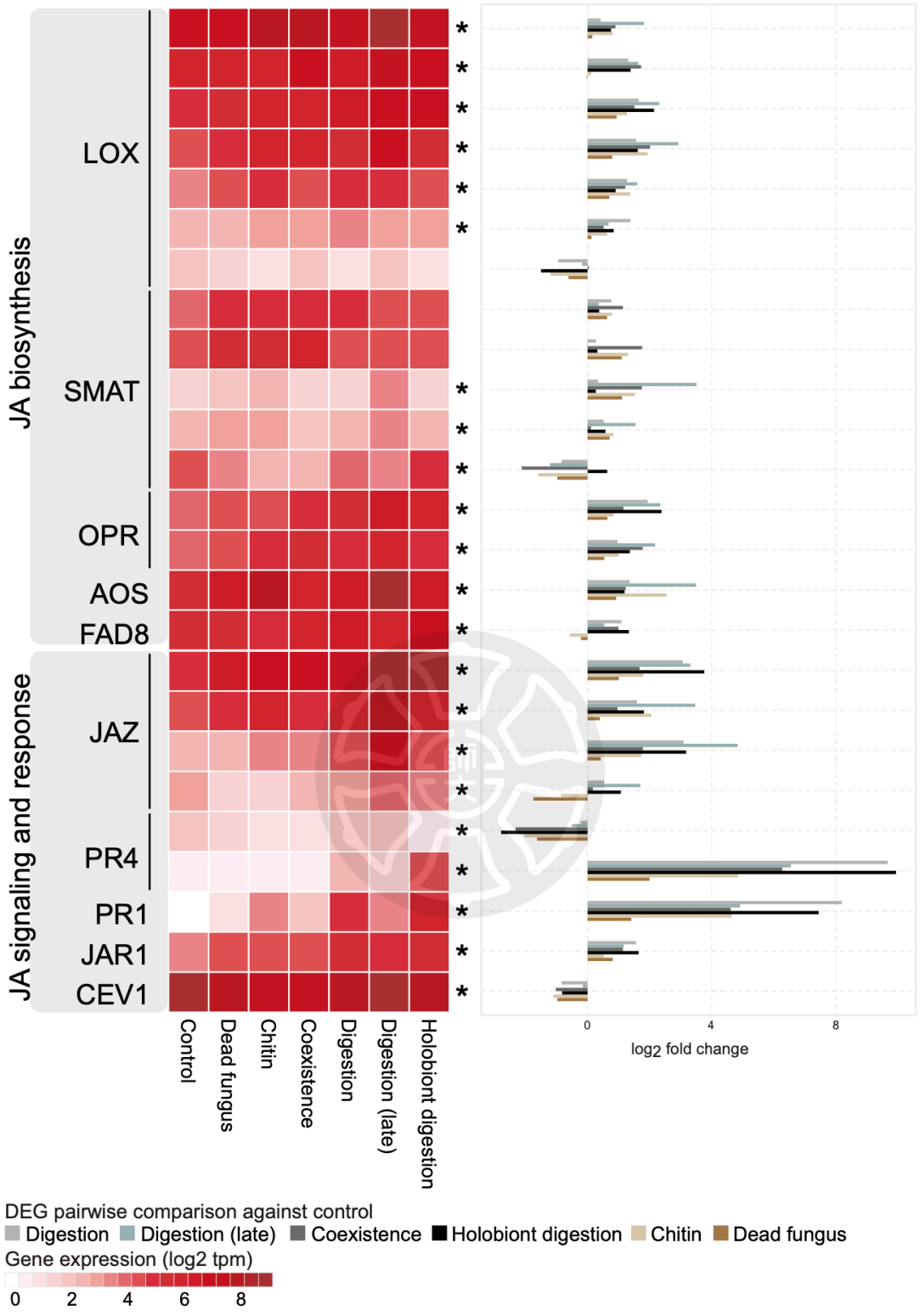

Fig. 3.26 Expression of genes involved in the JA signalling pathway during different phases. Asterisk denote genes that exhibited highest expression in either early or late digestion phase

3.4. Discussion

In this chapter, we elucidate a definitive symbiotic interaction between the carnivorous sundew *Drosera spatulata* and the acidophilic fungus *A. crateriforme*. Our results show that the digestion time of insects was reduced by almost 25% in the presence of the fungus. This cooperation is likely founded on the shared adaptive challenges that both carnivorous plants and extremophilic fungi encounter in harsh environments characterized by minimal nutrients. Besides, this study defines the symbiotic interaction between the carnivorous sundew *Drosera spatulata* and the acidophilic fungus *A. crateriforme* (**Fig. 3.25**), reshaping our view of botanical carnivory since Darwin's foundational work[157]

Upon colonizing *D. spatulata* stalk glands, *A. crateriforme* underwent a series of genomic alterations to adapt to the symbiotic lifestyle, may enhance prey capture by reducing digestion time. This implies that the coexistence is cooperative and may be mutualistic, as the level of prey capture is positively associated with plant fitness. This may be more correlated with carnivorous plants being considered sit-and-wait predators. Considering low nutrient uptake efficiency in carnivorous plants, such as nitrogen uptake levels ranging from 29% to 42%, it is plausible that *A. crateriforme* can utilize the unspent prey nutrients with other microbial members. As fungi serve as intermediaries between hosts and ecosystems, it remains to be determined whether *A. crateriforme* will exhibit a context-dependent trophic level throughout its life cycle within *D. spatulata* and other carnivorous plants. Interactions between species will be a crucial aspect of future cost-benefit models to explain how carnivorous plants survive in their harsh habitats.

The concept that plant carnivory genes evolved from defence mechanisms is generally accepted. The presence of symbiotic *A. crateriforme* and the transcriptomic landscape involving either single or dual species during the digestion phase provided us to delineate the relative contribution of fungus and plant as well as the role of each gene. In *D. spatulata*, the prevalence of co-opted genes seemed notably higher, with many maintaining consistent expression patterns throughout both the digestion and coexistence phases. This suggests that *D. spatulata* employs the same set of genes to mediate defence in response to biotic stimuli from microorganisms and prioritizes over digestion in the presence of prey which may be regulated by JA pathways. From a microbe’s perspective, the proteome of *A. crateriforme* also exhibitsgene co-

option and synergistic expression implying that the fungus has co-evolved with the sundew host to actively facilitate both processes in the shared environment[87]. For example, fungal sedolisins have been associated with increasing acidity and a plant-associated lifestyle[154]. The collective peptidases of both species can be utilized to degrade large peptides on acidic mucilage to generate nutrients in decomposing insect prey, potentially increasing overall digested nutrient levels.

In summary, the evolution of plant carnivory genes is believed to have originated from defence mechanisms, with a focus on the involvement of symbiotic *A. crateriforme* during the digestion phase. Transcriptomic analysis of *D. spatulata* unveiled a significant contribution of co-opted genes, especially in maintaining consistent expression patterns during both digestion and co-existence phases. This suggests that *D. spatulata* utilizes a common set of genes for defense against biotic stimuli and prioritizes this response over digestion in the presence of prey, potentially regulated by JA pathways. Moreover, the study highlights the extensive co-option of genes in the proteome of *A. crateriforme*, indicative of a co-evolutionary relationship with the sundew host. The co-expression of genes in both species, such as fungal sedolisins associated with acidity, suggests active facilitation of defence and digestion processes in their shared environment. Notably, the collaborative action of peptidases from both species is implicated in the degradation of peptides on acidic mucilage, thereby enhancing nutrient levels derived from decomposing insect prey. Overall, these findings underscore the intricate interplay and mutual adaptations between the sundew plant and its symbiotic fungus in the carnivorous lifestyle.

Chapter4

Conclusion

This study comprises two objectives: to characterize the diversity and composition of the *D. spatulata* mucilage microbiota and to investigate the host sundew-fungus interaction.

In characterizing the diversity of the *D. spatulata* mucilage microbiota, we have isolated a keystone fungus: *A. crateriforme*. In temporal experiment, we found that the dominant fungal species *A. crateriforme* is consistently present in *D. spatulata* mucilage. Spatial results suggest that *A. crateriforme* was identified as the most dominant fungal species not only in *D. spatulata* mucilage in Taiwan, but also in other *Drosera* species from the UK and USA. We also found that the mycelium of *A. crateriforme* was covered on *D. spatulata.* This suggests that *A. crateriforme* is able to interact with its host plant. In the past, *A. crateriforme* was previously considered to be ubiquitous across environments. In this study, it is now recognised as part of the sundew-fungus holobiont, with its presence and frequent dominance in several *Drosera* species worldwide. The dominance of this fungus in the *Drosera* microbiome, that was not observed in most other carnivorous plants. The reason may be related to the relative osmotic stress caused by the exposed mucilage, as opposed to the greater liquid medium contained in the traps of pitcher plants.

The study reveals a definitive symbiotic interaction between the carnivorous sundew and the acidophilic fungus. We provide the first direct evidence that *A. crateriforme* is essential for prey digestion in carnivorous sundews. *A. crateriforme* reduces the digestion time of insects, and enhances the digestion of *D. spatulata.* These results may lead to the digestion of more nutrients for both the fungus and the host plant, as evidenced by the upregulation of sundew's gene families involved in nitrogen assimilation, and transporters that were only up-regulated with *A. crateriforme* during prey digestion. Our study implies that the plant-fungal coexistence is cooperative. Prey capture rates are positively associated with plant fitness[158] and may be especially related with *Drosera* species, which are considered sit-and-wait predators.

In transcriptomic analysis reveals that the high extent of genes maintained similar expression in both digestion and co-existence phases in *D. spatulata*. This suggested that the sundew utilizes the shared gene pool for these

processes. Many plants will enter a priming phase and are known to enhance the ability of defend against pathogens in respond abiotic and biotic stimuli[159]. In *D. spatulata*, colonisation by *A. crateriforme* enable sundews to induce transcriptions changes before the prey is captured. This is similiar to the “posed to capture” phase described in the Venus flytrap *Dionaea muscipula*[149], or successful mycorrhization[156]. As almost half of the genes involved in digestion were already modulated in the priming phase, the actual digestion of prey required the transcription of fewer genes to be induced resulting in an overall faster digestion process.

In summary, our work provides the idea that plant-microbe interactions have been selected for during evolution to increase the overall fitness of the holobiont[87]. *Drosera-Acrodontium* is an amenable laboratory system since both can be grown separately and together in the laboratory. We hypothesised that just as plant carnivory has independently evolved with convergence in different plant groups, plant-microbial interactions capable of facilitating the process of digestion are likely to emerge in different carnivorous plants. Microbial ecosystems in other carnivorous plants can be highly complex and contain predators of microorganisms amongst inquilines[160], and we provide an initial framework for detangling these relationships.

Supplementary Table

Supplementary Table 1. Amplicon data of *D. spatulata* mucilage and surrounding plants

SampleID	Name	Date	month	Site	Collecting_Site	Habitat	Purpose	GPS_X	GPS_Y	Bacterial sample accession	Fungal sample accession
SH0275	Shuangxi2-Mucilage1	2021.07	July	Shuangxi	Shuangxi	Mucilage	Spatial distribution	121.825341	24.970089	NA	SAMN38109885
SH0276	Shuangxi2-Mucilage2	2021.07	July	Shuangxi	Shuangxi	Mucilage	Spatial distribution	121.825341	24.970089	NA	SAMN38109886
SH0277	Shuangxi2-Mucilage3	2021.07	July	Shuangxi	Shuangxi	Mucilage	Spatial distribution	121.825341	24.970089	NA	SAMN38109887
SH0278	Shuangxi3-Mucilage1	2021.07	July	Shuangxi	Shuangxi	Mucilage	Spatial distribution	121.837337	24.937508	NA	SAMN38109888
SH0279	Shuangxi3-Mucilage2	2021.07	July	Shuangxi	Shuangxi	Mucilage	Spatial distribution	121.837337	24.937508	NA	SAMN38109889
SH0280	Shuangxi3-Mucilage3	2021.07	July	Shuangxi	Shuangxi	Mucilage	Spatial distribution	121.837337	24.937508	NA	SAMN38109890

SH0263	Keelung2-Mucilage1	2021.07	July	Keelung2	Keelung	Mucilage	Spatial distribution	121.710643	25.155061	NA	SAMN38109875
SH0264	Keelung2-Mucilage2	2021.07	July	Keelung2	Keelung	Mucilage	Spatial distribution	121.710643	25.155061	NA	SAMN38109876
SH0265	Keelung2-Mucilage3	2021.07	July	Keelung2	Keelung	Mucilage	Spatial distribution	121.710643	25.155061	NA	SAMN38109877
SH0281	Yilan1-Mucilage1	2021.07	July	Yilan1	Yilan	Mucilage	Spatial distribution	121.77751	24.85931	NA	SAMN38109891
SH0282	Yilan1-Mucilage2	2021.07	July	Yilan1	Yilan	Mucilage	Spatial distribution	121.77751	24.85931	NA	SAMN38109892
SH0283	Yilan1-Mucilage3	2021.07	July	Yilan1	Yilan	Mucilage	Spatial distribution	121.77751	24.85931	NA	SAMN38109893
SH0284	Yilan2-Mucilage1	2021.07	July	Yilan2	Yilan	Mucilage	Spatial distribution	121.77647	24.84593	NA	SAMN38109894
SH0285	Yilan2-Mucilage2	2021.07	July	Yilan2	Yilan	Mucilage	Spatial distribution	121.77647	24.84593	NA	SAMN38109895

SH0286	Yilan2-Mucilage3	2021.07	July	Yilan2	Yilan	Mucilage	Spatial distribution	121.77647	24.84593	NA	SAMN38109896
SH0258	Keelung3-Mucilage1	2021.07	July	Keelung3	Keelung	Mucilage	Spatial distribution	121.709447	25.158397	NA	SAMN38109870
SH0259	Keelung3-Mucilage2	2021.07	July	Keelung3	Keelung	Mucilage	Spatial distribution	121.709447	25.158397	NA	SAMN38109871
SH0260	Keelung3-Mucilage3	2021.07	July	Keelung3	Keelung	Mucilage	Spatial distribution	121.709447	25.158397	NA	SAMN38109872
SH0255	Keelung1-Mucilage1	2021.07	July	Keelung1	Keelung	Mucilage	Spatial distribution	121.704949	25.159125	NA	SAMN38109867
SH0256	Keelung1-Mucilage2	2021.07	July	Keelung1	Keelung	Mucilage	Spatial distribution	121.704949	25.159125	NA	SAMN38109868
SH0257	Keelung1-Mucilage3	2021.07	July	Keelung1	Keelung	Mucilage	Spatial distribution	121.704949	25.159125	NA	SAMN38109869
SH0271	Houtong-Mucilage1	2021.07	July	Houtong	Houtong	Mucilage	Spatial distribution	121.827778	25.086944	NA	SAMN38109881

SH0272	Houtong-Mucilage2	2021.07	July	Houtong	Houtong	Mucilage	Spatial distribution	121.827778	25.086944	NA	SAMN38109882
SH0273	Houtong-Mucilage3	2021.07	July	Houtong	Houtong	Mucilage	Spatial distribution	121.827778	25.086944	NA	SAMN38109883
SH0274	Houtong-Mucilage4	2021.07	July	Houtong	Houtong	Mucilage	Spatial distribution	121.827778	25.086944	NA	SAMN38109884
SH0233	Nangang-Mucilage1	2021.07	July	Nangang	Nangang	Mucilage	Spatial distribution	121.639736	25.047277	NA	SAMN38109845
SH0234	Nangang-Mucilage2	2021.07	July	Nangang	Nangang	Mucilage	Spatial distribution	121.639736	25.047277	NA	SAMN38109846
SH0235	Nangang-Mucilage3	2021.07	July	Nangang	Nangang	Mucilage	Spatial distribution	121.639736	25.047277	NA	SAMN38109847
SH0236	Nangang-Mucilage4	2021.07	July	Nangang	Nangang	Mucilage	Spatial distribution	121.639736	25.047277	NA	SAMN38109848
SH0266	Buyanting-Mucilage1	2021.07	July	Buyanting	Buyanting	Mucilage	Spatial distribution	121.847242	25.090083	NA	SAMN38109878

SH0267	Buyanting-Mucilage2	2021.07	July	Buyanting	Buyanting	Mucilage	Spatial distribution	121.847242	25.090083	NA	SAMN38109879
SH0268	Buyanting-Mucilage3	2021.07	July	Buyanting	Buyanting	Mucilage	Spatial distribution	121.847242	25.090083	NA	SAMN38109880
SH0237	Pingxi1-Mucilage1	2021.07	July	Pingxi1	Pingxi	Mucilage	Spatial distribution	121.71027	25.06611	NA	SAMN38109849
SH0238	Pingxi1-Mucilage2	2021.07	July	Pingxi1	Pingxi	Mucilage	Spatial distribution	121.71027	25.06611	NA	SAMN38109850
SH0239	Pingxi1-Mucilage3	2021.07	July	Pingxi1	Pingxi	Mucilage	Spatial distribution	121.71027	25.06611	NA	SAMN38109851
SH0240	Pingxi2-Mucilage1	2021.07	July	Pingxi2	Pingxi	Mucilage	Spatial distribution	121.78554	25.061111	NA	SAMN38109852
SH0241	Pingxi2-Mucilage2	2021.07	July	Pingxi2	Pingxi	Mucilage	Spatial distribution	121.78554	25.061111	NA	SAMN38109853
SH0242	Pingxi2-Mucilage3	2021.07	July	Pingxi2	Pingxi	Mucilage	Spatial distribution	121.78554	25.061111	NA	SAMN38109854

SH0243	Pingxi3-Mucilage1	2021.07	July	Pingxi3	Pingxi	Mucilage	Spatial distribution	121.79306	25.07416	NA	SAMN38109855
SH0244	Pingxi3-Mucilage2	2021.07	July	Pingxi3	Pingxi	Mucilage	Spatial distribution	121.79306	25.07416	NA	SAMN38109856
SH0245	Pingxi3-Mucilage3	2021.07	July	Pingxi3	Pingxi	Mucilage	Spatial distribution	121.79306	25.07416	NA	SAMN38109857
SH0246	Pingxi4-Mucilage1	2021.07	July	Pingxi4	Pingxi	Mucilage	Spatial distribution	121.663487	24.992262	NA	SAMN38109858
SH0247	Pingxi4-Mucilage2	2021.07	July	Pingxi4	Pingxi	Mucilage	Spatial distribution	121.663487	24.992262	NA	SAMN38109859
SH0248	Shiding1-Mucilage1	2021.07	July	Shiding1	Shiding	Mucilage	Spatial distribution	121.614058	24.981645	NA	SAMN38109860
SH0249	Shiding1-Mucilage2	2021.07	July	Shiding1	Shiding	Mucilage	Spatial distribution	121.614058	24.981645	NA	SAMN38109861
SH0250	Shiding1-Mucilage3	2021.07	July	Shiding1	Shiding	Mucilage	Spatial distribution	121.614058	24.981645	NA	SAMN38109862

SH0251	Shiding2-Mucilage1	2021.07	July	Shiding2	Shiding	Mucilage	Spatial distribution	121.615112	24.97312	NA	SAMN38109863
SH0252	Shiding2-Mucilage2	2021.07	July	Shiding2	Shiding	Mucilage	Spatial distribution	121.615112	24.97312	NA	SAMN38109864
SH0253	Shiding2-Mucilage3	2021.07	July	Shiding2	Shiding	Mucilage	Spatial distribution	121.615112	24.97312	NA	SAMN38109865
SH0254	Shiding3-Mucilage1	2021.07	July	Shiding3	Shiding	Mucilage	Spatial distribution	121.624628	24.954655	NA	SAMN38109866
SH0261	Shiding3-Mucilage2	2021.07	July	Shiding3	Shiding	Mucilage	Spatial distribution	121.624628	24.954655	NA	SAMN38109873
SH0262	Shiding3-Mucilage3	2021.07	July	Shiding3	Shiding	Mucilage	Spatial distribution	121.624628	24.954655	NA	SAMN38109874
SH0135	Shuangxi--Mucilage1	2019.07	July	Shuangxi	Shuangxi	Mucilage	Initial survey	121.843341	25.066234	SAMN38109958	SAMN38109773
SH0136	Shuangxi-Mucilage2	2019.07	July	Shuangxi	Shuangxi	Mucilage	Initial survey	121.843341	25.066234	SAMN38109959	SAMN38109774
SH0137	Shuangxi-Mucilage3	2019.07	July	Shuangxi	Shuangxi	Mucilage	Initial survey	121.843341	25.066234	SAMN38109960	SAMN38109775

SH0138	Shuangxi-Mucilage4	2019.07	July	Shuangxi	Shuangxi	Mucilage	Initial survey	121.843341	25.066234	SAMN38109961	SAMN38109776
SH0139	Shuangxi-Mucilage5	2019.07	July	Shuangxi	Shuangxi	Mucilage	Initial survey	121.843341	25.066234	SAMN38109962	SAMN38109777
SH0140	Shuangxi-Mucilage6	2019.07	July	Shuangxi	Shuangxi	Mucilage	Initial survey	121.843341	25.066234	SAMN38109963	SAMN38109778
SH0141	Shuangxi-Mucilage7	2019.07	July	Shuangxi	Shuangxi	Mucilage	Initial survey	121.843341	25.066234	SAMN38109964	SAMN38109779
SH0142	Shuangxi-Mucilage8	2019.07	July	Shuangxi	Shuangxi	Mucilage	Initial survey	121.843341	25.066234	SAMN38109965	SAMN38109780
SH0143	Shuangxi-Mucilage9	2019.07	July	Shuangxi	Shuangxi	Mucilage	Initial survey	121.843341	25.066234	SAMN38109966	SAMN38109781
SH0144	Shuangxi-Mucilage10	2019.07	July	Shuangxi	Shuangxi	Mucilage	Initial survey	121.843341	25.066234	SAMN38109967	SAMN38109782
SH0145	Shuangxi-Moss1	2019.07	July	Shuangxi	Shuangxi	Moss	Initial survey	121.843341	25.066234	SAMN38109968	SAMN38109783
SH0146	Shuangxi-Moss2	2019.07	July	Shuangxi	Shuangxi	Moss	Initial survey	121.843341	25.066234	SAMN38109969	SAMN38109784
SH0147	Shuangxi-Moss3	2019.07	July	Shuangxi	Shuangxi	Moss	Initial survey	121.843341	25.066234	SAMN38109970	SAMN38109785
SH0148	Shuangxi-Moss4	2019.07	July	Shuangxi	Shuangxi	Moss	Initial survey	121.843341	25.066234	SAMN38109971	SAMN38109786
SH0149	Shuangxi-Moss5	2019.07	July	Shuangxi	Shuangxi	Moss	Initial survey	121.843341	25.066234	SAMN38109972	SAMN38109787

SH0150	Shuangxi-Moss6	2019.07	July	Shuangxi	Shuangxi	Moss	Initial survey	121.843341	25.066234	SAMN38109973	SAMN38109788
SH0151	Shuangxi-Plant1	2019.07	July	Shuangxi	Shuangxi	Plant	Initial survey	121.843341	25.066234	SAMN38109974	SAMN38109789
SH0152	Shuangxi-Plant2	2019.07	July	Shuangxi	Shuangxi	Plant	Initial survey	121.843341	25.066234	SAMN38109975	SAMN38109790
SH0153	Shuangxi-Plant3	2019.07	July	Shuangxi	Shuangxi	Plant	Initial survey	121.843341	25.066234	SAMN38109976	SAMN38109791
SH0154	Shuangxi-Plant4	2019.07	July	Shuangxi	Shuangxi	Plant	Initial survey	121.843341	25.066234	SAMN38109977	SAMN38109792
SH0155	Shuangxi-Plant5	2019.07	July	Shuangxi	Shuangxi	Plant	Initial survey	121.843341	25.066234	SAMN38109978	SAMN38109793
SH0156	Shuangxi-Plant6	2019.07	July	Shuangxi	Shuangxi	Plant	Initial survey	121.843341	25.066234	SAMN38109979	SAMN38109794
SH0101	Shumei-Mucilage1	2019.07	July	Shumei	Shumei	Mucilage	Initial survey	121.8609914	25.10146976	SAMN38109936	SAMN38109751
SH0102	Shumei-Mucilage2	2019.07	July	Shumei	Shumei	Mucilage	Initial survey	121.8609914	25.10146976	SAMN38109937	SAMN38109752
SH0103	Shumei-Mucilage3	2019.07	July	Shumei	Shumei	Mucilage	Initial survey	121.8609914	25.10146976	SAMN38109938	SAMN38109753
SH0104	Shumei-Mucilage4	2019.07	July	Shumei	Shumei	Mucilage	Initial survey	121.8609914	25.10146976	SAMN38109939	SAMN38109754
SH0105	Shumei-Mucilage5	2019.07	July	Shumei	Shumei	Mucilage	Initial survey	121.8609914	25.10146976	SAMN38109940	SAMN38109755

SH0106	Shumei-Mucilage6	2019.07	July	Shumei	Shumei	Mucilage	Initial survey	121.8609914	25.10146976	SAMN38109941	SAMN38109756
SH0107	Shumei-Mucilage7	2019.07	July	Shumei	Shumei	Mucilage	Initial survey	121.8609914	25.10146976	SAMN38109942	SAMN38109757
SH0108	Shumei-Mucilage8	2019.07	July	Shumei	Shumei	Mucilage	Initial survey	121.8609914	25.10146976	SAMN38109943	SAMN38109758
SH0109	Shumei-Mucilage9	2019.07	July	Shumei	Shumei	Mucilage	Initial survey	121.8609914	25.10146976	SAMN38109944	SAMN38109759
SH0110	Shumei-Mucilage10	2019.07	July	Shumei	Shumei	Mucilage	Initial survey	121.8609914	25.10146976	SAMN38109945	SAMN38109760
SH0111	Shumei-Moss1	2019.07	July	Shumei	Shumei	Moss	Initial survey	121.8609914	25.10146976	SAMN38109946	SAMN38109761
SH0112	Shumei-Moss2	2019.07	July	Shumei	Shumei	Moss	Initial survey	121.8609914	25.10146976	SAMN38109947	SAMN38109762
SH0113	Shumei-Moss3	2019.07	July	Shumei	Shumei	Moss	Initial survey	121.8609914	25.10146976	SAMN38109948	SAMN38109763
SH0114	Shumei-Moss4	2019.07	July	Shumei	Shumei	Moss	Initial survey	121.8609914	25.10146976	SAMN38109949	SAMN38109764
SH0115	Shumei-Moss5	2019.07	July	Shumei	Shumei	Moss	Initial survey	121.8609914	25.10146976	SAMN38109950	SAMN38109765
SH0116	Shumei-Moss6	2019.07	July	Shumei	Shumei	Moss	Initial survey	121.8609914	25.10146976	SAMN38109951	SAMN38109766
SH0117	Shumei-Plant1	2019.07	July	Shumei	Shumei	Plant	Initial survey	121.8609914	25.10146976	SAMN38109952	SAMN38109767

SH0118	Shumei-Plant2	2019.07	July	Shumei	Shumei	Plant	Initial survey	121.8609914	25.10146976	SAMN38109953	SAMN38109768
SH0119	Shumei-Plant3	2019.07	July	Shumei	Shumei	Plant	Initial survey	121.8609914	25.10146976	SAMN38109954	SAMN38109769
SH0120	Shumei-Plant4	2019.07	July	Shumei	Shumei	Plant	Initial survey	121.8609914	25.10146976	SAMN38109955	SAMN38109770
SH0121	Shumei-Plant5	2019.07	July	Shumei	Shumei	Plant	Initial survey	121.8609914	25.10146976	SAMN38109956	SAMN38109771
SH0122	Shumei-Plant6	2019.07	July	Shumei	Shumei	Plant	Initial survey	121.8609914	25.10146976	SAMN38109957	SAMN38109772
SH0188	Yangmingshan-Plant4	2019.07	July	Yangmingshan1	Yangmingshan	Plant	Initial survey	121.555332	25.181007	SAMN38110027	SAMN38109818
SH0165	Yangmingshan-Moss5	2019.07	July	Yangmingshan2	Yangmingshan	Moss	Initial survey	121.5580091	25.17691705	SAMN38110004	SAMN38109795
SH0166	Yangmingshan-Moss6	2019.07	July	Yangmingshan2	Yangmingshan	Moss	Initial survey	121.5580091	25.17691705	SAMN38110005	SAMN38109796
SH0167	Yangmingshan-Moss7	2019.07	July	Yangmingshan2	Yangmingshan	Moss	Initial survey	121.5580091	25.17691705	SAMN38110006	SAMN38109797
SH0168	Yangmingshan-Moss8	2019.07	July	Yangmingshan2	Yangmingshan	Moss	Initial survey	121.5580091	25.17691705	SAMN38110007	SAMN38109798
SH0169	Yangmingshan-Plant5	2019.07	July	Yangmingshan2	Yangmingshan	Plant	Initial survey	121.5580091	25.17691705	SAMN38110008	SAMN38109799
SH0170	Yangmingshan-Plant6	2019.07	July	Yangmingshan2	Yangmingshan	Plant	Initial survey	121.5580091	25.17691705	SAMN38110009	SAMN38109800

SH0171	Yangmingshan-Plant7	2019.07	July	Yangmingshan2	Yangmingshan	Plant	Initial survey	121.5580091	25.17691705	SAMN38110010	SAMN38109801
SH0172	Yangmingshan-Plant8	2019.07	July	Yangmingshan2	Yangmingshan	Plant	Initial survey	121.5580091	25.17691705	SAMN38110011	SAMN38109802
SH0223	Yangmingshan-Mucilage9	2019.07	July	Yangmingshan2	Yangmingshan	Mucilage	Initial survey	121.5580091	25.17691705	SAMN38109996	SAMN38109837
SH0224	Yangmingshan-Mucilage10	2019.07	July	Yangmingshan2	Yangmingshan	Mucilage	Initial survey	121.5580091	25.17691705	SAMN38109997	SAMN38109838
SH0225	Yangmingshan-Mucilage11	2019.07	July	Yangmingshan2	Yangmingshan	Mucilage	Initial survey	121.5580091	25.17691705	SAMN38109998	SAMN38109839
SH0226	Yangmingshan-Mucilage12	2019.07	July	Yangmingshan2	Yangmingshan	Mucilage	Initial survey	121.5580091	25.17691705	SAMN38109999	SAMN38109840
SH0227	Yangmingshan-Mucilage13	2019.07	July	Yangmingshan2	Yangmingshan	Mucilage	Initial survey	121.5580091	25.17691705	SAMN38110000	SAMN38109841
SH0228	Yangmingshan-Mucilage14	2019.07	July	Yangmingshan2	Yangmingshan	Mucilage	Initial survey	121.5580091	25.17691705	SAMN38110001	SAMN38109842
SH0229	Yangmingshan-Mucilage15	2019.07	July	Yangmingshan2	Yangmingshan	Mucilage	Initial survey	121.5580091	25.17691705	SAMN38110002	SAMN38109843
SH0230	Yangmingshan-Mucilage16	2019.07	July	Yangmingshan2	Yangmingshan	Mucilage	Initial survey	121.5580091	25.17691705	SAMN38110003	SAMN38109844
SH0173	Yangmingshan-Mucilage1	2019.07	July	Yangmingshan1	Yangmingshan	Mucilage	Initial survey	121.55 5332	25.181 007	SAMN38110012	SAMN38109803
SH0174	Yangmingshan-Mucilage2	2019.07	July	Yangmingshan1	Yangmingshan	Mucilage	Initial survey	121.55 5332	25.181 007	SAMN38110013	SAMN38109804

SH0175	Yangmingshan-Mucilage3	2019.07	July	Yangmingshan1	Yangmingshan	Mucilage	Initial survey	121.555332	25.181007	SAMN38110014	SAMN38109805
SH0176	Yangmingshan-Mucilage4	2019.07	July	Yangmingshan1	Yangmingshan	Mucilage	Initial survey	121.555332	25.181007	SAMN38110015	SAMN38109806
SH0177	Yangmingshan-Mucilage5	2019.07	July	Yangmingshan1	Yangmingshan	Mucilage	Initial survey	121.555332	25.181007	SAMN38110016	SAMN38109807
SH0178	Yangmingshan-Mucilage6	2019.07	July	Yangmingshan1	Yangmingshan	Mucilage	Initial survey	121.555332	25.181007	SAMN38110017	SAMN38109808
SH0179	Yangmingshan-Mucilage7	2019.07	July	Yangmingshan1	Yangmingshan	Mucilage	Initial survey	121.555332	25.181007	SAMN38110018	SAMN38109809
SH0180	Yangmingshan-Mucilage8	2019.07	July	Yangmingshan1	Yangmingshan	Mucilage	Initial survey	121.555332	25.181007	SAMN38110019	SAMN38109810
SH0181	Yangmingshan-Moss1	2019.07	July	Yangmingshan1	Yangmingshan	Moss	Initial survey	121.555332	25.181007	SAMN38110020	SAMN38109811
SH0182	Yangmingshan-Moss2	2019.07	July	Yangmingshan1	Yangmingshan	Moss	Initial survey	121.555332	25.181007	SAMN38110021	SAMN38109812
SH0183	Yangmingshan-Moss3	2019.07	July	Yangmingshan1	Yangmingshan	Moss	Initial survey	121.555332	25.181007	SAMN38110022	SAMN38109813
SH0184	Yangmingshan-Moss4	2019.07	July	Yangmingshan1	Yangmingshan	Moss	Initial survey	121.555332	25.181007	SAMN38110023	SAMN38109814
SH0185	Yangmingshan-Plant1	2019.07	July	Yangmingshan1	Yangmingshan	Plant	Initial survey	121.555332	25.181007	SAMN38110024	SAMN38109815
SH0186	Yangmingshan-Plant2	2019.07	July	Yangmingshan1	Yangmingshan	Plant	Initial survey	121.555332	25.181007	SAMN38110025	SAMN38109816

SH0187	Yangmingshan-Plant3	2019.07	July	Yangmingshan1	Yangmingshan	Plant	Initial survey	121.555332	25.181007	SAMN38110026	SAMN38109817
SH0207	Yangmingshan-Mucilage17	2019.07	July	Yangmingshan3	Yangmingshan	Mucilage	Initial survey	121.5494261	25.18002408	SAMN38109980	SAMN38109821
SH0208	Yangmingshan-Mucilage18	2019.07	July	Yangmingshan3	Yangmingshan	Mucilage	Initial survey	121.5494261	25.18002408	SAMN38109981	SAMN38109822
SH0209	Yangmingshan-Mucilage19	2019.07	July	Yangmingshan3	Yangmingshan	Mucilage	Initial survey	121.5494261	25.18002408	SAMN38109982	SAMN38109823
SH0210	Yangmingshan-Mucilage20	2019.07	July	Yangmingshan3	Yangmingshan	Mucilage	Initial survey	121.5494261	25.18002408	SAMN38109983	SAMN38109824
SH0211	Yangmingshan-Mucilage21	2019.07	July	Yangmingshan3	Yangmingshan	Mucilage	Initial survey	121.5494261	25.18002408	SAMN38109984	SAMN38109825
SH0212	Yangmingshan-Mucilage22	2019.07	July	Yangmingshan3	Yangmingshan	Mucilage	Initial survey	121.5494261	25.18002408	SAMN38109985	SAMN38109826
SH0213	Yangmingshan-Mucilage23	2019.07	July	Yangmingshan3	Yangmingshan	Mucilage	Initial survey	121.5494261	25.18002408	SAMN38109986	SAMN38109827
SH0214	Yangmingshan-Mucilage24	2019.07	July	Yangmingshan3	Yangmingshan	Mucilage	Initial survey	121.5494261	25.18002408	SAMN38109987	SAMN38109828
SH0215	Yangmingshan-Moss9	2019.07	July	Yangmingshan3	Yangmingshan	Moss	Initial survey	121.5494261	25.18002408	SAMN38109988	SAMN38109829
SH0216	Yangmingshan-Moss10	2019.07	July	Yangmingshan3	Yangmingshan	Moss	Initial survey	121.5494261	25.18002408	SAMN38109989	SAMN38109830
SH0217	Yangmingshan-Moss11	2019.07	July	Yangmingshan3	Yangmingshan	Moss	Initial survey	121.5494261	25.18002408	SAMN38109990	SAMN38109831

SH0218	Yangmingshan-Moss12	2019.07	July	Yangmingshan3	Yangmingshan	Moss	Initial survey	121.5494261	25.18002408	SAMN38109991	SAMN38109832
SH0219	Yangmingshan-Plant9	2019.07	July	Yangmingshan3	Yangmingshan	Plant	Initial survey	121.5494261	25.18002408	SAMN38109992	SAMN38109833
SH0220	Yangmingshan-Plant10	2019.07	July	Yangmingshan3	Yangmingshan	Plant	Initial survey	121.5494261	25.18002408	SAMN38109993	SAMN38109834
SH0221	Yangmingshan-Plant11	2019.07	July	Yangmingshan3	Yangmingshan	Plant	Initial survey	121.5494261	25.18002408	SAMN38109994	SAMN38109835
SH0222	Yangmingshan-Plant12	2019.07	July	Yangmingshan3	Yangmingshan	Plant	Initial survey	121.5494261	25.18002408	SAMN38109995	SAMN38109836
SH0316	Shuangxi-June1	2018.06.07	June	Shuangxi	Shuangxi	Mucilage	Temporal variation	121.843341	25.066234	NA	SAMN38109900
SH0317	Shuangxi-June2	2018.06.07	June	Shuangxi	Shuangxi	Mucilage	Temporal variation	121.843341	25.066234	NA	SAMN38109901
SH0320	Shuangxi-July1	2018.07.18	July	Shuangxi	Shuangxi	Mucilage	Temporal variation	121.843341	25.066234	NA	SAMN38109904
SH0321	Shuangxi-July2	2018.07.18	July	Shuangxi	Shuangxi	Mucilage	Temporal variation	121.843341	25.066234	NA	SAMN38109905
SH0324	Shuangxi-August1	2018.08.21	August	Shuangxi	Shuangxi	Mucilage	Temporal variation	121.843341	25.066234	NA	SAMN38109908
SH0325	Shuangxi-August2	2018.08.21	August	Shuangxi	Shuangxi	Mucilage	Temporal variation	121.843341	25.066234	NA	SAMN38109909
SH0328	Shuangxi-November1	2018.11.16	November	Shuangxi	Shuangxi	Mucilage	Temporal variation	121.843341	25.066234	NA	SAMN38109912

SH0329	Shuangxi-November2	2018.11.16	November	Shuangxi	Shuangxi	Mucilage	Temporal variation	121.843341	25.066234	NA	SAMN38109913
SH0332	Shuangxi-December1	2018.12.18	December	Shuangxi	Shuangxi	Mucilage	Temporal variation	121.843341	25.066234	NA	SAMN38109916
SH0333	Shuangxi-December2	2018.12.18	December	Shuangxi	Shuangxi	Mucilage	Temporal variation	121.843341	25.066234	NA	SAMN38109917
SH0336	Shuangxi-January1	2019.01.18	January	Shuangxi	Shuangxi	Mucilage	Temporal variation	121.843341	25.066234	NA	SAMN38109920
SH0337	Shuangxi-January2	2019.01.18	January	Shuangxi	Shuangxi	Mucilage	Temporal variation	121.843341	25.066234	NA	SAMN38109921
SH0340	Shuangxi-Febrary1	2019.02.28	Febrary	Shuangxi	Shuangxi	Mucilage	Temporal variation	121.843341	25.066234	NA	SAMN38109924
SH0341	Shuangxi-Febrary2	2019.02.28	Febrary	Shuangxi	Shuangxi	Mucilage	Temporal variation	121.843341	25.066234	NA	SAMN38109925
SH0344	Shuangxi-March1	2019.03.28	March	Shuangxi	Shuangxi	Mucilage	Temporal variation	121.843341	25.066234	NA	SAMN38109928
SH0345	Shuangxi-March2	2019.03.28	March	Shuangxi	Shuangxi	Mucilage	Temporal variation	121.843341	25.066234	NA	SAMN38109929
SH0348	Shuangxi-April1	2019.04.23	April	Shuangxi	Shuangxi	Mucilage	Temporal variation	121.843341	25.066234	NA	SAMN38109932
SH0349	Shuangxi-April2	2019.04.23	April	Shuangxi	Shuangxi	Mucilage	Temporal variation	121.843341	25.066234	NA	SAMN38109933
SH0314	Shumei- June1	2018.06.07	June	Shumei	Shumei	Mucilage	Temporal variation	121.8609914	25.10146976	NA	SAMN38109898

SH0315	Shumei- June2	2018.06.07	June	Shumei	Shumei	Mucilage	Temporal variation	121.8609914	25.10146976	NA	SAMN38109899
SH0318	Shumei-July1	2018.07.18	July	Shumei	Shumei	Mucilage	Temporal variation	121.8609914	25.10146976	NA	SAMN38109902
SH0319	Shumei-July2	2018.07.18	July	Shumei	Shumei	Mucilage	Temporal variation	121.8609914	25.10146976	NA	SAMN38109903
SH0322	Shumei-August1	2018.08.21	August	Shumei	Shumei	Mucilage	Temporal variation	121.8609914	25.10146976	NA	SAMN38109906
SH0323	Shumei-August2	2018.08.21	August	Shumei	Shumei	Mucilage	Temporal variation	121.8609914	25.10146976	NA	SAMN38109907
SH0326	Shumei-November1	2018.11.16	November	Shumei	Shumei	Mucilage	Temporal variation	121.8609914	25.10146976	NA	SAMN38109910
SH0327	Shumei-November2	2018.11.16	November	Shumei	Shumei	Mucilage	Temporal variation	121.8609914	25.10146976	NA	SAMN38109911
SH0330	Shumei-December1	2018.12.18	December	Shumei	Shumei	Mucilage	Temporal variation	121.8609914	25.10146976	NA	SAMN38109914
SH0331	Shumei-December2	2018.12.18	December	Shumei	Shumei	Mucilage	Temporal variation	121.8609914	25.10146976	NA	SAMN38109915
SH0334	Shumei-January1	2019.01.18	January	Shumei	Shumei	Mucilage	Temporal variation	121.8609914	25.10146976	NA	SAMN38109918
SH0335	Shumei-January2	2019.01.18	January	Shumei	Shumei	Mucilage	Temporal variation	121.8609914	25.10146976	NA	SAMN38109919
SH0338	Shumei-Febrary1	2019.02.28	Febrary	Shumei	Shumei	Mucilage	Temporal variation	121.8609914	25.10146976	NA	SAMN38109922

SH0339	Shumei-Febrary2	2019.02.28	Febrary	Shumei	Shumei	Mucilage	Temporal variation	121.8609914	25.10146976	NA	SAMN38109923
SH0342	Shumei-March1	2019.03.28	March	Shumei	Shumei	Mucilage	Temporal variation	121.8609914	25.10146976	NA	SAMN38109926
SH0343	Shumei-March2	2019.03.28	March	Shumei	Shumei	Mucilage	Temporal variation	121.8609914	25.10146976	NA	SAMN38109927
SH0346	Shumei-April1	2019.04.23	April	Shumei	Shumei	Mucilage	Temporal variation	121.8609914	25.10146976	NA	SAMN38109930
SH0347	Shumei-April2	2019.04.23	April	Shumei	Shumei	Mucilage	Temporal variation	121.8609914	25.10146976	NA	SAMN38109931

Supplementary Table 2. Bacterial OTU table of *D. spatulata* mucilage and surrounding plants

Numbers in cells denote relative abundances (%)

OTU Taxa	Sm-Mu	Sm-Mo	Sm-Pl	Sx--Mu	Sx-Mo	Sx-Pl	Yms-Mu	Yms--Mo	Yms-Pl
Beijerinckiaceae	6.801	8.196666667	7.91	7.387	4.356666667	9.501666667	13.87041667	11.80833333	13.69916667
Caulobacteraceae	5.678	1.57	6.755	1.552	1.656666667	3.031666667	4.325	5.645833333	3.985833333
Acetobacteraceae	2.102	13.20333333	0.281666667	0.146	0.306666667	0.066666667	3.486666667	6.785	0.618333333
Methylobacteriaceae	0.759	0.346666667	3.031666667	2.244	1.856666667	6.42	1.132083333	0.216666667	6.6225

Acetobacteraceae	9.012	7.001666667	4.326666667	1.045	2.086666667	0.768333333	0.6	0.4075	0.135
unknown	3.22	1.535	11.42666667	0.109	0.106666667	0.165	1.494166667	1.065	2.476666667
Acidiphilium	3.848	12.92166667	1.248333333	0.618	3.573333333	0.193333333	0.6825	0.979166667	0.6425
Acetobacteraceae	0.001	0.016666667	0	0	0.001666667	0.001666667	3.2975	3.938333333	2.76
unknown	1.717	2.94	0.986666667	0.21	0.69	0.146666667	1.520416667	4.72	0.949166667
Sphingomonadaceae	1.059	0.206666667	1.795	1.812	0.56	5.17	1.020833333	0.186666667	3.6025
unknown	0.635	0.271666667	4.265	0.191	0.058333333	0.251666667	0.430416667	0.205833333	6.055
unknown	3.042	1.436666667	3.973333333	0.36	0.59	0.371666667	0.857083333	0.81	1.195
Acetobacteraceae	2.45	1.595	2.805	0.345	1.128333333	0.353333333	1.06	0.595	1.2
Sphingomonadaceae	0.639	0.081666667	0.713333333	1.953	0.563333333	2.43	1.267083333	0.1225	2.039166667
Burkholderiaceae	0.446	0.141666667	0.251666667	1.655	0.795	0.838333333	2.07125	0.91	0.79
Enterobacter	0.258	0.006666667	0.71	5.453	0.015	0.35	1.422916667	0.005	0.421666667

Enterobacter	6.301	0.013333333	0	1.812	0	0.506666667	0.390416667	0.696666667	0.003333333
Burkholderiaceae	0.488	0.033333333	0.341666667	1.535	0.07	0.233333333	3.082083333	0.095833333	0.0925
Acetobacteraceae	4.39	1.443333333	2.798333333	0.401	0.906666667	0.248333333	0.31875	0.585833333	0.020833333
Acetobacteraceae	1.179	0.5	0.851666667	0.489	0.106666667	2.538333333	1.170416667	1.034166667	1.155

Sm: Shumei, Sx: Shuangxi, Yms: Yangmingshan; Mu: Mucilage, Mo: Moss, Pl: Plant

Supplementary Table 3 Metadata from Globalfungi

Paper ID	Longitude	Latitude	Continent	Sample type	ITS1 extracted	ITS2 extracted	ITS total	Biome	Year of sampling	*Acrodontium* reads	Acrodontium abundance (%)
URen_2019_add	14.3216	60.8919	Europe	lichen	0	10528	10528	forest	2012	3801	36.1%
Toju_2018_56FC	141.623	42.6766	Asia	root	34	0	34	forest	2011	9	26.5%
URen_2019_add	14.3209	60.8918	Europe	lichen	0	6255	6255	forest	2012	1027	16.4%
Abrego_2018_CA	25.48	62.22	Europe	air	0	2984	2984	forest	2010	390	13.1%
Abrego_2018_CA	25.48	62.22	Europe	air	0	3942	3942	forest	2010	412	10.5%

Toju_2019_89C0	138.349	36.524	Asia	shoot	3242	0	3242	grassland	2017	254	7.8%
URen_2019_add	-73.0732	52.4132	North America	lichen	0	9376	9376	forest	2011	622	6.6%
URen_2019_add	14.3209	60.8918	Europe	shoot	0	5680	5680	forest	2012	374	6.6%
Toju_2019_89C0	138.349	36.524	Asia	shoot	198	0	198	grassland	2017	13	6.6%
Abrego_2018_CA	25.55	63.37	Europe	air	0	683	683	forest	2009	41	6.0%
Abrego_2018_CA	25.55	63.37	Europe	air	0	711	711	forest	2009	36	5.1%
Abrego_2018_CA	25.48	62.22	Europe	air	0	4681	4681	forest	2010	173	3.7%
Nguyen_2016_D8E8	23.9	52.7	Europe	shoot	0	86	86	forest	2013	3	3.5%
Abrego_2018_CA	25.55	63.37	Europe	air	0	634	634	forest	2009	22	3.5%
Abrego_2018_CA	25.55	63.37	Europe	air	0	719	719	forest	2009	23	3.2%
Toju_2019_89C0	138.349	36.524	Asia	shoot	6243	0	6243	grassland	2017	197	3.2%
Abrego_2018_CA	25.55	63.37	Europe	air	0	3674	3674	forest	2009	115	3.1%

URen_2019_add	-111.552	59.7183	North America	lichen	0	8702	8702	forest	2013	246	2.8%
Abrego_2018_CA	25.55	63.37	Europe	air	0	676	676	forest	2009	16	2.4%
Abrego_2018_CA	25.55	63.37	Europe	air	0	2083	2083	forest	2009	47	2.3%
Toju_2019_89C0	138.349	36.524	Asia	shoot	1313	0	1313	grassland	2017	28	2.1%
Toju_2019_89C0	138.349	36.524	Asia	shoot	3348	0	3348	grassland	2017	69	2.1%
Abrego_2018_CA	25.48	62.22	Europe	air	0	3336	3336	forest	2010	68	2.0%
Toju_2019_89C0	138.349	36.524	Asia	shoot	8142	0	8142	grassland	2017	165	2.0%
Toju_2019_89C0	138.349	36.524	Asia	shoot	11181	0	11181	grassland	2017	222	2.0%
Abrego_2018_CA	25.48	62.22	Europe	air	0	7012	7012	forest	2010	121	1.7%
Abrego_2018_CA	25.55	63.37	Europe	air	0	1017	1017	forest	2009	17	1.7%
Toju_2019_89C0	138.349	36.524	Asia	shoot	425	0	425	grassland	2017	7	1.6%
Toju_2019_89C0	138.349	36.524	Asia	shoot	1916	0	1916	grassland	2017	30	1.6%

URen_2019_add	-88.08	46.9	North America	shoot	0	6752	6752	forest	2013	103	1.5%
Toju_2018_56FC	142.022	45.0421	Asia	root	861	0	861	forest	2012	12	1.4%
Abrego_2018_CA	25.55	63.37	Europe	air	0	4352	4352	forest	2009	60	1.4%
URen_2019_add	135.957	47.8163	Asia	lichen	0	8057	8057	forest	2013	109	1.4%
Toju_2019_89C0	138.349	36.524	Asia	shoot	1308	0	1308	grassland	2017	16	1.2%
Baldrian_2016_DE02	14.7057	48.6653	Europe	deadwood	0	11804	11804	forest	2013	144	1.2%
DeBeeck_2014_14DC	5.37278	51.1258	Europe	soil	492	0	492	forest	2009	6	1.2%
URen_2019_add	-73.0725	52.4126	North America	shoot	0	13879	13879	forest	2011	163	1.2%
Darcy_2020_CT	-156.919	21.1174	North America	shoot	24567	0	24567	forest	2016	287	1.2%
Abrego_2018_CA	25.55	63.37	Europe	air	0	3275	3275	forest	2009	37	1.1%
Abrego_2018_CA	25.55	63.37	Europe	air	0	3409	3409	forest	2009	38	1.1%

Toju_2019_89C0	138.349	36.524	Asia	shoot	4356	0	4356	grassland	2017	48	1.1%
Abrego_2018_CA	25.48	62.22	Europe	air	0	2400	2400	forest	2010	25	1.0%
Abrego_2018_CA	25.55	63.37	Europe	air	0	773	773	forest	2009	8	1.0%
Abrego_2018_CA	25.55	63.37	Europe	air	0	3325	3325	forest	2009	34	1.0%
Toju_2019_89C0	138.349	36.524	Asia	shoot	98	0	98	grassland	2017	1	1.0%
Toju_2019_89C0	138.349	36.524	Asia	shoot	2680	0	2680	grassland	2017	27	1.0%
URen_2019_add	-111.552	59.7184	North America	lichen	0	4647	4647	forest	2013	46	1.0%
Abrego_2018_CA	25.55	63.37	Europe	air	0	1588	1588	forest	2009	15	0.9%
Baldrian_2016_DE02	14.7093	48.666	Europe	deadwood	0	12084	12084	forest	2013	114	0.9%
Abrego_2018_CA	25.55	63.37	Europe	air	0	774	774	forest	2009	7	0.9%
Abrego_2018_CA	25.48	62.22	Europe	air	0	3383	3383	forest	2010	30	0.9%
DeBeeck_2014_14DC	5.37278	51.1258	Europe	soil	0	115	115	forest	2009	1	0.9%

Abrego_2018_CA	25.55	63.37	Europe	air	0	2840	2840	forest	2009	24	0.8%
Abrego_2018_CA	25.48	62.22	Europe	air	0	3704	3704	forest	2010	31	0.8%
Toju_2019_89C0	138.349	36.524	Asia	shoot	4911	0	4911	grassland	2017	41	0.8%
Abrego_2018_CA	25.55	63.37	Europe	air	0	490	490	forest	2009	4	0.8%
Toju_2019_89C0	138.349	36.524	Asia	shoot	12923	0	12923	grassland	2017	105	0.8%
Abrego_2018_CA	25.55	63.37	Europe	air	0	774	774	forest	2009	6	0.8%
Toju_2019_89C0	138.349	36.524	Asia	root	266	0	266	grassland	2017	2	0.8%
Abrego_2018_CA	25.55	63.37	Europe	air	0	685	685	forest	2009	5	0.7%
Abrego_2018_CA	25.48	62.22	Europe	air	0	1460	1460	forest	2010	10	0.7%
Abrego_2018_CA	25.55	63.37	Europe	air	0	321	321	forest	2009	2	0.6%
DeBeeck_2014_14DC	5.37278	51.1258	Europe	soil	0	806	806	forest	2009	5	0.6%
URen_2019_add	-88.0708	46.8539	North America	lichen	0	12481	12481	forest	2013	77	0.6%

Toju_2019_89C0	138.349	36.524	Asia	shoot	1400	0	1400	grassland	2017	8	0.6%
Toju_2019_89C0	138.349	36.524	Asia	shoot	7119	0	7119	grassland	2017	38	0.5%
Abrego_2018_CA	25.55	63.37	Europe	air	0	378	378	forest	2009	2	0.5%
Nguyen_2016_D8E8	23.9	52.7	Europe	shoot	0	190	190	forest	2013	1	0.5%
Baldrian_2016_DE02	14.7058	48.6674	Europe	deadwood	0	21686	21686	forest	2013	111	0.5%
Abrego_2018_CA	25.55	63.37	Europe	air	0	793	793	forest	2009	4	0.5%
Abrego_2018_CA	25.55	63.37	Europe	air	0	826	826	forest	2009	4	0.5%
Abrego_2020_CV	23.9833	61.5089	Europe	air	0	32590	32590	forest	2019	155	0.5%
Abrego_2018_CA	25.55	63.37	Europe	air	0	2360	2360	forest	2009	11	0.5%
Abrego_2018_CA	25.55	63.37	Europe	air	0	2885	2885	forest	2009	13	0.5%
Ovaskainen_2019_air	14.1938	46.5723	Europe	air	0	7696	7696	forest	2018	34	0.4%
Toju_2019_89C0	138.349	36.524	Asia	shoot	2324	0	2324	grassland	2017	10	0.4%

Abrego_2018_CA	25.48	62.22	Europe	air	0	4235	4235	forest	2010	18	0.4%
Toju_2019_89C0	138.349	36.524	Asia	shoot	18914	0	18914	grassland	2017	80	0.4%
Toju_2019_89C0	138.349	36.524	Asia	shoot	1205	0	1205	grassland	2017	5	0.4%
Abrego_2018_CA	25.48	62.22	Europe	air	0	2959	2959	forest	2010	12	0.4%
Clemmensen_2021_OP	18.8536	68.3265	Europe	litter	0	1243	1243	tundra	2008	5	0.4%
Abrego_2018_CA	25.55	63.37	Europe	air	0	2640	2640	forest	2009	10	0.4%
Abrego_2018_CA	25.55	63.37	Europe	air	0	4230	4230	forest	2009	16	0.4%
Darcy_2020_CT	-156.93	21.1191	North America	shoot	6885	0	6885	forest	2016	26	0.4%
Abrego_2018_CA	25.48	62.22	Europe	air	0	1631	1631	forest	2010	6	0.4%
Abrego_2018_CA	25.55	63.37	Europe	air	0	1961	1961	forest	2009	7	0.4%
Abrego_2018_CA	25.48	62.22	Europe	air	0	4504	4504	forest	2010	16	0.4%
Toju_2019_89C0	138.349	36.524	Asia	root	853	0	853	grassland	2017	3	0.4%

Toju_2019_89C0	138.349	36.524	Asia	shoot	3131	0	3131	grassland	2017	11	0.4%
Abrego_2018_CA	25.55	63.37	Europe	air	0	3428	3428	forest	2009	12	0.4%
URen_2019_add	-87.9251	46.8504	North America	shoot	1	14104	14105	forest	2013	49	0.3%
Abrego_2018_CA	25.55	63.37	Europe	air	0	865	865	forest	2009	3	0.3%
Kovalchuk_2018_EDF8	25.2233	60.7531	Europe	root	0	298	298	forest	2016	1	0.3%
URen_2019_add	14.3209	60.8918	Europe	lichen	0	18377	18377	forest	2012	61	0.3%
Abrego_2018_CA	25.55	63.37	Europe	air	0	2137	2137	forest	2009	7	0.3%
Abrego_2018_CA	25.55	63.37	Europe	air	0	2455	2455	forest	2009	8	0.3%
Talas_2021_OR	27.1492	56.7602	Europe	sedimentt	0	23239	23239	aquatic	2013	75	0.3%
Abrego_2020_CV	24.5166	60.2943	Europe	air	0	16802	16802	forest	2019	54	0.3%
Toju_2019_89C0	138.349	36.524	Asia	shoot	940	0	940	grassland	2017	3	0.3%
Toju_2019_89C0	138.349	36.524	Asia	shoot	6953	0	6953	grassland	2017	22	0.3%

Toju_2019_89C0	138.349	36.524	Asia	shoot	3212	0	3212	grassland	2017	10	0.3%
Abrego_2018_CA	25.48	62.22	Europe	air	0	3271	3271	forest	2010	10	0.3%
Abrego_2018_CA	25.55	63.37	Europe	air	0	673	673	forest	2009	2	0.3%
Abrego_2018_CA	25.55	63.37	Europe	air	0	1029	1029	forest	2009	3	0.3%
URen_2019_add	135.957	47.8165	Asia	lichen	0	10032	10032	forest	2013	29	0.3%
Abrego_2020_CV	24.95	60.1724	Europe	air	0	167338	1673 38	anthropogenic	2019	478	0.3%
Toju_2019_89C0	138.349	36.524	Asia	shoot	2150	0	2150	grassland	2017	6	0.3%
Davey_2014_2252	10.6967	60.1399	Europe	shoot	0	4424	4424	forest	2010	12	0.3%
Abrego_2018_CA	25.48	62.22	Europe	air	0	7795	7795	forest	2010	21	0.3%
Clemmensen_2015_B0AE	17.738	66.0441	Europe	litter	0	1504	1504	forest	2009	4	0.3%
Abrego_2018_CA	25.55	63.37	Europe	air	0	1507	1507	forest	2009	4	0.3%
Abrego_2018_CA	25.55	63.37	Europe	air	0	395	395	forest	2009	1	0.3%

Toju_2019_89C0	138.349	36.524	Asia	shoot	4029	0	4029	grassland	2017	10	0.2%
Woo_2018_BY	126.955	37.4653	Asia	dust	65170	0	65170	anthropogenic	2015	160	0.2%
Abrego_2018_CA	25.55	63.37	Europe	air	0	825	825	forest	2009	2	0.2%
Abrego_2018_CA	25.482	62.22	Europe	air	0	4954	4954	forest	2010	12	0.2%
Toju_2019_89C0	138.349	36.524	Asia	shoot	4159	0	4159	grassland	2017	10	0.2%
Baldrian_2016_DE02	14.7066	48.6661	Europe	deadwood	0	10024	10024	forest	2013	24	0.2%
Abrego_2018_CA	25.55	63.37	Europe	air	0	2092	2092	forest	2009	5	0.2%
Toju_2019_89C0	138.349	36.524	Asia	shoot	4746	0	4746	grassland	2017	11	0.2%
Davey_2012_6F6A	10.845	59.6614	Europe	shoot	0	433	433	forest	2009 to 2010	1	0.2%
Abrego_2018_CA	25.482	62.22	Europe	air	0	3095	3095	forest	2010	7	0.2%
Toju_2019_89C0	138.349	36.524	Asia	shoot	5776	0	5776	grassland	2017	13	0.2%
DeBeeck_2014_14DC	5.37278	51.1258	Europe	soil	0	908	908	forest	2009	2	0.2%

Nguyen_2016_D8E8	29.9	62.6	Europe	shoot	0	455	455	forest	2012	1	0.2%
Davey_2012_6F6A	10.845	59.614	Europe	shoot	0	921	921	forest	2009 to 2010	2	0.2%
Clemmensen_2015_B0AE	17.7149	66.1376	Europe	litter	0	467	467	forest	2009	1	0.2%
URen_2019_add	14.3205	60.8919	Europe	lichen	0	21104	21104	forest	2012	45	0.2%
Anthony_2020_mBY	-72.1875	42.4836	North America	soil	0	7783	7783	forest	2016	16	0.2%
Abrego_2018_CA	25.55	63.37	Europe	air	0	2476	2476	forest	2009	5	0.2%
Toju_2019_89C0	138.349	36.524	Asia	shoot	2556	0	2556	grassland	2017	5	0.2%
Clemmensen_2015_B0AE	17.7438	66.0254	Europe	litter	0	516	516	forest	2009	1	0.2%
Nguyen_2016_D8E8	29.9	62.6	Europe	shoot	0	516	516	forest	2012	1	0.2%
URen_2019_add	135.957	47.8167	Asia	shoot	0	9860	9860	forest	2013	19	0.2%
Davey_2012_6F6A	10.845	59.614	Europe	shoot	0	1040	1040	forest	2009 to 2010	2	0.2%
Toju_2019_89C0	138.349	36.524	Asia	shoot	6775	0	6775	grassland	2017	13	0.2%

Toju_2019_89C0	138.349	36.524	Asia	shoot	5874	0	5874	grassland	2017	11	0.2%
Abrego_2018_CA	25.55	63.37	Europe	air	0	1088	1088	forest	2009	2	0.2%
Woo_2018_BY	126.955	37.4653	Asia	dust	93351	0	93351	anthropogenic	2015	171	0.2%
Abrego_2020_CV	25.7346	62.1444	Europe	air	0	148042	148042	forest	2019	268	0.2%
Toju_2019_89C0	138.349	36.524	Asia	shoot	4476	0	4476	grassland	2017	8	0.2%
Davey_2014_2252	10.7626	60.1295	Europe	shoot	0	1741	1741	forest	2010	3	0.2%
Abrego_2018_CA	25.55	63.37	Europe	air	0	1742	1742	forest	2009	3	0.2%
Yang_2019_D4B1	128.162	42.2722	Asia	soil	39256	0	39256	forest	2016	64	0.2%
Talas_2021_ORR	27.1492	56.7602	Europe	sedimentt	0	115345	11534 5	aquatic	2013	188	0.2%
Rajala_2015_1113	26.12	60.66	Europe	deadwood	4321	0	4321	forest	2008	7	0.2%
Mikryukov_2021_SP	59.863	56.848	Asia	litter	0	39216	39216	forest	2017	63	0.2%
Abrego_2020_CV	24.4511	60.2911	Europe	air	0	45497	45497	forest	2019	73	0.2%

Abrego_2018_CA	25.55	63.37	Europe	air	0	652	652	forest	2009	1	0.2%
Abrego_2018_CA	25.55	63.37	Europe	air	0	4000	4000	forest	2009	6	0.2%
Davey_2012_6F6A	10.845	59.614	Europe	shoot	0	667	667	forest	2009 to 2010	1	0.1%
Abrego_2018_CA	25.55	63.37	Europe	air	0	680	680	forest	2009	1	0.1%
Clemmensen_2015_B0AE	17.7158	66.1406	Europe	litter	0	689	689	forest	2009	1	0.1%
URen_2019_add	135.957	47.8165	Asia	shoot	0	8295	8295	forest	2013	12	0.1%
Rajala_2015_1113	25.11	61.35	Europe	deadwood	3487	0	3487	forest	2009	5	0.1%
Davey_2014_2252	10.6888	60.1307	Europe	shoot	0	2812	2812	forest	2010	4	0.1%
Darcy_2020_CT	-155.401	19.674	North America	shoot	8537	0	8537	forest	2015	12	0.1%
Toju_2019_89C0	138.349	36.524	Asia	shoot	8605	0	8605	grassland	2017	12	0.1%
Toju_2019_89C0	138.349	36.524	Asia	root	1447	0	1447	grassland	2017	2	0.1%
Abrego_2018_CA	25.55	63.37	Europe	air	0	726	726	forest	2009	1	0.1%

Lepinay_2021_SO	16.9436	48.6813	Europe	deadwood	0	8775	8775	forest	2016	12	0.1%
Darcy_2020_CT	-155.238	19.414	North America	shoot	21315	0	21315	forest	2014	29	0.1%
Abrego_2018_CA	25.55	63.37	Europe	air	0	1475	1475	forest	2009	2	0.1%
Abrego_2018_CA	25.55	63.37	Europe	air	0	1499	1499	forest	2009	2	0.1%
URen_2019_add	-73.0725	52.4126	North America	shoot	0	27388	27388	forest	2011	36	0.1%
Tedersoo_2021_TJ	26.6047	57.669	Europe	soil	739	804	1543	forest	2013	2	0.1%
Abrego_2018_CA	25.55	63.37	Europe	air	0	3086	3086	forest	2009	4	0.1%
Abrego_2018_CA	25.48	62.22	Europe	air	0	9308	9308	forest	2010	12	0.1%
Clemmensen_2015_B0AE	17.819	65.9687	Europe	litter	0	778	778	forest	2009	1	0.1%
Toju_2016_23219	137.579	36.579	Asia	root	22717	0	22717	tundra	2013	29	0.1%
Davey_2014_2252	10.7486	60.1296	Europe	shoot	0	1567	1567	forest	2010	2	0.1%

URen_2019_add	14.32 09	60.8 918	Europe	shoot	0	14925	1492 5	forest	2012	19	0.1%
Abrego_2020_C V	30.10 21	62.6 287	Europe	air	0	40488	4048 8	forest	2019	51	0.1%
Abrego_2018_C A	25.2	60.4 6	Europe	air	802	0	802	forest	2009	1	0.1%
Davey_2012_6F6 A	10.84 5	59.6 614	Europe	shoot	0	1646	1646	forest	2009 to 2010	2	0.1%
URen_2019_add	-87.92 51	46.8 504	North America	shoot	0	10718	1071 8	forest	2013	13	0.1%
Clemmensen_20 15_B0AE	17.84 59	65.9 558	Europe	litter	0	833	833	forest	2009	1	0.1%
URen_2019_add	-88.07 08	46.8 539	North America	shoot	0	12619	1261 9	forest	2013	15	0.1%
Clemmensen_20 21_OP	18.84 81	68.3 304	Europe	litter	0	862	862	forest	2008	1	0.1%
Clemmensen_20 15_B0AE	17.76 11	66.1 417	Europe	litter	0	866	866	forest	2009	1	0.1%
Toju_2019_89C0	138.3 49	36.5 24	Asia	shoot	4363	0	4363	grassla nd	2017	5	0.1%
Davey_2012_6F6 A	10.84 5	59.6 614	Europe	shoot	0	1747	1747	forest	2009 to 2010	2	0.1%

URen_2019_add	135.957	47.8167	Asia	shoot	0	3533	3533	forest	2013	4	0.1%
Abrego_2018_CA	25.48	62.22	Europe	air	0	2730	2730	forest	2010	3	0.1%
Abrego_2020_CV	23.9833	61.5089	Europe	air	0	163805	163805	forest	2019	175	0.1%
Abrego_2018_CA	25.55	63.37	Europe	air	0	941	941	forest	2009	1	0.1%
Toju_2019_89C0	138.349	36.524	Asia	shoot	3801	0	3801	grassland	2017	4	0.1%
Abrego_2018_CA	22.4988	59.7233	Europe	air	0	955	955	desert	2010	1	0.1%
Wurth_2019_0DBA	-148.281	64.7666	North America	shoot	0	18192	18192	forest	2016	19	0.1%
Toju_2019_89C0	138.349	36.524	Asia	shoot	7680	0	7680	grassland	2017	8	0.1%
Abrego_2018_CA	25.48	62.22	Europe	air	0	967	967	forest	2010	1	0.1%
URen_2019_add	14.3205	60.8919	Europe	lichen	0	17486	17486	forest	2012	18	0.1%
George_2019_9BEA	-4.83509	51.8894	Europe	soil	190926	0	190926	cropland	2013 to 2014	196	0.1%

Mikryukov_2021_SP	59.425	56.801	Asia	litter	0	40064	40064	forest	2017	41	0.1%
Toju_2019_89C0	138.349	36.524	Asia	shoot	5902	0	5902	grassland	2017	6	0.1%
Abrego_2018_CA	25.48	62.22	Europe	air	0	3937	3937	forest	2010	4	0.1%
Toju_2019_89C0	138.349	36.524	Asia	shoot	5997	0	5997	grassland	2017	6	0.1%
Clemmensen_2015_B0AE	17.7438	66.0254	Europe	litter	0	1029	1029	forest	2009	1	0.1%
Baldrian_2016_DE02	14.706	48.6643	Europe	deadwood	0	13550	13550	forest	2013	13	0.1%
Toju_2019_89C0	138.349	36.524	Asia	root	3129	0	3129	grassland	2017	3	0.1%
Toju_2019_89C0	138.349	36.524	Asia	shoot	10471	0	10471	grassland	2017	10	0.1%
Abrego_2020_CV	25.7946	61.1032	Europe	air	0	43391	43391	forest	2019	41	0.1%
Darcy_2020_CT	-155.927	19.615	North America	shoot	18700	0	18700	forest	2015	17	0.1%
Davey_2012_6F6A	10.845	59.6614	Europe	shoot	0	1102	1102	forest	2009 to 2010	1	0.1%
Toju_2019_89C0	138.349	36.524	Asia	root	1104	0	1104	grassland	2017	1	0.1%

Toju_2019_89C0	138.349	36.524	Asia	shoot	9968	0	9968	grassland	2017	9	0.1%
Kovalchuk_2018_EDF8	25.2594	60.7542	Europe	shoot	0	121457	121457	forest	2016	108	0.1%
Toju_2019_89C0	138.349	36.524	Asia	shoot	9138	0	9138	grassland	2017	8	0.1%
Abrego_2018_CA	25.55	63.37	Europe	air	0	2303	2303	forest	2009	2	0.1%
Davey_2014_2252	10.7155	60.1454	Europe	shoot	0	3468	3468	forest	2010	3	0.1%
Abrego_2020_CV	25.8065	61.0995	Europe	air	0	65969	65969	forest	2019	56	0.1%
Clemmensen_2015_B0AE	17.7438	66.0254	Europe	litter	0	1181	1181	forest	2009	1	0.1%
Toju_2019_89C0	138.349	36.524	Asia	shoot	2389	0	2389	grassland	2017	2	0.1%
Davey_2014_2252	10.7128	60.1439	Europe	shoot	0	2408	2408	forest	2010	2	0.1%
Clemmensen_2015_B0AE	17.8711	65.9451	Europe	litter	0	1210	1210	forest	2009	1	0.1%
Toju_2019_89C0	138.349	36.524	Asia	shoot	2424	0	2424	grassland	2017	2	0.1%
Davey_2012_6F6A	10.845	59.6614	Europe	shoot	0	1221	1221	forest	2009 to 2010	1	0.1%

Clemmensen_2015_B0AE	17.8436	65.9468	Europe	litter	0	1222	1222	forest	2009	1	0.1%
Abrego_2020_CV	25.5972	62.2189	Europe	air	0	198494	198494	forest	2019	162	0.1%
Zhao_2019_0D8E	117.575	32.0548	Asia	soil	0	7635	7635	cropland	2015	6	0.1%
Davey_2012_6F6A	10.845	59.6614	Europe	shoot	0	1278	1278	forest	2009 to 2010	1	0.1%
Darcy_2020_CT	-158.136	21.5119	North America	shoot	16782	0	16782	forest	2015	13	0.1%
Clemmensen_2015_B0AE	17.8711	65.9451	Europe	litter	0	1306	1306	forest	2009	1	0.1%
Toju_2019_89C0	138.349	36.524	Asia	shoot	10460	0	10460	grassland	2017	8	0.1%
Davey_2012_6F6A	10.845	59.6614	Europe	shoot	0	1335	1335	forest	2009 to 2010	1	0.1%
Davey_2013_7683	9.80203	61.1072	Europe	shoot	0	1350	1350	forest	2009	1	0.1%
Toju_2019_89C0	138.349	36.524	Asia	shoot	5417	0	5417	grassland	2017	4	0.1%
Ovaskainen_2019_air	14.1938	46.5723	Europe	air	0	5430	5430	forest	2018	4	0.1%
Abrego_2018_CA	25.2	60.46	Europe	air	1362	0	1362	forest	2009	1	0.1%

Abrego_2018_CA	25.55	63.37	Europe	air	0	2736	2736	forest	2009	2	0.1%
George_2019_9BEA	-3.86744	53.0776	Europe	soil	30920	0	30920	grassland	2013 to 2014	22	0.1%
Davey_2012_6F6A	10.845	59.614	Europe	shoot	0	1408	1408	forest	2009 to 2010	1	0.1%
Davey_2014_2252	10.6903	60.1302	Europe	shoot	0	4234	4234	forest	2010	3	0.1%
Toju_2016_2321	137.61	36.57	Asia	root	12950	0	12950	tundra	2013	9	0.1%
Mikryukov_2021_SP	59.827	56.85	Asia	litter	0	50362	50362	forest	2017	35	0.1%
Clemmensen_2015_B0AE	17.819	65.9687	Europe	litter	0	2880	2880	forest	2009	2	0.1%
Clemmensen_2015_B0AE	17.8436	65.9468	Europe	litter	0	4358	4358	forest	2009	3	0.1%
Toju_2019_89C0	138.349	36.524	Asia	root	4368	0	4368	grassland	2017	3	0.1%
Toju_2019_89C0	138.349	36.524	Asia	shoot	5855	0	5855	grassland	2017	4	0.1%
Toju_2019_89C0	138.349	36.524	Asia	shoot	4454	0	4454	grassland	2017	3	0.1%
Clemmensen_2015_B0AE	17.8711	65.9451	Europe	litter	0	1490	1490	forest	2009	1	0.1%

Clemmensen_2015_B0AE	17.71 49	66.1 376	Europe	litter	0	1527	1527	forest	2009	1	0.1%
Toju_2019_89C0	138.3 49	36.5 24	Asia	shoot	3103	0	3103	grassland	2017	2	0.1%
Clemmensen_2015_B0AE	17.71 58	66.1 406	Europe	litter	0	1557	1557	forest	2009	1	0.1%
URen_2019_add	14.32 16	60.8 919	Europe	lichen	0	9382	9382	forest	2012	6	0.1%
Clemmensen_2015_B0AE	17.74 92	66.1 452	Europe	soil	0	1564	1564	forest	2009	1	0.1%
Abrego_2018_CA	25.48	62.2 2	Europe	air	0	3140	3140	forest	2010	2	0.1%
Clemmensen_2015_B0AE	17.76 46	66.1 412	Europe	litter	0	1585	1585	forest	2009	1	0.1%
Baldrian_2016_DE02	14.70 88	48.6 666	Europe	deadwood	0	14580	1458 0	forest	2013	9	0.1%
Abrego_2018_CA	25.55	63.3 7	Europe	air	0	1625	1625	forest	2009	1	0.1%
URen_2019_add	92.82 92	55.9 311	Asia	lichen	0	16341	1634 1	forest	2012	10	0.1%
Toju_2019_89C0	138.3 49	36.5 24	Asia	shoot	4964	0	4964	grassland	2017	3	0.1%
Kovalchuk_2018_EDF8	25.22 33	60.7 531	Europe	shoot	0	60305	6030 5	forest	2016	36	0.1%

Walker_2014_22C1	-83.7647	41.0601	North America	topsoil	0	1690	1690	forest	2013	1	0.1%
Siciliano_2014_FF	-110.53	-66.31	Antarctica	soil	10197	1	10198	desert	2005 to 2008	6	0.1%
Ji_2016_C06E	-110.55	-66.31	Antarctica	soil	10198	1	10199	desert	2006	6	0.1%
Baldrian_2016_DE02	14.704	48.671	Europe	deadwood	0	12070	12070	forest	2013	7	0.1%
Clemmensen_2021_OP	18.8481	68.3304	Europe	litter	0	1761	1761	forest	2008	1	0.1%
Rajala_2015_1113	26.123	60.66	Europe	deadwood	5435	0	5435	forest	2008	3	0.1%
Blaalid_2013_HK	7.41667	60.55	Europe	root	0	1816	1816	tundra	NA_	1	0.1%
Abrego_2018_CA	25.55	63.37	Europe	air	0	1823	1823	forest	2009	1	0.1%
Davey_2014_2252	10.7152	60.1478	Europe	shoot	0	3658	3658	forest	2010	2	0.1%
Davey_2014_2252	10.6898	60.1303	Europe	shoot	0	3846	3846	forest	2010	2	0.1%
Abrego_2020_CV	29.783	62.6103	Europe	air	0	50325	50325	anthropogenic	2019	26	0.1%

Clemmensen_2015_B0AE	17.7492	66.1452	Europe	litter	0	3886	3886	forest	2009	2	0.1%
Joergensen_2021_TK	18.77	64.5087	Europe	topsoil	0	1952	1952	forest	2016	1	0.1%
Joergensen_2021_TK	16.3	63.8244	Europe	topsoil	0	1984	1984	forest	2016	1	0.1%
Abrego_2020_CV	25.5972	62.2189	Europe	air	0	226316	2263 16	forest	2019	113	0.0%
George_2019_9BEA	-3.55608	52.7224	Europe	soil	125339	0	1253 39	forest	2013 to 2014	62	0.0%
Abrego_2020_CV	30.1629	62.618	Europe	air	0	208110	2081 10	forest	2019	102	0.0%
Davey_2014_2252	10.7177	60.1438	Europe	shoot	0	6127	6127	forest	2010	3	0.0%
RoyBolduc_2016_E50C	-61.7546	47.4434	North America	root	4324	3851	8175	forest	2010	4	0.0%
Davey_2014_2252	10.7174	60.1438	Europe	shoot	0	4126	4126	forest	2010	2	0.0%
Davey_2014_2252	10.7008	60.1418	Europe	shoot	0	2087	2087	forest	2010	1	0.0%
Toju_2018_56FC	142.022	45.0421	Asia	root	2114	0	2114	forest	2012	1	0.0%

Abrego_2018_CA	25.55	63.37	Europe	air	0	2130	2130	forest	2009	1	0.0%
Baldrian_2016_DE02	14.7097	48.66661	Europe	deadwood	0	4266	4266	forest	2013	2	0.0%
Abrego_2020_CV	29.783	62.6103	Europe	air	0	81873	81873	anthropogenic	2019	38	0.0%
Abrego_2018_CA	25.55	63.37	Europe	air	0	4324	4324	forest	2009	2	0.0%
Baldrian_2016_DE02	14.7054	48.66678	Europe	deadwood	0	10878	10878	forest	2013	5	0.0%
Davey_2014_2252	10.7537	60.1303	Europe	shoot	0	4363	4363	forest	2010	2	0.0%
Davey_2014_2252	10.7486	60.1929	Europe	shoot	0	2195	2195	forest	2010	1	0.0%
Toju_2019_89C0	138.349	36.524	Asia	shoot	6601	0	6601	grassland	2017	3	0.0%
Clemmensen_2015_B0AE	17.7994	66.1251	Europe	litter	0	2204	2204	forest	2009	1	0.0%
Froeslev_2019_CA74	8.3724	56.1707	Europe	soil	0	11024	11024	shrubland	2014	5	0.0%
Zheng_2021_QP	112.333	16.8333	Asia	soil	0	28805	28805	woodland	2014	13	0.0%
URen_2019_add	92.7704	55.8859	Asia	lichen	0	11134	11134	forest	2012	5	0.0%

Abrego_2020_CV	24.4511	60.2911	Europe	air	0	147277	147277	forest	2019	66	0.0%
Darcy_2020_CT	-156.919	21.1174	North America	shoot	24679	0	24679	forest	2016	11	0.0%
Mikryukov_2021_SP	59.827	56.85	Asia	litter	0	40509	40509	forest	2017	18	0.0%
Darcy_2020_CT	-158.137	21.512	North America	shoot	13740	0	13740	forest	2015	6	0.0%
Abrego_2018_CA	25.48	62.22	Europe	air	0	6881	6881	forest	2010	3	0.0%
Clemmensen_2015_B0AE	17.819	65.9687	Europe	litter	0	2308	2308	forest	2009	1	0.0%
Toju_2019_89C0	138.349	36.524	Asia	shoot	6992	0	6992	grassland	2017	3	0.0%
Tedersoo_2016_ISME	27.4353	59.0729	Europe	soil	0	4699	4699	forest	2013	2	0.0%
Kovalchuk_2018_EDF8	25.2233	60.7531	Europe	shoot	0	83903	83903	forest	2016	35	0.0%
Zhao_2019_0D8E	117.654	32.084	Asia	soil	0	21730	21730	cropland	2015	9	0.0%
Joergensen_2021_TK	19.82	64.3555	Europe	topsoil	0	2424	2424	forest	2016	1	0.0%

Toju_2019_89C0	138.349	36.524	Asia	shoot	4865	0	4865	grassland	2017	2	0.0%
Abrego_2020_CV	25.7441	62.2303	Europe	air	0	112494	112494	anthropogenic	2019	46	0.0%
Toju_2019_89C0	138.349	36.524	Asia	shoot	2451	0	2451	grassland	2017	1	0.0%
Duan_2018_DJ	-76.6707	34.7181	North America	water	9805	0	9805	aquatic	2012	4	0.0%
Abrego_2020_CV	24.1159	61.5944	Europe	air	0	231488	231488	forest	2019	94	0.0%
Zhou_2016_A8F1	-72.19	42.53	North America	soil	0	29568	29568	forest	2012	12	0.0%
Abrego_2018_CA	25.48	62.22	Europe	air	0	2491	2491	forest	2010	1	0.0%
Joergensen_2021_TK	19.82	64.3555	Europe	topsoil	0	2500	2500	forest	2016	1	0.0%
Sun_2021_PK	101.574	21.612	Asia	topsoil	0	22754	22754	forest	2015	9	0.0%
Tedersoo_2014_B9DD	53.0757	57.1041	Asia	soil	0	5191	5191	forest	2011	2	0.0%
Abrego_2018_CA	25.55	63.37	Europe	air	0	2596	2596	forest	2009	1	0.0%
Mikryukov_2021_SP	59.863	56.848	Asia	litter	0	36490	36490	forest	2017	14	0.0%

Toju_2019_89C0	138.349	36.524	Asia	shoot	5234	0	5234	grassland	2017	2	0.0%
Davey_2014_2252	10.7005	60.1418	Europe	shoot	0	2619	2619	forest	2010	1	0.0%
George_2019_9BEA	-3.55608	52.7224	Europe	soil	13176	0	13176	grassland	2013 to 2014	5	0.0%
Ovaskainen_2019_air	14.1938	46.5723	Europe	air	0	15927	15927	forest	2018	6	0.0%
Rajala_2015_1113	24.17	60.79	Europe	deadwood	2728	0	2728	forest	2008	1	0.0%
Rajala_2015_1113	25.11	61.35	Europe	deadwood	2736	0	2736	forest	2009	1	0.0%
Clemmensen_2015_B0AE	17.7492	66.1452	Europe	litter	0	2762	2762	forest	2009	1	0.0%
Toju_2019_89C0	138.349	36.524	Asia	shoot	5535	0	5535	grassland	2017	2	0.0%
Abrego_2020_CV	25.7346	62.1444	Europe	air	0	172149	172149	forest	2019	62	0.0%
Kovalchuk_2018_EDF8	25.2594	60.7542	Europe	shoot	0	100065	100065	forest	2016	36	0.0%
Fukasawa_2015_1109	135.48	35.02	Asia	deadwood	2814	0	2814	forest	2009	1	0.0%
Oja_2015_88D4	23.551	58.5552	Europe	soil	1423	1425	2848	forest	2011	1	0.0%

Abrego_2018_CA	25.55	63.37	Europe	air	0	2863	2863	forest	2009	1	0.0%
Abrego_2020_CV	25.7946	61.1032	Europe	air	0	220372	220372	forest	2019	74	0.0%
George_2019_9BEA	-3.82956	52.1779	Europe	soil	94163	0	94163	shrubland	2013 to 2014	31	0.0%
Zhao_2019_0D8E	117.575	32.0548	Asia	soil	0	12155	121555	cropland	2015	4	0.0%
URen_2019_add	14.3209	60.8918	Europe	shoot	0	15211	152111	forest	2012	5	0.0%
Toju_2019_89C0	138.349	36.524	Asia	shoot	6090	0	6090	grassland	2017	2	0.0%
Yang_2019_D4B1	118.14	29.257	Asia	soil	33783	0	33783	forest	2016	11	0.0%
Kyaschenko_2017_89D4	17.5037	60.0813	Europe	litter	0	3078	3078	forest	2012	1	0.0%
George_2019_9BEA	-3.55929	52.8123	Europe	soil	68076	0	68076	shrubland	2013 to 2014	22	0.0%
Tedersoo_2021_TJ	26.2646	58.7188	Europe	soil	3407	2792	6199	forest	2017	2	0.0%
Toju_2019_89C0	138.349	36.524	Asia	shoot	3148	0	3148	grassland	2017	1	0.0%

Anthony_2020_mBY	-72.1875	42.4836	North America	soil	0	28360	28360	forest	2016	9	0.0%
Toju_2019_89C0	138.349	36.524	Asia	root	3224	0	3224	grassland	2017	1	0.0%
Davey_2014_2252	10.6999	60.1422	Europe	shoot	0	3240	3240	forest	2010	1	0.0%
Hoppe_2015_BE27	9.26136	48.3962	Europe	deadwood	1329	1952	3281	forest	2009	1	0.0%
Kovalchuk_2018_EDF8	25.2233	60.7531	Europe	shoot	0	49455	49455	forest	2016	15	0.0%
Abrego_2020_CV	25.6093	62.2043	Europe	air	0	223420	22342	forest	2019	67	0.0%
Toju_2019_89C0	138.349	36.524	Asia	shoot	3342	0	3342	grassland	2017	1	0.0%
Baldrian_2016_DE02	14.7031	48.6644	Europe	deadwood	0	3348	3348	forest	2013	1	0.0%
Toju_2019_89C0	138.349	36.524	Asia	shoot	3361	0	3361	grassland	2017	1	0.0%
Yang_2016_0B27	128.065	42.058	Asia	shoot	13492	0	13492	forest	2013	4	0.0%
George_2019_9BEA	-3.70758	52.8102	Europe	soil	138654	0	138654	shrubland	2013 to 2014	40	0.0%

Schappe_2017_BF24	-79.78	9.33389	North America	soil	3493	0	3493	forest	2015	1	0.0%
Kovalchuk_2018_EDF8	25.2594	60.7542	Europe	shoot	0	148176	148176	forest	2016	42	0.0%
Abrego_2020_CV	25.7346	62.1444	Europe	air	0	219599	219599	forest	2019	62	0.0%
Davey_2014_2252	10.6851	60.1292	Europe	shoot	0	3589	3589	forest	2010	1	0.0%
Froeslev_2019_CA74	8.19077	55.6942	Europe	soil	0	25560	25560	forest	2014	7	0.0%
Tedersoo_2021_TJ	26.7213	58.3849	Europe	soil	4013	3297	7310	anthropogenic	2017	2	0.0%
Kovalchuk_2018_EDF8	25.2233	60.7531	Europe	shoot	0	69588	69588	forest	2016	19	0.0%
Abrego_2018_CA	25.55	63.37	Europe	air	0	3736	3736	forest	2009	1	0.0%
Mikryukov_2021_SP	59.425	56.801	Asia	litter	0	26285	26285	forest	2017	7	0.0%
Mikryukov_2021_SP	59.827	56.85	Asia	deadwood	0	48869	48869	forest	2017	13	0.0%
Toju_2016_2321	137.675	36.5	Asia	root	19146	0	19146	tundra	2013	5	0.0%
Toju_2019_89C0	138.349	36.524	Asia	shoot	7913	0	7913	grassland	2017	2	0.0%

Froeslev_2019_CA74	9.73053	55.6919	Europe	soil	0	16052	16052	forest	2014	4	0.0%
Yang_2019_D4B1	110.491	31.3245	Asia	soil	32235	0	32235	forest	2015	8	0.0%
Davey_2014_2252	10.7156	60.1478	Europe	shoot	0	4030	4030	forest	2010	1	0.0%
Ji_2016_C06E	110.55	-66.31	Antarctica	soil	4122	0	4122	desert	2006	1	0.0%
Siciliano_2014_FF	110.53	-66.31	Antarctica	soil	4122	0	4122	desert	2005 to 2008	1	0.0%
Clemmensen_2015_B0AE	17.8466	65.9548	Europe	litter	0	4143	4143	forest	2009	1	0.0%
Froeslev_2019_CA74	10.4717	56.2873	Europe	soil	0	20916	20916	forest	2014	5	0.0%
Kovalchuk_2018_EDF8	25.2233	60.7531	Europe	shoot	0	239665	239665	forest	2016	57	0.0%
Tedersoo_2014_B9DD	53.2202	57.0739	Asia	soil	0	4237	4237	forest	2011	1	0.0%
Yang_2019_D4B1	119.442	30.3251	Asia	soil	30238	0	30238	forest	2015	7	0.0%
Davey_2014_2252	10.6897	60.1301	Europe	shoot	0	4326	4326	forest	2010	1	0.0%

Ihrmark_2012_3AE5	18.816	68.3544	Europe	soil	0	4331	4331	forest	NA_	1	0.0%
Oh_2021_IE	126.728	33.478	Asia	soil	0	43655	43655	woodland	2015	10	0.0%
Davey_2014_2252	10.6902	60.1301	Europe	shoot	0	4372	4372	forest	2010	1	0.0%
Abrego_2018_CA	22.4988	59.7233	Europe	air	0	4409	4409	desert	2010	1	0.0%
URen_2019_add	-87.9251	46.8504	North America	shoot	0	13297	13297	forest	2013	3	0.0%
Clemmensen_2015_B0AE	17.8436	65.9468	Europe	litter	0	4440	4440	forest	2009	1	0.0%
Ovaskainen_2019_air	14.1938	46.5723	Europe	air	0	8899	8899	forest	2018	2	0.0%
Kovalchuk_2018_EDF8	25.2214	60.7475	Europe	shoot	0	62928	62928	forest	2016	14	0.0%
Toju_2019_89C0	138.349	36.524	Asia	shoot	9041	0	9041	grassland	2017	2	0.0%
Kovalchuk_2018_EDF8	25.2233	60.7531	Europe	shoot	0	153931	153931	forest	2016	34	0.0%
Abrego_2020_CV	23.7489	61.5036	Europe	air	0	139517	139517	anthropogenic	2019	30	0.0%
Yang_2019_D4B1	110.424	31.6792	Asia	soil	37464	0	37464	forest	2015	8	0.0%

Tedersoo_2014_B9DD	-69.54	-4.025	South America	soil	0	4706	4706	forest	2011	1	0.0%
Yang_2019_D4B1	110.492	31.3235	Asia	soil	33507	0	33507	forest	2015	7	0.0%
Abrego_2020_CV	30.1733	62.6131	Europe	air	0	100989	100989	forest	2019	21	0.0%
Kovalchuk_2018_EDF8	25.2594	60.7542	Europe	shoot	0	53061	53061	forest	2016	11	0.0%
Toju_2019_89C0	138.349	36.524	Asia	shoot	4847	0	4847	grassland	2017	1	0.0%
van_der_Wal_2017_3070	5.63	52.25	Europe	soil	0	4930	4930	forest	2012	1	0.0%
RoyBolduc_2015_ED	-61.7413	47.4756	North America	soil	5405	4512	9917	wetland	2011	2	0.0%
RoyBolduc_2016_F11B	-61.7413	47.4756	North America	soil	5405	4512	9917	forest	2011	2	0.0%
Tedersoo_2016_ISME	21.7	61.7	Europe	soil	0	4988	4988	forest	2011	1	0.0%
Toju_2019_89C0	138.349	36.524	Asia	shoot	5079	0	5079	grassland	2017	1	0.0%

	-111.552	59.7184	North America	shoot	0	15364	15364	forest	2013	3	0.0%
Mikryukov_2021_SP	59.425	56.801	Asia	deadwood	0	51302	51302	forest	2017	10	0.0%
Tedersoo_2016_ISME	21.77	61.77	Europe	soil	0	5143	5143	forest	2011	1	0.0%
Tedersoo_2014_B9DD	-69.8947	-3.9997	South America	soil	0	5323	5323	forest	2011	1	0.0%
Mikryukov_2021_SP	59.827	56.85	Asia	litter	0	54544	54544	forest	2017	10	0.0%
Tedersoo_2014_B9DD	-69.913	-4.133	South America	soil	0	5553	5553	forest	2011	1	0.0%
Poosakkannu_2017_B342	24.7036	68.4878	Europe	rhizosphere soil	0	5806	5806	desert	2011	1	0.0%
Kovalchuk_2018_EDF8	25.2233	60.7531	Europe	root	0	181801	181801	forest	2016	31	0.0%
Abrego_2020_CV	23.7617	61.4997	Europe	air	0	152673	152673	anthropogenic	2019	26	0.0%
Yang_2019_D4B1	110.491	31.3266	Asia	soil	58973	0	58973	forest	2015	10	0.0%
Mikryukov_2021_SP	59.863	56.848	Asia	litter	0	82744	82744	forest	2017	14	0.0%

Vasutova_2021_b815	15.2449	50.8313	Europe	shoot	0	5919	5919	wetland	2016	1	0.0%
Tedersoo_2016_ISME	21.7	61.7	Europe	soil	0	5949	5949	forest	2011	1	0.0%
Ovaskainen_2019_air	14.1938	46.5723	Europe	air	0	29886	29886	forest	2018	5	0.0%
Mikryukov_2021_SP	59.827	56.85	Asia	litter	0	18067	18067	forest	2017	3	0.0%
Zheng_2021_QP	112.333	16.8333	Asia	soil	0	24166	24166	woodland	2014	4	0.0%
Mikryukov_2021_SP	59.425	56.801	Asia	litter	0	24272	24272	forest	2017	4	0.0%
Veloso_2020_EB	-41.0261	-20.1617	South America	shoot	42729	0	42729	cropland	2016	7	0.0%
Yang_2019_D4B1	118.144	29.2586	Asia	soil	36756	0	36756	forest	2016	6	0.0%
Tedersoo_2016_ISME	27.3238	58.2778	Europe	soil	0	6149	6149	forest	2011	1	0.0%
Elfstrand_2019_29C7	13.9871	55.9027	Europe	shoot	1	43421	43422	forest	2013 to 2014	7	0.0%
Toju_2019_89C0	138.349	36.524	Asia	shoot	6313	0	6313	grassland	2017	1	0.0%
Toju_2016_2321	137.6	36.573	Asia	root	12718	0	12718	tundra	2013	2	0.0%

TignatPerrier_2020_addCL	2.95	45.77	Europe	air	0	31874	31874	grassland	2016	5	0.0%
Abrego_2018_CA	25.48	62.22	Europe	air	0	6459	6459	forest	2010	1	0.0%
Darcy_2020_CT	-155.82	19.115	North America	shoot	6507	0	6507	forest	2015	1	0.0%
Mikryukov_2021_SP	59.863	56.848	Asia	litter	0	45910	45910	forest	2017	7	0.0%
Mikryukov_2021_SP	59.425	56.801	Asia	litter	0	32852	32852	forest	2017	5	0.0%
Kovalchuk_2018_EDF8	25.2233	60.7531	Europe	shoot	0	52603	52603	forest	2016	8	0.0%
Tedersoo_2014_B9DD	-69.8983	-4.0175	South America	soil	0	6607	6607	forest	2011	1	0.0%
Toju_2019_89C0	138.349	36.524	Asia	shoot	6686	0	6686	grassland	2017	1	0.0%
Ovaskainen_2019_air	14.1938	46.5723	Europe	air	0	27350	27350	forest	2018	4	0.0%
Elfstrand_2019_29C7	13.9871	55.9027	Europe	shoot	1	51057	51058	forest	2013 to 2014	7	0.0%
Toju_2019_89C0	138.349	36.524	Asia	shoot	7301	0	7301	grassland	2017	1	0.0%

Mikryukov_2021_SP	59.827	56.85	Asia	litter	0	29625	29625	forest	2017	4	0.0%
URen_2019_add	-88.0708	46.8539	North America	shoot	0	14873	14873	forest	2013	2	0.0%
RoyBolduc_2016_E50C	-61.754	47.453	North America	root	4068	3389	7457	forest	2010	1	0.0%
Mikryukov_2021_SP	59.827	56.85	Asia	litter	0	82694	82694	forest	2017	11	0.0%
Harantova_2017_FU	12.6584	50.2383	Europe	soil	0	7720	7720	grassland	2008	1	0.0%
Cross_2017_2AFC	10.7753	59.6789	Europe	shoot	0	7796	7796	forest	2011	1	0.0%
Ritter_2020_BI	-60.3228	-2.56035	South America	soil	3905	3894	7799	forest	2015	1	0.0%
Polackova_2016_KRTINY	16.6178	49.3077	Europe	soil	0	7951	7951	forest	2013	1	0.0%
Tedersoo_2016_ISME	21.7	61.7	Europe	soil	0	7982	7982	forest	2011	1	0.0%
Mikryukov_2021_SP	59.425	56.801	Asia	litter	0	40231	40231	forest	2017	5	0.0%

Siciliano_2014_F	110.53	-66.31	Antarctica	soil	8080	0	8080	desert	2005 to 2008	1	0.0%
Ji_2016_C06E	110.55	-66.31	Antarctica	soil	8080	0	8080	desert	2006	1	0.0%
Cross_2017_2AFC	10.7753	59.6789	Europe	shoot	0	16454	16454	forest	2011	2	0.0%
Kovalchuk_2018_EDF8	25.2594	60.7542	Europe	root	0	131792	131792	forest	2016	16	0.0%
Lepinay_2021_SO	16.9463	48.6773	Europe	deadwood	0	8333	8333	forest	2016	1	0.0%
Kovalchuk_2018_EDF8	25.2594	60.7542	Europe	root	0	209094	209094	forest	2016	25	0.0%
Kovalchuk_2018_EDF8	25.2214	60.7475	Europe	shoot	0	184599	184599	forest	2016	22	0.0%
Ovaskainen_2019_air	14.1938	46.5723	Europe	air	0	25861	25861	forest	2018	3	0.0%
URen_2019_add	-73.0713	52.4132	North America	shoot	0	9115	9115	forest	2011	1	0.0%
Liu_2020_add	108.85	18.7333	Asia	soil	0	36554	36554	forest	2014	4	0.0%
Boeraeve_2019_1AJ	4.90378	50.8656	Europe	soil	0	9143	9143	forest	2018	1	0.0%

Kovalchuk_2018_EDF8	25.2594	60.7542	Europe	shoot	0	184900	184900	forest	2016	20	0.0%
Mikryukov_2021_SP	59.827	56.85	Asia	litter	0	27901	27901	forest	2017	3	0.0%
Zhang_2017_02C2	124.95	41.85	Asia	topsoil	0	46705	46705	forest	2013	5	0.0%
Mikryukov_2021_SP	59.425	56.801	Asia	litter	0	18790	18790	forest	2017	2	0.0%
TignatPerrier_2020_addCL	2.95	45.77	Europe	air	0	18974	18974	grassland	2017	2	0.0%
Polackova_2016_KRTINY	16.6541	49.3214	Europe	litter	0	9682	9682	forest	2013	1	0.0%
Kovalchuk_2018_EDF8	25.2594	60.7542	Europe	shoot	0	107057	107057	forest	2016	11	0.0%
URen_2019_add	134.783	48.2195	Asia	lichen	0	9737	9737	forest	2013	1	0.0%
Abrego_2020_CV	25.759	62.1538	Europe	air	0	178052	178052	anthropogenic	2019	18	0.0%
Zhang_2016_DO	126.905	27.8078	Pacific Ocean	sediment	9913	0	9913	aquatic	2014	1	0.0%
Elfstrand_2019_29C7	13.9871	55.9027	Europe	shoot	0	20181	20181	forest	2013 to 2014	2	0.0%
Baldrian_2016_DE02	14.7099	48.6645	Europe	deadwood	0	10193	10193	forest	2013	1	0.0%

Yang_2019_D4B1	118.141	29.2564	Asia	soil	30662	0	30662	forest	2016	3	0.0%
URen_2019_add	134.783	48.2195	Asia	lichen	0	10228	10228	forest	2013	1	0.0%
Yang_2019_D4B1	119.432	30.3482	Asia	soil	71731	0	71731	forest	2015	7	0.0%
Toju_2019_89C0	138.349	36.524	Asia	shoot	10255	0	10255	grassland	2017	1	0.0%
Ovaskainen_2019_air	14.1938	46.5723	Europe	air	0	31079	31079	forest	2018	3	0.0%
Mikryukov_2021_SP	59.827	56.85	Asia	deadwood	0	41760	41760	forest	2017	4	0.0%
Polackova_2016_KRTINY	16.6237	49.2637	Europe	soil	0	31634	31634	forest	2013	3	0.0%
Sukdeo_2018_1DF4	-123.267	54.3333	North America	soil	0	164989	164989	forest	2015	15	0.0%
Sun_2021_PK	101.02	24.53	Asia	topsoil	0	879975	879975	forest	2014	80	0.0%
Merges_2018_DD53	9.90382	46.8015	Europe	soil	0	22007	22007	forest	2015	2	0.0%
Elfstrand_2019_29C7	13.9871	55.9027	Europe	shoot	0	22558	22558	forest	2013 to 2014	2	0.0%
Mikryukov_2021_SP	59.863	56.848	Asia	litter	0	56959	56959	forest	2017	5	0.0%

Mikryukov_2021_SP	59.827	56.85	Asia	litter	0	57049	57049	forest	2017	5	0.0%
Darcy_2020_CT	-158.136	21.5119	North America	shoot	23115	0	23115	forest	2015	2	0.0%
Lepinay_2021_SO	16.9472	48.679	Europe	deadwood	0	11592	11592	forest	2016	1	0.0%
Kovalchuk_2018_EDF8	25.2594	60.7542	Europe	root	0	105119	105119	forest	2016	9	0.0%
Zheng_2021_QP	114.014	21.8465	Asia	soil	0	35156	35156	woodland	2014	3	0.0%
Froeslev_2019_CA74	8.38886	56.1673	Europe	soil	0	23550	23550	shrubland	2014	2	0.0%
Abrego_2020_CV	30.1733	62.6131	Europe	air	0	259908	259908	forest	2019	22	0.0%
Kovalchuk_2018_EDF8	25.2233	60.7531	Europe	shoot	0	216139	216139	forest	2016	18	0.0%
Sun_2021_PK	101.02	24.53	Asia	topsoil	0	1118060	1118060	forest	2017	92	0.0%
Siciliano_2014_FF	-110.53	-66.31	Antarctica	soil	12318	5	12323	desert	2005 to 2008	1	0.0%
Ji_2016_C06E	-110.55	-66.31	Antarctica	soil	12318	5	12323	desert	2006	1	0.0%

Froeslev_2019_CA74	12.2928	55.9846	Europe	soil	0	12341	12341	shrubland	2014	1	0.0%
TignatPerrier_2020_addCL	2.95	45.77	Europe	air	0	24962	24962	grassland	2016	2	0.0%
Yang_2019_D4B1	110.354	31.4925	Asia	soil	74976	0	74976	forest	2015	6	0.0%
URen_2019_add	-73.0732	52.4132	North America	shoot	0	25028	25028	forest	2011	2	0.0%
Yang_2019_D4B1	128.353	42.3777	Asia	soil	39200	0	39200	forest	2016	3	0.0%
Mikryukov_2021_SP	59.863	56.848	Asia	deadwood	0	78912	78912	forest	2017	6	0.0%
Mikryukov_2021_SP	59.863	56.848	Asia	litter	0	67073	67073	forest	2017	5	0.0%
Mikryukov_2021_SP	59.827	56.85	Asia	litter	0	26932	26932	forest	2017	2	0.0%
Polackova_2016_KRTINY	16.7457	49.3021	Europe	litter	0	13577	13577	forest	2013	1	0.0%
Mikryukov_2021_SP	59.827	56.85	Asia	litter	0	68975	68975	forest	2017	5	0.0%
Yang_2019_D4B1	118.14	29.2569	Asia	soil	42368	0	42368	forest	2016	3	0.0%
Liu_2020_add	108.983	18.75	Asia	soil	0	56911	56911	forest	2014	4	0.0%

Sun_2021_PK	101.02	24.53	Asia	topsoil	0	956396	956396	forest	2014	67	0.0%
PradaSalcedo_2021_GT	26.05	47.31	Europe	soil	0	57344	57344	forest	2017	4	0.0%
Sun_2021_PK	101.016	24.533	Asia	topsoil	0	58432	58432	forest	2015	4	0.0%
George_2019_9BEA	-4.16128	52.9827	Europe	soil	87899	0	87899	grassland	2013 to 2014	6	0.0%
Zhang_2017_02C2	124.95	41.85	Asia	soil	0	44650	44650	forest	2013	3	0.0%
Sun_2021_PK	101.574	21.612	Asia	topsoil	0	60000	60000	forest	2015	4	0.0%
Abrego_2020_CV	24.0294	61.5378	Europe	air	0	30340	30340	forest	2019	2	0.0%
Kovalchuk_2018_EDF8	25.2233	60.7531	Europe	root	0	169320	169320	forest	2016	11	0.0%
UOBC_2016_5CA6	-83.37	46.42	North America	soil	0	15653	15653	forest	2011	1	0.0%
Shigyo_2021_TF	138.804	35.9367	Asia	soil	0	31625	31625	forest	2014	2	0.0%
Baldrian_2016_DE02	14.7055	48.6666	Europe	deadwood	0	15849	15849	forest	2013	1	0.0%
Samonil_2020_GB	14.7095	48.6641	Europe	soil	0	15973	15973	forest	2015	1	0.0%

Abrego_2020_C	25.66	61.0					1498	anthrop			
V	53	086	Europe	air	0	149823	23	ogenic	2019	9	0.0%
Abrego_2020_C	30.17	62.6					1831				
V	33	131	Europe	air	0	183172	72	forest	2019	11	0.0%
Mikryukov_2021_	59.82	56.8					1673				
SP	7	5	Asia	litter	0	16739	9	forest	2017	1	0.0%
Yang_2019_D4B	118.1	29.2					3356				
1	25	466	Asia	soil	33561	0	1	forest	2016	2	0.0%
Yang_2019_D4B	118.1	29.2					3400				
1	44	516	Asia	soil	34005	0	5	forest	2016	2	0.0%
Mikryukov_2021_	59.86	56.8					8537				
SP	3	48	Asia	litter	0	85378	8	forest	2017	5	0.0%
Mikryukov_2021_	59.82	56.8		deadwo			6890				
SP	7	5	Asia	od	0	68909	9	forest	2017	4	0.0%
	-										
DelgadoBaqueriz	1.673	37.8					8875	shrubla			
o_2017_BB88	75	212	Europe	soil	0	88758	8	nd	2006	5	0.0%
Lepinay_2021_S	16.94	48.6		deadwo			1841				
O	81	781	Europe	od	0	18416	6	forest	2016	1	0.0%
	-	-									
Detheridge_2020	5.679	15.9					3692	woodla			
_Z	31	489	Africa	soil	0	36922	2	nd	2018	2	0.0%
Mikryukov_2021_	59.42	56.8					7464				
SP	5	01	Asia	litter	0	74644	4	forest	2017	4	0.0%

Benucci_2020_1AF	174.721	-41.2989	Australia	root	730450	98244	828694	forest	2014	44	0.0%
Guo_2018_0653	-97.5167	34.9833	North America	topsoil	0	19004	190004	grassland	2013	1	0.0%
Mikryukov_2021_SP	59.827	56.85	Asia	litter	0	19294	192944	forest	2017	1	0.0%
Odriozola_2021_QY	13.9411	48.8133	Europe	litter	0	19315	193155	forest	2016	1	0.0%
Zhang_2017_02C2	124.9	41.85	Asia	topsoil	0	58619	586199	forest	2013	3	0.0%
Zhao_2019_0D8E	117.575	32.055	Asia	soil	0	19760	197600	cropland	2015	1	0.0%
Mikryukov_2021_SP	59.827	56.85	Asia	deadwood	0	40366	403666	forest	2017	2	0.0%
Harantova_2017_FU	12.6793	50.2421	Europe	soil	0	20236	202366	shrubland	2006	1	0.0%
Zhang_2017_02C2	124.9	41.85	Asia	topsoil	0	61082	610822	forest	2013	3	0.0%
Oh_2021_IE	126.728	33.478	Asia	shoot	0	193103	19310303	woodland	2015	9	0.0%
URen_2019_add	135.957	47.8167	Asia	lichen	0	21570	215700	forest	2013	1	0.0%

Sun_2021_PK	101.57	21.61	Asia	topsoil	0	389827	389827	forest	2017	18	0.0%
Kovalchuk_2018_EDF8	25.2594	60.7542	Europe	shoot	0	200790	200790	forest	2016	9	0.0%
Mikryukov_2021_SP	59.425	56.801	Asia	litter	0	23272	23272	forest	2017	1	0.0%
Darcy_2020_CT	-158.136	21.5119	North America	shoot	23337	0	23337	forest	2015	1	0.0%
Shigyo_2021_TF	138.827	35.9272	Asia	soil	0	23401	23401	forest	2014	1	0.0%
Mikryukov_2021_SP	59.425	56.801	Asia	litter	0	71144	71144	forest	2017	3	0.0%
TignatPerrier_2020_addCL	2.95	45.77	Europe	air	0	23794	23794	grassland	2016	1	0.0%
Sun_2021_PK	101.57	21.61	Asia	topsoil	0	357923	357923	forest	2017	15	0.0%
Mikryukov_2021_SP	59.863	56.848	Asia	deadwood	0	24001	24001	forest	2017	1	0.0%
Sun_2021_PK	101.57	21.61	Asia	topsoil	0	409653	409653	forest	2016	17	0.0%
Polackova_2016_KRTINY	16.6786	49.2674	Europe	soil	0	48308	48308	forest	2013	2	0.0%

Darcy_2020_CT	-155.82	19.115	North America	shoot	24267	0	24267	forest	2015	1	0.0%
Lepinay_2021_SO	16.947	48.6793	Europe	deadwood	0	24413	24413	forest	2016	1	0.0%
Kovalchuk_2018_EDF8	25.2594	60.7542	Europe	shoot	0	198169	198169	forest	2016	8	0.0%
Darcy_2020_CT	-156.93	21.1191	North America	shoot	24931	0	24931	forest	2016	1	0.0%
Sun_2021_PK	101.02	24.53	Asia	topsoil	0	150105	150105	forest	2014	6	0.0%
Nakayama_2019_3780	144.64	43.4018	Asia	soil	25065	0	25065	forest	2012	1	0.0%
Ovaskainen_2019_air	14.1938	46.5723	Europe	air	0	25209	25209	forest	2018	1	0.0%
Mikryukov_2021_SP	59.863	56.848	Asia	deadwood	0	50969	50969	forest	2017	2	0.0%
Yang_2016_DA04	128.067	42.073	Asia	shoot	26047	0	26047	forest	2013	1	0.0%
Kovalchuk_2018_EDF8	25.2594	60.7542	Europe	shoot	0	191417	191417	forest	2016	7	0.0%
Ovaskainen_2019_air	14.1938	46.5723	Europe	air	0	28741	28741	forest	2018	1	0.0%

Mikryukov_2021_SP	59.425	56.801	Asia	litter	0	28959	28959	forest	2017	1	0.0%
Kovalchuk_2018_EDF8	25.2214	60.7475	Europe	shoot	0	28971	28971	forest	2016	1	0.0%
Zheng_2021_QP	114.014	21.8465	Asia	soil	0	29439	29439	woodland	2014	1	0.0%
Zhang_2017_02C2	124.95	41.85	Asia	topsoil	0	58893	58893	forest	2013	2	0.0%
Ovaskainen_2019_air	8.5511	47.3962	Europe	air	0	29608	29608	anthropogenic	2018	1	0.0%
Elfstrand_2019_29C7	13.9871	55.9027	Europe	shoot	0	29882	29882	forest	2013 to 2014	1	0.0%
Woo_2018_BY	126.955	37.4653	Asia	dust	89677	0	89677	anthropogenic	2015	3	0.0%
Oh_2021_IE	126.728	33.478	Asia	shoot	0	180051	180051	woodland	2015	6	0.0%
Abrego_2020_CV	25.6093	62.2043	Europe	air	0	210955	210955	forest	2019	7	0.0%
Veloso_2020_EB	-41.0261	-20.1617	South America	shoot	30342	0	30342	cropland	2016	1	0.0%
Yang_2019_D4B1	128.162	42.2728	Asia	soil	30518	0	30518	forest	2016	1	0.0%
TignatPerrier_2020_addCL	2.95	45.77	Europe	air	0	30606	30606	grassland	2016	1	0.0%

Sun_2021_PK	101.02	24.53	Asia	topsoil	0	159618	159618	forest	2014	5	0.0%
Lanzen_2016_CCBC	0.077	42.676	Europe	soil	128370	0	128370	grassland	2013	4	0.0%
TignatPerrier_2020_addCL	2.95	45.77	Europe	air	0	32501	32501	grassland	2017	1	0.0%
Yang_2019_D4B1	119.424	30.3498	Asia	soil	65428	0	65428	forest	2015	2	0.0%
Boeraeve_2018_B175	4.95	50.88	Europe	root	32790	0	32790	forest	2015	1	0.0%
Sun_2021_PK	101.02	24.53	Asia	topsoil	0	1265810	1265810	forest	2017	38	0.0%
Sun_2021_PK	101.02	24.53	Asia	topsoil	0	68526	68526	forest	2014	2	0.0%
Samonil_2020_GB	14.7048	48.6767	Europe	soil	0	34725	34725	forest	2015	1	0.0%
Semenova-Nelsen_2019_add	-84	30.75	North America	litter	0	34773	34773	forest	2014	1	0.0%
Boeraeve_2018_17A7	4.384	50.916	Europe	root	35489	0	35489	forest	2016	1	0.0%
Yang_2019_D4B1	128.059	42.5685	Asia	soil	36740	0	36740	forest	2016	1	0.0%
Polackova_2016_KRTINY	16.6452	49.3178	Europe	litter	0	37407	37407	forest	2013	1	0.0%

Anthony_2017_647F	-73.2508	42.1291	North America	soil	0	114015	114015	forest	2013	3	0.0%
Sun_2021_PK	101.02	24.53	Asia	topsoil	0	1142008	1142008	forest	2014	30	0.0%
Yang_2019_D4B1	128.1	42.4029	Asia	soil	38325	0	38325	forest	2016	1	0.0%
Semenova-Nelsen_2019_add	-84	30.75	North America	litter	0	38609	38609	forest	2014	1	0.0%
Liu_2019_A7FB	127.461	50.2533	Asia	rhizosphere soil	39303	0	39303	cropland	2015	1	0.0%
Liu_2020_M	127.461	50.2533	Asia	rhizosphere soil	39303	0	39303	cropland	2015	1	0.0%
Mikryukov_2021_SP	59.827	56.85	Asia	litter	0	79504	79504	forest	2017	2	0.0%
Yang_2019_D4B1	128.163	42.2734	Asia	soil	39959	0	39959	forest	2016	1	0.0%
Woo_2018_BY	126.955	37.4653	Asia	dust	82346	0	82346	anthropogenic	2015	2	0.0%
Zhang_2017_02C2	124.9	41.85	Asia	soil	0	41200	41200	forest	2013	1	0.0%
George_2019_9BEA	-4.84076	51.9792	Europe	soil	84605	0	84605	shrubland	2013 to 2014	2	0.0%

Yang_2019_D4B1	110.483	31.3215	Asia	soil	42352	0	42352	forest	2015	1	0.0%
Kovalchuk_2018_EDF8	25.2233	60.7531	Europe	shoot	0	212188	212188	forest	2016	5	0.0%
Mikryukov_2021_SP	59.863	56.848	Asia	litter	0	84970	84970	forest	2017	2	0.0%
Yang_2019_D4B1	118.144	29.2535	Asia	soil	43958	0	43958	forest	2016	1	0.0%
Yang_2019_D4B1	118.144	29.256	Asia	soil	44206	0	44206	forest	2016	1	0.0%
Teng_2021_PZ	112.1	36.7	Asia	topsoil	44372	0	44372	forest	2013	1	0.0%
Yang_2019_D4B1	118.144	29.2571	Asia	soil	44623	0	44623	forest	2016	1	0.0%
Yang_2019_D4B1	118.144	29.2586	Asia	soil	44683	0	44683	forest	2016	1	0.0%
Mikryukov_2021_SP	59.425	56.801	Asia	litter	0	44816	44816	forest	2017	1	0.0%
Yang_2019_D4B1	128.06	42.5676	Asia	soil	44865	0	44865	forest	2016	1	0.0%
Zhou_2016_A8F1	-72.19	42.53	North America	soil	0	44925	44925	forest	2012	1	0.0%
Lepinay_2021_SO	16.9476	48.6774	Europe	deadwood	0	45256	45256	forest	2016	1	0.0%

Kovalchuk_2018_EDF8	25.2233	60.7531	Europe	shoot	0	182256	182256	forest	2016	4	0.0%
Kovalchuk_2018_EDF8	25.2214	60.7475	Europe	shoot	0	137138	137138	forest	2016	3	0.0%
Semenova-Nelsen_2019_add	-84	30.75	North America	litter	0	45858	45858	forest	2014	1	0.0%
Yang_2019_D4B1	119.435	30.3459	Asia	soil	47673	0	47673	forest	2015	1	0.0%
Sun_2021_PK	101.02	24.53	Asia	topsoil	0	1885233	1885233	forest	2014	39	0.0%
Bissett_AAAA_2016	148.831	-35.3365	Australia	soil	45399	3123	48522	forest	2013	1	0.0%
Brown_2019_add	-83.5345	35.6953	North America	soil	0	49309	49309	forest	2017	1	0.0%
Boeraeve_2021_II	4.4643	50.8151	Europe	root	0	49588	49588	forest	2019	1	0.0%
Kovalchuk_2018_EDF8	25.2214	60.7475	Europe	shoot	0	149375	149375	forest	2016	3	0.0%
Sun_2021_PK	101.016	24.533	Asia	topsoil	0	49896	49896	forest	2015	1	0.0%
Elfstrand_2019_29C7	13.9871	55.9027	Europe	shoot	0	50270	50270	forest	2013 to 2014	1	0.0%

George_2019_9BEA	-3.71466	52.99	Europe	soil	101506	0	101506	cropland	2013 to 2014	2	0.0%
Sun_2021_PK	101.02	24.53	Asia	topsoil	0	1851839	1851839	forest	2014	36	0.0%
Kovalchuk_2018_EDF8	25.2594	60.7542	Europe	shoot	0	155166	155166	forest	2016	3	0.0%
Woo_2018_BY	126.955	37.4653	Asia	air	53203	0	53203	anthropogenic	2015	1	0.0%
Shigyo_2021_TF	138.825	35.9505	Asia	soil	0	53243	53243	forest	2014	1	0.0%
Mikryukov_2021_SP	59.827	56.85	Asia	litter	0	53480	53480	forest	2017	1	0.0%
Zhang_2017_02C2	124.95	41.85	Asia	soil	0	54380	54380	forest	2013	1	0.0%
Kovalchuk_2018_EDF8	25.2214	60.7475	Europe	shoot	0	109620	109620	forest	2016	2	0.0%
Oh_2021_IE	126.728	33.478	Asia	soil	0	55357	55357	woodland	2015	1	0.0%
Zhang_2017_02C2	124.95	41.85	Asia	soil	0	55382	55382	forest	2013	1	0.0%
George_2019_9BEA	-3.66333	51.642	Europe	soil	278361	0	278361	grassland	2013 to 2014	5	0.0%

Kovalchuk_2018_EDF8	25.2594	60.7542	Europe	shoot	0	226645	226645	forest	2016	4	0.0%
Cai_2020_addG	99.49	26.52	Asia	shoot	56974	0	56974	cropland	2017	1	0.0%
Sun_2021_PK	101.02	24.53	Asia	topsoil	0	1662226	1662226	forest	2014	29	0.0%
Nakayama_2019_3780	144.654	43.3463	Asia	soil	57903	0	57903	forest	2012	1	0.0%
Fan_2019_BU	116.48	39.88	Asia	air	59362	0	59362	anthropogenic	2014	1	0.0%
Mikryukov_2021_SP	59.425	56.801	Asia	litter	0	60013	60013	forest	2017	1	0.0%
Sukdeo_2018_1DF4	-123.267	54.3333	North America	soil	0	240953	240953	forest	2014	4	0.0%
Mikryukov_2021_SP	59.863	56.848	Asia	litter	0	60353	60353	forest	2017	1	0.0%
Sun_2021_PK	101.02	24.53	Asia	topsoil	0	1579818	1579818	forest	2017	26	0.0%
Sun_2021_PK	101.02	24.53	Asia	topsoil	0	1217512	1217512	forest	2017	20	0.0%
Cregger_2018_added	-83.96	35.84	North America	shoot	0	182688	182688	forest	2014	3	0.0%
Zhang_2017_02C2	124.9	41.85	Asia	topsoil	0	60993	60993	forest	2013	1	0.0%

Zhang_2017_02 C2	124.9	41.8 5	Asia	topsoil	0	61388	6138 8	forest	2013	1	0.0%
Sun_2021_PK	101.0 2	24.5 3	Asia	topsoil	0	1663763	1663 763	forest	2014	27	0.0%
Sun_2021_PK	101.0 2	24.5 3	Asia	topsoil	0	432006	4320 06	forest	2017	7	0.0%
Sun_2021_PK	101.0 2	24.5 3	Asia	topsoil	0	1896327	1896 327	forest	2017	30	0.0%
Talas_2021_OR	27.14 92	56.7 602	Europe	sedimen t	0	64066	6406 6	aquatic	2013	1	0.0%
Anthony_2017_6 47F	- 73.25 08	42.1 291	North America	soil	0	131926	1319 26	forest	2013	2	0.0%
Mikryukov_2021_ SP	59.82 7	56.8 5	Asia	litter	0	66506	6650 6	forest	2017	1	0.0%
Kovalchuk_2018 _EDF8	25.25 94	60.7 542	Europe	shoot	0	69399	6939 9	forest	2016	1	0.0%
George_2019_9B EA	- 3.686 78	52.2 711	Europe	soil	213653	0	2136 53	shrubla nd	2013 to 2014	3	0.0%
Bayranvand_202 0_FT	52.08 19	36.3 713	Asia	soil	0	71430	7143 0	forest	2018	1	0.0%
Kovalchuk_2018 _EDF8	25.22 33	60.7 531	Europe	shoot	0	215002	2150 02	forest	2016	3	0.0%

	-83.2344	35.082	North America	soil	0	73869	73869	forest	2017	1	0.0%
Mikryukov_2021_SP	59.425	56.801	Asia	deadwood	0	74477	74477	forest	2017	1	0.0%
Kovalchuk_2018_EDF8	25.2214	60.7475	Europe	shoot	0	74825	74825	forest	2016	1	0.0%
Boeraeve_2018_17A7	2.787	50.866	Europe	root	75393	0	75393	forest	2016	1	0.0%
Mikryukov_2021_SP	59.425	56.801	Asia	deadwood	0	75984	75984	forest	2017	1	0.0%
Park_2020_609a	128.463	38.0321	Asia	rhizosphere soil	0	152677	152677	forest	2018	2	0.0%
Kovalchuk_2018_EDF8	25.2214	60.7475	Europe	shoot	0	76908	76908	forest	2016	1	0.0%
Brown_2019_add	-83.2344	35.082	North America	soil	0	77438	77438	forest	2017	1	0.0%
Sun_2021_PK	101.02	24.53	Asia	topsoil	0	156791	156791	forest	2014	2	0.0%
Sun_2021_PK	101.02	24.53	Asia	topsoil	0	396293	396293	forest	2014	5	0.0%
He_2021_mEA	112.167	23.1667	Asia	soil	0	79657	79657	forest	2016	1	0.0%

Kovalchuk_2018_EDF8	25.2594	60.7542	Europe	shoot	0	167577	167577	forest	2016	2	0.0%
Park_2020_609a	128.463	38.0321	Asia	rhizosphere soil	0	167938	167938	forest	2018	2	0.0%
Sun_2021_PK	101.02	24.53	Asia	topsoil	0	430552	430552	forest	2014	5	0.0%
George_2019_9BEA	-3.39661	52.3648	Europe	soil	266779	0	266779	forest	2013 to 2014	3	0.0%
Mikryukov_2021_SP	59.425	56.801	Asia	deadwood	0	92175	92175	forest	2017	1	0.0%
Gomes_2017_2AFC	150.275	-33.6478	Australia	soil	0	185924	185924	forest	2012	2	0.0%
Woo_2018_BY	126.955	37.4653	Asia	dust	94732	0	94732	anthropogenic	2015	1	0.0%
Boeraeve_2018_17A7	4.114	50.869	Europe	root	288563	0	288563	forest	2016	3	0.0%
Kovalchuk_2018_EDF8	25.2594	60.7542	Europe	shoot	0	193216	193216	forest	2016	2	0.0%
Kovalchuk_2018_EDF8	25.2594	60.7542	Europe	root	0	97236	97236	forest	2016	1	0.0%
Sun_2021_PK	101.02	24.53	Asia	topsoil	0	1217578	1217578	forest	2014	12	0.0%

	101.02	24.53					922592				
Sun_2021_PK			Asia	topsoil	0			forest	2014	9	0.0%
Yang_2019_D4B1	119.439	30.3439	Asia	soil	102835	0	102835	forest	2015	1	0.0%
	101.02	24.53					1137139				
Sun_2021_PK			Asia	topsoil	0	1137139		forest	2017	11	0.0%
	101.02	24.53					980326				
Sun_2021_PK			Asia	topsoil	0	980326		forest	2014	9	0.0%
	101.02	24.53					917814				
Sun_2021_PK			Asia	topsoil	0	917814		forest	2014	8	0.0%
Kovalchuk_2018_EDF8	25.2233	60.7531	Europe	shoot	0	114962	114962	forest	2016	1	0.0%
	101.02	24.53					935057				
Sun_2021_PK			Asia	topsoil	0	935057		forest	2014	8	0.0%
Kovalchuk_2018_EDF8	25.2214	60.7475	Europe	root	0	117600	117600	forest	2016	1	0.0%
Kovalchuk_2018_EDF8	25.2233	60.7531	Europe	shoot	0	119545	119545	forest	2016	1	0.0%
	101.02	24.53					1819929				
Sun_2021_PK			Asia	topsoil	0	1819929		forest	2017	15	0.0%
Kovalchuk_2018_EDF8	25.2233	60.7531	Europe	shoot	0	121585	121585	forest	2016	1	0.0%
	101.02	24.53					1099464				
Sun_2021_PK			Asia	topsoil	0	1099464		forest	2017	9	0.0%

Kovalchuk_2018_EDF8	25.22 14	60.7 475	Europe	shoot	1	128124	1281 25	forest	2016	1	0.0%
Kovalchuk_2018_EDF8	25.22 33	60.7 531	Europe	shoot	0	128457	1284 57	forest	2016	1	0.0%
Sun_2021_PK	101.0 2	24.5 3	Asia	topsoil	0	1689355	1689 355	forest	2017	13	0.0%
Franzetti_2020_GF	10.58 51	46.4 049	Europe	soil	137974	0	1379 74	tundra	2015	1	0.0%
Park_2020_609a	128.4 63	38.0 321	Asia	rhizosphere soil	0	140661	1406 61	forest	2018	1	0.0%
Saitta_2018_51C8	12.00 22	36.7 808	Europe	soil	0	287082	2870 82	forest	2013	2	0.0%
Franzetti_2020_GF	10.58 45	46.4 056	Europe	soil	583776	0	5837 76	tundra	2015	4	0.0%
Kovalchuk_2018_EDF8	25.22 33	60.7 531	Europe	shoot	0	146089	1460 89	forest	2016	1	0.0%
Sun_2021_PK	101.0 2	24.5 3	Asia	topsoil	0	1319159	1319 159	forest	2014	9	0.0%
Woo_2018_BY	126.9 55	37.4 653	Asia	dust	154682	0	1546 82	anthropogenic	2015	1	0.0%
Kovalchuk_2018_EDF8	25.22 14	60.7 475	Europe	shoot	0	156583	1565 83	forest	2016	1	0.0%
Kovalchuk_2018_EDF8	25.25 94	60.7 542	Europe	root	0	158503	1585 03	forest	2016	1	0.0%

Sun_2021_PK	101.02	24.53	Asia	topsoil	0	1430097	1430097	forest	2014	9	0.0%
Nunez_2019_BS	-3.72514	40.446	Europe	air	0	159066	159066	anthropogenic	2015	1	0.0%
Kovalchuk_2018_EDF8	25.2233	60.7531	Europe	shoot	0	161667	161667	forest	2016	1	0.0%
Park_2020_609a	128.463	38.0321	Asia	rhizosphere soil	0	162403	162403	forest	2018	1	0.0%
Sun_2021_PK	101.02	24.53	Asia	topsoil	0	1028561	1028561	forest	2014	6	0.0%
Sun_2021_PK	101.02	24.53	Asia	topsoil	0	873469	873469	forest	2017	5	0.0%
Kovalchuk_2018_EDF8	25.2233	60.7531	Europe	shoot	0	181051	181051	forest	2016	1	0.0%
Sun_2021_PK	101.02	24.53	Asia	topsoil	0	1752547	1752547	forest	2014	9	0.0%
Kovalchuk_2018_EDF8	25.2594	60.7542	Europe	shoot	0	197510	197510	forest	2016	1	0.0%
Sun_2021_PK	101.57	21.61	Asia	topsoil	0	200173	200173	forest	2017	1	0.0%
Sun_2021_PK	101.02	24.53	Asia	topsoil	0	1651283	1651283	forest	2014	7	0.0%
Kovalchuk_2018_EDF8	25.2594	60.7542	Europe	shoot	0	246234	246234	forest	2016	1	0.0%

Sun_2021_PK	101.57	21.61	Asia	topsoil	0	252813	252813	forest	2016	1	0.0%
Benucci_2020_1AF	170.157	-43.249	Australia	root	706373	339599	1045972	forest	2014	4	0.0%
Saitta_2018_51C8	12.015	36.8185	Europe	soil	0	264711	2647211	forest	2013	1	0.0%
Saitta_2018_51C8	12.0423	36.785	Europe	soil	0	279954	2799054	forest	2013	1	0.0%
Sun_2021_PK	101.02	24.53	Asia	topsoil	0	1121182	1121182	forest	2017	4	0.0%
Saitta_2018_51C8	11.9752	36.794	Europe	soil	1	323750	3237051	forest	2013	1	0.0%
Saitta_2018_51C8	12.0182	36.7878	Europe	soil	0	327753	3277053	forest	2013	1	0.0%
Sun_2021_PK	101.57	21.61	Asia	topsoil	0	694925	6949025	forest	2017	2	0.0%
Sun_2021_PK	101.02	24.53	Asia	topsoil	0	1760148	1760148	forest	2014	5	0.0%
Sun_2021_PK	100.17	27.12	Asia	topsoil	0	356350	3563050	forest	2014	1	0.0%
Saitta_2018_51C8	12.0302	36.7388	Europe	soil	0	394657	3946057	forest	2013	1	0.0%
Sun_2021_PK	101.02	24.53	Asia	topsoil	0	1678287	1678287	forest	2014	4	0.0%

Saitta_2018_51C8	12.021	36.7584	Europe	soil	0	437042	437042	forest	2013	1	0.0%
Sun_2021_PK	101.57	21.61	Asia	topsoil	0	482553	4825053	forest	2017	1	0.0%
Sun_2021_PK	101.02	24.53	Asia	topsoil	0	514714	5147014	forest	2017	1	0.0%
Sun_2021_PK	101.57	21.61	Asia	topsoil	0	644759	6447059	forest	2017	1	0.0%
Sun_2021_PK	101.02	24.53	Asia	topsoil	0	741972	7419072	forest	2014	1	0.0%
Sun_2021_PK	101.02	24.53	Asia	topsoil	0	795905	7959005	forest	2014	1	0.0%
Sun_2021_PK	100.17	27.12	Asia	topsoil	0	806713	8067013	forest	2014	1	0.0%
Sun_2021_PK	100.17	27.12	Asia	topsoil	0	1243887	1243887	forest	2014	1	0.0%
Sun_2021_PK	101.02	24.53	Asia	topsoil	0	1263089	1263089	forest	2014	1	0.0%
Sun_2021_PK	101.02	24.53	Asia	topsoil	0	1420912	1420912	forest	2014	1	0.0%

Supplementary Table 4 Distribution of CAZymes in representative fungal species used in this study

GH	*A. cra*	*A. ric*	*C. may*	*E. faw*	*H. wer*	*P. ton*	*S. mus*	*D. aci*	*F. end*	*P. fij*	*A. nam*	*T. nub*	*D. sep*	*M. dur*	*F. sim*	*B. pan*	*Z. cel*	*E. amp*	*P. nod*	*S. tha*	*C. bet*	*H. aci*	*Z. tri*	*P. ful*	*P. hor*

AA1	6	5	7	9	5	5	2	7	2	7	5	5	6	7	8	4	10	5	8	2	7	2	5	8	1
AA11	5	1	5	3	6	3	5	2	4	5	3	3	5	1	7	4	5	3	5	4	5	1	5	5	5
AA12	1	0	1	1	2	1	0	1	1	1	1	0	1	1	1	1	1	1	3	1	1	1	1	2	0
AA13	0	0	0	1	0	0	0	0	0	0	0	0	0	0	0	0	0	1	1	0	0	0	0	0	0
AA14	0	0	0	0	0	0	0	0	0	0	0	0	0	0	1	0	0	0	1	0	0	0	0	0	0
AA16	0	1	1	2	4	0	1	0	1	1	1	1	1	1	1	0	2	2	2	1	1	0	0	1	0
AA1_2	1	2	1	1	0	1	1	1	1	1	3	1	1	1	1	1	1	1	1	1	1	1	1	1	1
AA1_3	5	5	5	2	19	9	5	3	7	7	6	7	7	4	8	6	17	2	2	9	8	5	2	9	8
AA2	2	3	3	4	6	3	3	3	1	3	5	4	4	3	3	4	5	4	9	2	4	0	3	5	2
AA3	1	1	0	1	1	1	0	1	2	2	1	2	2	1	2	2	2	1	3	2	1	0	3	2	0
AA3_1	0	1	3	5	4	1	3	0	1	3	3	1	3	0	1	0	4	4	5	1	3	0	2	2	1
AA3_2	6	6	14	14	38	7	15	6	7	15	20	14	15	12	15	11	38	14	23	13	25	13	13	20	0
AA3_3	2	1	3	2	4	1	2	0	1	2	2	2	2	1	2	2	3	2	4	1	3	1	2	4	0
AA4	1	3	2	3	2	1	2	0	2	2	2	0	1	1	4	2	2	3	3	1	1	1	0	1	1
AA5	1	0	1	0	0	1	0	0	0	2	0	0	1	1	1	1	1	0	1	0	1	0	0	1	0
AA5_1	0	0	1	1	0	0	1	1	1	0	2	1	1	0	1	1	1	0	1	0	1	0	0	2	0
AA5_2	1	0	5	3	0	0	0	0	0	0	0	0	1	3	0	0	2	2	3	0	6	0	1	1	0
AA6	1	1	1	1	2	2	1	3	1	2	1	1	1	1	1	1	1	1	1	1	2	1	1	1	1
AA7	12	11	16	27	25	8	14	14	4	19	4	13	11	17	5	6	41	17	42	7	25	10	15	22	1
AA8	1	3	3	3	4	1	3	0	3	3	2	1	3	1	3	2	2	3	6	2	3	4	4	3	0
AA9	0	2	3	12	8	0	2	1	1	3	6	1	2	3	1	1	3	16	28	1	3	0	2	2	0
CBM13	0	0	0	0	0	0	0	0	0	0	0	0	0	1	0	0	0	0	0	0	0	0	0	0	0
CBM20	1	2	3	2	2	4	3	1	2	2	3	4	2	1	3	1	3	2	3	1	3	0	3	4	2
CBM21	1	1	1	1	2	1	1	1	1	1	1	1	1	1	2	1	1	1	1	1	1	1	1	1	2
CBM32	0	0	0	0	0	0	0	0	0	0	0	0	0	0	0	0	1	0	0	0	1	0	0	1	0

CBM42	2	0	1	1	1	0	1	1	0	1	2	2	1	1	0	0	4	1	1	1	1	2	0	1	0
CBM43	1	2	2	1	2	1	1	1	1	2	2	0	1	1	2	1	2	1	0	1	2	0	1	1	1
CBM46	0	0	0	1	0	0	0	0	0	0	0	0	0	0	0	0	0	1	1	0	0	0	0	0	0
CBM52	0	1	0	1	2	1	0	0	1	0	1	0	0	1	1	1	1	1	0	0	1	0	0	1	1
CBM6	0	0	0	0	0	0	0	0	0	0	1	0	0	0	0	0	0	0	1	0	0	0	0	0	0
CBM63	0	1	1	1	2	0	1	0	1	0	1	2	1	1	2	0	1	1	1	1	0	0	0	1	0
CBM66	0	0	0	0	0	0	0	0	0	0	0	0	0	0	0	0	1	0	0	0	0	0	0	0	0
CBM67	1	2	0	4	0	0	1	0	0	1	4	0	0	0	0	1	3	3	2	0	0	0	1	0	0
CBM87	0	0	1	1	2	0	0	0	0	0	1	0	0	1	0	0	0	1	1	0	1	0	0	0	0
CBM91	0	1	1	6	7	0	0	0	2	1	5	0	0	0	6	1	1	3	4	1	1	0	1	1	0
CE1	3	3	3	3	12	3	3	3	5	7	7	2	4	3	6	5	6	4	11	3	3	1	3	4	1
CE12	0	0	1	3	4	0	2	0	0	2	2	0	1	1	0	0	1	2	3	1	2	0	0	2	0
CE13	0	0	0	1	0	0	0	0	0	0	0	0	0	0	0	0	0	0	0	0	0	0	0	0	0
CE15	0	1	0	1	2	0	0	0	0	0	1	0	0	0	1	1	0	1	1	0	0	0	0	0	0
CE16	0	3	2	3	7	1	1	4	3	3	4	4	5	5	2	2	10	3	2	4	2	3	2	7	4
CE18	0	0	1	1	2	0	0	0	0	0	1	0	0	1	0	0	0	1	1	0	1	0	0	0	0
CE2	0	0	0	2	4	0	0	0	1	1	1	1	1	0	0	0	2	2	1	1	0	0	0	1	0
CE3	3	1	4	2	2	0	4	5	0	5	0	3	3	4	4	0	12	2	4	3	7	0	3	3	3
CE4	1	4	2	5	5	2	3	1	3	5	6	4	3	2	6	5	6	4	11	3	2	4	5	3	0
CE5	4	3	9	13	15	3	6	8	4	7	9	7	3	9	5	3	12	15	11	6	10	0	6	11	0
CE8	2	3	1	8	6	0	0	0	0	1	6	2	2	6	10	1	1	6	6	3	1	0	1	2	0
CE9	2	2	2	1	4	2	1	0	2	2	2	3	1	2	2	2	3	1	2	2	2	1	0	2	0
GH1	2	4	3	3	4	2	0	1	4	4	6	2	2	2	6	3	4	2	2	2	3	1	2	3	0
GH10	0	3	2	4	8	0	0	0	2	1	4	1	0	1	3	4	2	5	8	0	4	0	2	1	0
GH105	3	2	5	3	8	1	4	1	1	4	2	3	3	0	1	1	5	3	2	3	6	0	2	6	0

GH106	0	0	0	0	5	0	0	0	0	0	0	1	0	0	0	0	2	0	0	2	2	0	0	2	0
GH109	2	6	1	0	2	0	1	0	2	0	1	1	3	2	1	2	7	0	2	0	1	3	1	2	0
GH11	0	3	2	3	6	1	1	0	4	0	5	1	2	2	5	2	2	5	7	1	4	0	1	2	0
GH114	1	1	2	3	3	1	0	0	0	0	1	0	1	3	1	0	1	3	2	0	2	1	1	1	0
GH115	1	0	1	1	2	0	0	0	0	3	1	0	0	0	3	1	0	1	2	0	1	0	1	1	0
GH12	0	3	2	2	8	0	2	1	1	2	2	3	3	1	5	1	1	3	4	3	3	2	1	4	0
GH125	2	2	3	2	4	2	4	1	2	3	2	2	2	3	3	2	4	2	3	2	3	1	3	3	2
GH127	1	3	0	2	0	1	0	0	1	1	1	0	0	1	2	0	2	2	0	0	1	1	1	1	0
GH128	4	4	4	9	9	4	4	4	4	4	6	5	3	3	4	4	4	7	5	5	4	4	4	5	4
GH130	0	0	2	0	1	0	0	0	0	0	0	0	0	0	0	0	2	0	0	0	1	0	0	1	0
GH131	0	1	1	2	2	0	1	0	1	1	1	1	1	1	1	0	1	2	5	0	1	0	1	1	0
GH132	1	1	1	1	2	1	1	1	1	1	1	1	1	1	1	1	1	1	1	1	1	1	1	1	1
GH134	0	0	0	1	0	0	0	0	0	0	0	0	0	0	0	0	0	0	0	0	0	0	0	0	0
GH135	1	3	2	2	2	1	1	0	1	0	2	1	3	2	1	0	1	3	4	1	2	0	0	3	0
GH139	0	1	0	0	0	0	0	0	0	0	0	0	0	0	0	0	0	0	1	0	1	1	0	0	0
GH13_1	1	2	4	2	6	4	4	1	3	3	3	5	4	1	4	2	7	1	1	3	4	0	3	4	3
GH13_22	0	0	2	2	4	2	2	2	2	4	6	2	3	0	2	2	2	2	0	2	4	2	6	4	2
GH13_25	1	1	1	1	2	1	1	1	1	1	1	1	1	1	1	1	1	1	1	1	1	1	1	1	1
GH13_31	0	0	0	0	0	0	0	0	0	0	0	0	0	0	0	0	0	0	1	0	0	0	0	0	0
GH13_40	4	3	6	2	4	4	4	1	4	4	6	2	3	2	2	2	7	2	2	2	5	2	4	5	0
GH13_5	3	1	2	2	2	3	3	2	2	2	2	2	3	1	4	2	3	2	1	2	3	1	2	3	1
GH13_8	1	1	1	1	1	1	1	1	1	1	1	1	1	1	1	1	1	1	1	1	1	1	1	1	1
GH141	0	1	0	0	0	0	0	0	0	0	0	0	0	0	0	0	0	0	1	0	1	0	0	0	0
GH142	0	1	1	1	2	1	1	0	1	1	1	1	0	1	1	1	2	1	1	2	1	0	1	1	0
GH146	0	1	0	2	0	0	0	0	0	0	0	0	0	0	0	0	0	2	1	0	0	0	0	0	0

GH15	2	2	1	2	2	3	3	0	1	2	3	2	2	2	1	1	2	2	3	1	2	1	1	2	1
GH152	1	1	1	1	2	1	1	1	1	1	1	1	1	1	1	1	1	1	1	1	1	1	1	1	1
GH154	1	2	1	1	2	0	0	0	0	1	2	0	0	1	2	1	1	1	2	0	2	0	1	1	0
GH16	0	0	0	0	0	0	0	0	0	0	0	0	0	0	0	0	0	0	0	0	0	0	0	0	1
GH16_1	4	4	4	4	10	3	2	1	4	4	6	5	5	4	5	5	6	4	5	5	4	3	3	5	2
GH16_10	0	0	0	1	0	0	0	0	0	1	0	0	0	0	0	0	0	0	0	0	0	0	0	0	0
GH16_18	3	3	4	3	6	3	4	3	3	5	4	5	3	3	6	3	5	3	3	3	4	2	4	3	5
GH16_19	1	1	1	1	2	1	1	1	1	1	1	1	1	1	1	1	1	1	1	1	1	1	1	1	1
GH16_2	2	2	2	2	4	2	2	2	2	2	2	2	2	2	2	2	2	2	2	2	2	2	2	2	2
GH16_22	1	0	0	0	0	0	0	0	1	0	0	0	0	0	0	1	0	0	1	0	0	0	0	0	0
GH16_23	4	2	4	3	4	3	4	2	1	4	8	4	3	2	2	1	4	4	2	3	4	0	1	3	2
GH16_3	0	0	1	2	0	0	1	0	0	0	1	0	1	1	0	0	1	3	2	0	1	0	1	1	0
GH16_4	1	1	2	2	2	1	1	0	1	1	1	1	1	2	2	2	2	2	2	1	2	1	1	1	0
GH17	3	4	6	5	7	5	6	4	2	6	5	6	7	4	2	4	7	4	4	5	4	3	4	5	3
GH18	9	6	10	10	13	12	5	17	3	9	6	5	7	14	5	4	17	13	14	4	7	3	8	10	3
GH2	6	7	5	5	14	3	4	2	4	7	2	4	4	3	7	5	10	3	10	4	6	4	8	5	2
GH20	3	2	1	1	4	1	2	1	1	2	1	2	1	1	2	1	2	1	3	2	1	2	1	2	1
GH24	0	0	1	0	0	0	0	0	0	0	0	0	0	0	0	0	1	0	0	0	1	0	0	2	0
GH25	1	1	0	0	2	1	0	1	0	1	0	0	1	0	0	0	1	0	0	0	0	2	0	0	4
GH26	0	1	0	0	0	1	0	1	0	0	0	0	0	0	0	0	0	0	0	0	0	0	0	0	0
GH27	3	6	2	4	5	1	1	0	2	1	4	4	2	2	1	1	7	3	3	3	3	3	1	1	1
GH28	4	9	5	11	18	1	5	0	0	5	9	10	4	6	7	6	9	11	5	8	5	0	2	14	0
GH29	0	1	2	0	2	0	3	0	0	1	1	1	1	0	1	0	1	0	0	1	3	0	1	1	0
GH3	7	11	16	16	32	6	10	8	11	15	20	13	10	7	16	9	22	13	15	12	16	4	16	18	1
GH30	0	0	0	0	0	0	0	0	0	0	0	0	0	0	1	0	0	0	0	0	0	0	0	1	0

GH30_3	1	1	1	0	2	1	2	1	1	1	0	2	2	1	1	1	2	0	0	1	1	1	1	0	0
GH30_4	0	1	0	0	0	1	0	2	0	0	0	1	0	0	0	0	0	0	0	0	0	0	0	0	0
GH30_7	0	1	0	0	2	0	0	0	2	0	1	0	0	0	3	2	1	1	2	0	1	0	0	0	0
GH31	5	9	8	7	21	9	9	6	11	10	7	8	8	7	18	6	14	7	10	8	8	4	7	12	4
GH32	3	1	3	4	3	7	2	1	2	4	5	2	2	5	2	2	5	2	4	3	3	1	4	4	2
GH33	0	0	0	0	2	0	0	0	0	0	0	0	0	0	0	0	1	0	0	0	1	0	0	0	0
GH35	3	9	1	5	8	1	1	1	2	3	4	3	1	2	5	3	4	4	4	3	2	4	2	6	0
GH36	0	1	1	0	2	1	1	1	1	1	1	0	1	0	2	1	1	0	1	1	1	1	1	1	0
GH37	1	1	2	1	4	2	1	2	1	2	1	2	1	1	1	1	1	1	2	2	2	1	2	2	0
GH38	1	2	1	1	2	1	1	1	1	1	1	1	1	1	2	1	1	1	1	1	1	1	1	1	1
GH39	0	2	1	1	0	0	0	0	1	0	0	0	0	0	2	0	0	0	0	0	0	0	0	0	2
GH42	0	0	0	0	2	0	1	0	0	1	0	0	1	0	0	0	1	0	0	0	1	0	0	1	0
GH43_1	1	1	1	1	2	0	0	0	1	1	1	0	0	1	4	1	1	1	2	0	1	0	1	1	0
GH43_11	0	0	0	0	0	0	0	0	1	0	0	0	0	0	2	0	0	0	1	0	0	0	0	0	0
GH43_12	0	0	0	0	0	0	0	0	0	0	1	0	0	0	0	0	0	0	0	0	0	0	0	1	0
GH43_13	0	0	0	2	0	0	0	0	0	0	1	0	0	0	0	0	0	1	0	1	0	0	0	0	0
GH43_14	0	1	1	3	8	0	0	0	0	1	3	0	0	0	3	1	1	2	2	0	1	0	1	1	0
GH43_21	0	0	2	4	0	0	1	0	0	0	2	1	0	0	0	0	1	4	0	0	2	0	1	2	0
GH43_22	0	0	1	1	2	0	1	0	0	1	1	0	1	0	0	0	1	1	1	1	1	0	1	1	0
GH43_24	0	1	3	1	4	1	2	0	0	2	0	1	1	0	0	0	3	1	2	0	3	1	1	3	0
GH43_26	1	2	1	4	6	2	1	1	2	2	4	1	1	2	3	0	7	4	2	2	2	1	1	3	1
GH43_29	0	0	0	1	0	0	0	0	0	1	1	0	0	0	0	0	1	1	1	0	0	0	0	1	0
GH43_30	3	3	3	4	10	5	2	1	4	5	5	3	4	3	6	2	8	3	0	5	4	1	2	5	4
GH43_34	0	0	1	1	2	0	0	0	0	1	1	1	1	0	0	0	1	1	1	1	1	0	1	1	0
GH43_36	0	0	0	1	2	0	0	0	1	0	1	0	0	0	2	0	0	1	1	0	0	0	0	0	0

GH43_37	0	2	0	0	0	0	0	0	0	1	1	0	1	1	0	1	1	0	0	0	0	1	0	1	0
GH43_5	0	0	0	1	2	0	0	0	0	0	0	0	0	0	0	0	0	0	0	0	0	0	1	0	0
GH43_6	0	2	2	1	5	0	1	0	0	1	2	1	2	1	1	0	5	1	2	4	2	0	0	2	0
GH45	0	1	0	1	2	0	0	0	1	0	1	1	1	1	1	0	0	1	3	1	0	0	1	1	0
GH47	6	11	8	7	16	9	9	7	7	11	7	10	8	8	8	10	12	7	9	6	9	6	8	8	7
GH49	0	0	0	0	0	0	0	0	0	0	1	0	0	0	0	0	0	0	0	0	0	0	0	0	0
GH51	1	3	2	4	8	2	2	0	2	3	3	2	1	2	3	3	3	3	2	3	2	2	2	2	0
GH53	1	1	1	3	4	0	2	0	1	2	2	2	1	1	1	0	2	3	1	2	1	0	2	2	0
GH54	3	2	1	1	1	0	1	1	0	1	2	2	1	1	0	0	6	1	1	1	1	2	1	1	0
GH55	4	2	4	4	6	4	2	6	4	4	5	3	4	3	3	3	6	3	3	3	5	3	3	4	1
GH5_12	1	1	1	1	2	1	1	1	1	1	1	1	1	1	1	1	1	1	1	1	1	1	1	1	1
GH5_15	0	0	0	0	0	0	0	0	0	0	0	0	0	0	0	0	1	0	1	0	1	0	0	0	0
GH5_16	1	1	2	1	4	0	1	0	0	1	2	0	1	0	0	1	3	0	3	0	3	0	2	1	0
GH5_22	1	2	1	1	2	0	0	0	1	0	1	0	0	1	3	2	1	2	1	1	1	0	1	1	0
GH5_23	0	0	0	3	2	0	0	0	0	1	5	0	0	0	0	0	1	2	0	0	0	0	0	3	0
GH5_24	1	1	1	0	2	0	1	1	1	1	0	1	1	0	1	1	1	0	0	0	1	1	0	1	0
GH5_31	0	0	0	0	0	0	0	0	0	0	0	0	0	2	0	0	1	0	2	0	0	0	1	1	0
GH5_36	0	0	0	0	0	0	0	0	0	0	0	0	0	0	0	0	1	0	0	0	0	0	0	0	0
GH5_4	0	0	0	1	0	0	0	0	0	0	1	0	0	0	0	0	0	1	1	0	0	0	0	0	0
GH5_41	0	1	0	0	0	0	0	0	1	0	0	0	0	1	0	1	0	0	0	0	0	1	0	0	0
GH5_44	0	0	0	0	0	0	0	0	1	0	0	0	0	0	0	0	0	0	0	0	0	0	0	0	0
GH5_49	1	1	1	1	2	1	1	1	1	1	1	1	1	1	1	1	1	1	1	1	1	1	1	1	1
GH5_5	2	2	2	2	10	1	1	0	1	1	3	1	2	2	2	2	6	2	3	2	2	0	0	2	0
GH5_7	0	1	0	3	4	1	0	0	1	1	2	0	1	0	0	1	1	3	2	1	0	0	0	1	0
GH5_9	4	5	3	4	11	5	2	5	5	3	6	6	4	5	6	6	5	5	4	6	4	2	3	4	5

GH6	0	1	0	2	2	0	0	0	0	0	2	0	0	1	0	1	0	2	4	0	0	0	0	0	0
GH62	0	0	1	1	2	0	0	0	2	1	1	0	1	0	6	1	0	2	3	0	1	0	1	0	0
GH63	1	2	1	1	2	1	1	1	1	1	1	1	1	1	2	1	1	1	2	1	1	1	1	1	1
GH64	3	6	4	4	6	2	6	3	4	4	2	4	6	3	4	3	5	3	1	3	4	4	4	5	1
GH65	1	1	1	1	2	1	1	1	1	1	1	1	1	1	1	1	1	1	1	0	1	1	1	1	1
GH67	0	1	1	1	4	0	0	0	1	1	1	1	1	1	1	1	1	1	1	1	1	0	0	1	0
GH7	1	2	1	2	6	0	0	0	1	1	2	0	1	1	2	2	0	2	5	2	1	0	1	2	0
GH71	2	2	1	0	2	3	2	2	2	2	2	1	1	0	9	1	4	0	1	1	2	1	1	2	1
GH72	5	6	7	4	14	8	5	3	5	7	7	6	6	4	5	4	9	3	7	7	8	6	5	8	4
GH74	0	1	0	0	0	0	0	0	0	0	0	0	0	0	0	0	0	0	0	0	0	0	0	0	0
GH75	1	0	0	0	0	0	0	0	0	0	0	0	1	1	0	0	0	0	1	0	0	3	1	1	0
GH76	11	10	9	6	16	9	7	6	8	8	10	8	7	7	11	8	14	5	8	9	10	6	6	9	4
GH78	2	9	2	8	6	1	2	0	1	8	11	2	1	0	5	3	9	6	4	2	2	0	2	5	0
GH79	3	1	3	4	4	2	2	0	0	3	3	1	4	3	0	1	6	4	2	3	3	1	3	4	1
GH81	1	1	1	1	2	1	1	1	1	1	1	1	1	1	1	1	1	1	2	1	1	1	1	1	1
GH85	0	0	1	0	0	0	0	0	0	0	0	0	0	0	0	0	0	0	1	0	1	0	1	0	0
GH88	2	2	0	1	2	0	0	0	0	0	1	0	0	0	0	0	1	2	1	1	2	0	0	2	0
GH89	1	1	0	0	2	0	1	0	1	1	0	0	0	0	1	1	1	0	0	0	0	0	0	0	0
GH9	0	0	0	0	2	0	0	0	1	0	1	0	0	0	2	1	0	0	0	0	0	0	0	0	0
GH92	3	4	6	2	10	3	5	1	1	7	1	6	7	0	4	3	10	0	8	5	7	2	7	6	0
GH93	0	2	0	3	3	0	1	0	1	1	2	1	1	2	3	2	2	1	3	1	0	0	1	2	0
GH94	0	0	0	0	0	0	0	0	0	0	0	0	0	0	0	0	0	0	1	0	0	0	0	0	0
GH95	0	2	0	1	4	0	1	0	2	1	1	1	0	0	2	0	2	1	2	1	1	1	0	0	0
GH97	0	0	0	0	0	0	0	0	0	0	0	0	0	0	0	1	1	0	0	0	0	0	0	0	0
GT1	4	4	3	7	8	3	3	4	2	3	8	3	3	6	2	5	6	5	7	4	6	4	4	4	1

GT109	3	0	0	2	2	2	0	2	0	1	2	1	1	3	0	0	3	2	1	1	0	1	1	1	0
GT13	0	0	0	0	0	0	0	0	0	0	0	0	0	0	0	0	1	0	0	0	0	1	0	0	0
GT15	3	3	3	4	6	4	3	3	3	4	4	3	4	4	3	3	3	4	3	3	4	3	3	3	3
GT17	2	1	2	0	2	1	1	0	1	1	0	1	3	0	1	1	2	0	0	1	2	1	2	3	1
GT20	3	3	3	3	6	3	3	3	3	3	3	3	3	3	3	3	3	3	3	3	3	3	3	3	3
GT21	1	1	1	1	2	1	1	1	1	1	1	1	1	1	1	1	1	1	1	1	1	1	1	1	1
GT22	4	4	4	4	8	4	4	4	4	4	4	4	4	4	5	4	4	4	4	4	4	4	3	4	4
GT24	1	1	1	1	2	1	1	1	1	1	1	1	1	1	2	1	1	1	1	1	1	1	1	1	1
GT25	2	2	5	2	0	1	3	2	1	3	2	2	5	0	1	0	2	0	0	3	5	3	3	2	0
GT3	1	1	1	1	2	1	1	1	1	1	1	1	1	1	1	1	1	1	1	1	1	1	1	1	1
GT32	5	6	4	5	11	2	3	7	2	5	3	5	5	6	1	1	7	7	5	5	5	6	4	4	3
GT33	1	1	1	1	2	1	1	1	1	1	1	1	1	1	1	1	1	1	1	1	1	1	1	1	1
GT34	2	2	6	5	10	4	5	2	3	4	5	4	5	4	4	3	3	5	6	3	7	2	6	6	2
GT35	1	1	1	1	2	1	1	1	1	1	1	1	1	1	2	1	1	1	1	0	1	1	1	1	1
GT39	3	3	3	3	6	3	3	3	3	3	4	3	3	3	3	3	3	3	3	3	3	3	3	3	3
GT4	4	6	4	3	12	3	5	4	4	4	3	5	5	3	4	5	5	3	4	4	4	4	4	5	3
GT48	1	1	1	1	2	1	1	1	1	1	1	1	1	1	1	1	1	1	1	1	1	1	1	1	1
GT5	0	0	0	0	0	0	0	0	0	0	0	0	1	0	0	0	0	0	0	0	0	0	0	0	0
GT50	1	1	1	1	2	1	1	1	1	1	1	1	1	1	1	1	1	1	1	2	1	1	1	1	1
GT55	0	0	0	0	0	0	0	0	0	0	0	0	0	0	0	0	0	0	1	0	0	0	0	0	0
GT57	2	3	3	3	6	3	3	2	3	3	3	3	3	2	2	3	3	3	3	3	3	3	3	3	2
GT58	1	1	1	1	2	1	2	1	1	2	1	1	1	1	2	1	1	1	1	1	1	1	1	1	1
GT59	1	1	1	1	2	1	1	1	1	1	1	1	1	1	1	1	1	1	1	1	1	1	1	0	1
GT61	1	2	0	1	0	0	1	2	0	0	0	1	0	0	0	0	0	1	0	0	0	0	0	0	0
GT62	4	4	3	4	6	3	3	3	4	3	4	4	3	5	5	4	3	4	4	3	3	3	3	3	4

GT64	0	0	1	0	0	0	0	0	0	0	0	0	0	0	0	0	0	0	0	0	1	0	1	0	0
GT66	1	1	1	1	2	1	1	1	1	1	1	1	1	1	1	1	1	1	1	1	1	1	1	1	1
GT69	2	2	2	2	2	1	2	1	1	2	1	1	2	1	2	1	1	2	3	1	2	2	1	2	1
GT71	0	3	2	2	3	0	1	2	1	0	5	2	4	13	2	3	3	2	1	1	4	0	2	4	1
GT76	1	1	1	1	2	1	1	0	2	1	1	1	1	1	1	1	1	1	1	1	1	1	1	0	1
GT77	1	1	0	0	0	0	1	0	0	0	0	1	1	1	0	0	0	0	0	0	0	0	0	1	1
GT8	6	6	8	8	14	10	9	5	4	9	9	10	8	16	9	6	8	9	6	7	11	5	9	9	3
GT90	5	4	13	8	8	4	9	5	7	12	5	6	15	8	11	6	13	9	4	5	12	6	8	11	3
GT91	0	0	0	0	0	0	0	0	0	0	0	0	1	2	0	0	0	0	0	0	2	0	0	0	0
PL1	0	0	0	1	0	0	0	0	0	0	0	0	0	0	0	0	0	1	0	0	0	0	0	1	0
PL1_10	0	0	1	1	0	0	0	0	0	0	1	0	0	0	0	0	1	1	1	0	1	0	1	0	0
PL1_2	0	0	0	1	0	0	0	0	0	0	0	0	0	0	0	0	0	1	1	0	0	0	0	0	0
PL1_4	0	0	1	4	5	0	1	1	0	1	3	1	1	1	0	0	1	1	1	1	1	0	0	1	0
PL1_7	0	0	1	1	4	0	1	0	0	1	0	1	0	1	0	0	1	1	0	0	1	0	1	1	0
PL1_9	0	0	0	0	0	0	0	0	0	0	0	0	0	0	0	0	0	0	2	0	0	0	0	0	0
PL26	0	1	1	0	2	0	0	0	0	1	1	1	0	0	0	0	0	0	1	0	1	0	0	1	0
PL36_2	0	0	0	0	0	0	0	0	0	0	0	0	1	0	0	0	0	0	0	0	0	0	0	0	0
PL3_2	0	0	1	5	8	0	2	0	0	1	2	0	0	0	0	0	2	5	2	2	2	0	1	4	0
PL42	0	1	0	0	0	0	0	0	0	0	0	0	0	0	0	0	0	0	1	0	0	0	0	0	0
PL4_1	0	0	1	1	0	0	1	0	0	1	1	0	1	0	0	0	1	0	2	0	1	0	0	1	0
PL4_3	0	0	0	1	2	0	1	0	0	1	1	1	1	0	0	0	1	1	1	1	0	0	0	1	0
PL4_5	0	0	0	2	0	0	0	0	0	0	2	0	0	0	0	0	0	2	1	0	0	0	0	0	0
PL7_4	1	0	0	0	0	0	0	0	0	0	0	0	0	1	0	0	2	0	0	0	0	0	0	1	0
PL9_3	0	0	0	1	2	0	0	0	0	0	0	0	0	0	0	0	0	1	0	0	0	0	0	0	0

A. cra= Acrodontium crateriforme, A. ric= Acidomyces richmondensis, C. may= Cercospora zeae-maydis, E. faw= Elsinoe fawcettii,H. wer= Hortaea werneckii, P. ton= Polychaeton citri, S. mus= Sphaerulina musiva,

D. aci= Dissoconium aciculare, F. end= Friedmanniomyces endolithicus,P. fij= Pseudocercospora fijiensis, A. nam= Aureobasidium namibiae, T. nub= Teratosphaeria nubilosa, D. sep= Dothistroma septosporum, M. dur= Myriangium duriaei,

F. sim= Friedmanniomyces simplex,B. pan= Baudoinia panamericana, Z. cel= Zasmidium cellare, E. amp= Elsinoe ampelina, P. nod= Parastagonospora nodorum, S. tha= Salinomyces thailandica, C. bet= Cercospora beticola,

H. aci= Hortaea acidophila, Z. tri= Zymoseptoria tritici, P. ful= Passalora fulva, P. hor= Piedraia hortae.

Reference

1 Čapek, P. *et al.* A plant–microbe interaction framework explaining nutrient effects on primary production. *Nature ecology & evolution* **2**, 1588-1596 (2018).

2 Mehmood, A. *et al.* In vitro production of IAA by endophytic fungus Aspergillus awamori and its growth promoting activities in Zea mays. *Symbiosis* **77**, 225-235 (2019).

3 Shalev, O. *et al.* Commensal Pseudomonas strains facilitate protective response against pathogens in the host plant. *Nature ecology & evolution* **6**, 383-396 (2022).

4 Ling, S. *et al.* Enhanced anti-herbivore defense of tomato plants against Spodoptera litura by their rhizosphere bacteria. *BMC Plant Biology* **22**, 254 (2022).

5 Van Noorden, G. E. *et al.* Molecular signals controlling the inhibition of nodulation by nitrate in Medicago truncatula. *International Journal of Molecular Sciences* **17**, 1060 (2016).

6 Kuang, W. *et al.* Genome and transcriptome sequencing analysis of Fusarium commune provides insights into the pathogenic mechanisms of the lotus rhizome rot. *Microbiology spectrum* **10**, e00175-00122 (2022).

7 Wan, C. *et al.* A serine-rich effector from the stripe rust pathogen targets a Raf-like kinase to suppress host immunity. *Plant Physiology* **190**, 762-778 (2022).

8 Yao, H. *et al.* Phyllosphere epiphytic and endophytic fungal community and network structures differ in a tropical mangrove ecosystem. *Microbiome* **7**, 1-15 (2019).

9 Svistoonoff, S. *et al.* The independent acquisition of plant root nitrogen-fixing symbiosis in Fabids recruited the same genetic pathway for nodule organogenesis. *PLoS One* **8**, e64515 (2013).

10 Liu, X. *et al.* Phyllosphere microbiome induces host metabolic defence against rice false-smut disease. *Nature Microbiology*, 1-15 (2023).

11 Iqbal, M. *et al.* Plant microbe mediated enhancement in growth and yield of canola (Brassica napus L.) plant through auxin production and increased nutrient acquisition. *Journal of Soils and Sediments* **23**, 1233-1249 (2023).

12 Vadassery, J. *et al.* The role of auxins and cytokinins in the mutualistic interaction between Arabidopsis and Piriformospora indica. *Molecular Plant-Microbe Interactions* **21**, 1371-1383 (2008).

13 Chen, C., Gao, M., Liu, J. & Zhu, H. Fungal symbiosis in rice requires an ortholog of a legume common symbiosis gene encoding a Ca2+/calmodulin-dependent protein kinase. *Plant physiology* **145**, 1619-1628 (2007).

14 Venkatachalam, S. *et al.* Diversity and functional traits of culturable microbiome members, including cyanobacteria in the rice phyllosphere. *Plant Biology* **18**, 627-637 (2016).

15 Romero, F. M., Marina, M. & Pieckenstain, F. L. Novel components of leaf bacterial communities of field-grown tomato plants and their potential for plant growth promotion and biocontrol of tomato diseases. *Research in microbiology* **167**, 222-233 (2016).

16 Freund, M. *et al.* The digestive systems of carnivorous plants. *Plant physiology* **190**, 44-59 (2022).

17 Mithöfer, A. Carnivorous plants and their biotic interactions. *Journal of Plant Interactions* **17**, 333-343 (2022).

18 Procko, C. *et al.* Dynamic calcium signals mediate the feeding response of the carnivorous sundew plant. *Proceedings of the National Academy of Sciences* **119**, e2206433119 (2022).

19 Palfalvi, G. *et al.* Genomes of the venus flytrap and close relatives unveil the roots of plant carnivory. *Current Biology* **30**, 2312-2320. e2315 (2020).

20 Chan, X. Y., Hong, K. W., Yin, W. F. & Chan, K. G. Microbiome and Biocatalytic Bacteria in Monkey Cup (Nepenthes Pitcher) Digestive Fluid. *Sci Rep* **6**, 20016, doi:10.1038/srep20016 (2016).

21 Caravieri, F. A. *et al.* Bacterial community associated with traps of the carnivorous plants Utricularia hydrocarpa and Genlisea filiformis. *Aquatic botany* **116**, 8-12 (2014).

22 Sickel, W., Grafe, T. U., Meuche, I., Steffan-Dewenter, I. & Keller, A. Bacterial diversity and community structure in two Bornean Nepenthes species with differences in nitrogen acquisition strategies. *Microbial ecology* **71**, 938-953 (2016).

23 Li, Y. *et al.* Microbial taxonomical composition in spruce phyllosphere, but not community functional structure, varies by geographical location. *PeerJ* **7**, e7376 (2019).

24 Grothjan, J. J. & Young, E. B. Diverse microbial communities hosted by the model carnivorous pitcher plant Sarracenia purpurea: analysis of both bacterial and eukaryotic composition across distinct host plant populations. *PeerJ* **7**, e6392 (2019).

25 Alcaraz, L. D., Martinez-Sanchez, S., Torres, I., Ibarra-Laclette, E. & Herrera-Estrella, L. The metagenome of utricularia gibba's traps: Into the microbial input to a carnivorous plant. *PloS one* **11**, e0148979 (2016).

26 Matušíková, I. *et al.* Tentacles of in vitro-grown round-leaf sundew (Drosera rotundifoliaL.) show induction of chitinase activity upon mimicking the presence of prey. *Planta* **222**, 1020-1027 (2005).

27 Poppinga, S., Hartmeyer, S. R., Masselter, T., Hartmeyer, I. & Speck, T. Trap diversity and evolution in the family Droseraceae. *Plant signaling & behavior* **8**, e24685 (2013).

28 El-Sayed, A. M., Byers, J. A. & Suckling, D. M. Pollinator-prey conflicts in carnivorous plants: when flower and trap properties mean life or death. *Scientific reports* **6**, 21065 (2016).

29 Hanslin, H. & Karlsson, P. Nitrogen uptake from prey and substrate as affected by prey capture level and plant reproductive status in four carnivorous plant species. *Oecologia* **106**, 370-375 (1996).

30 Millett, J., Jones, R. I. & Waldron, S. The contribution of insect prey to the total nitrogen content of sundews (Drosera spp.) determined in situ by stable isotope analysis. *New Phytologist* **158**, 527-534 (2003).

31 Fu, S.-F. *et al.* Plant growth-promoting traits of yeasts isolated from the phyllosphere and rhizosphere of Drosera spatulata Lab. *Fungal biology* **120**, 433-448 (2016).

32 Chambers, S. M., Curlevski, N. J. & Cairney, J. W. Ericoid mycorrhizal fungi are common root inhabitants of non-Ericaceae plants in a south-eastern Australian sclerophyll forest. *FEMS Microbiol Ecol* **65**, 263-270, doi:10.1111/j.1574-6941.2008.00481.x (2008).

33 Nakano, M., Kinoshita, E. & Ueda, K. Life history traits and coexistence of an amphidiploid, Drosera tokaiensis, and its parental species, D. rotundifolia and D. spatulata (Droseraceae). *Plant Species Biology* **19**, 59-72 (2004).

34 Krausko, M. *et al.* The role of electrical and jasmonate signalling in the recognition of captured prey in the carnivorous sundew plant Drosera capensis. *New Phytologist* **213**, 1818-1835 (2017).

35 Bauer, U., Müller, U. K. & Poppinga, S. Complexity and diversity of motion amplification and control strategies in motile carnivorous plant traps. *Proceedings of the Royal Society B* **288**, 20210771 (2021).

36 Roy, J. C. *et al.* Solubility of chitin: solvents, solution behaviors and their related mechanisms. *Solubility of polysaccharides* **10** (2017).

37 Hatcher, C. R., Ryves, D. B. & Millett, J. The function of secondary metabolites in plant carnivory. *Annals of botany* **125**, 399-411 (2020).
38 Takeuchi, Y. *et al.* Bacterial diversity and composition in the fluid of pitcher plants of the genus Nepenthes. *Systematic and applied microbiology* **38**, 330-339 (2015).
39 Boynton, P. J., Peterson, C. N. & Pringle, A. Superior dispersal ability can lead to persistent ecological dominance throughout succession. *Applied and environmental microbiology* **85**, e02421-02418 (2019).
40 Sirová, D. *et al.* Microbial community development in the traps of aquatic Utricularia species. *Aquatic Botany* **90**, 129-136 (2009).
41 Cao, H. X. *et al.* Metatranscriptome analysis reveals host-microbiome interactions in traps of carnivorous Genlisea species. *Frontiers in microbiology* **6**, 526 (2015).
42 Fleischmann, A., Cross, A., Gibson, R., Gonella, P. & Dixon, K. in *Carnivorous plants: physiology, ecology, and evolution* 45-57 (2018).
43 Poppinga, S., Hartmeyer, S. R., Masselter, T., Hartmeyer, I. & Speck, T. Trap diversity and evolution in the family Droseraceae. *Plant Signal Behav* **8**, e24685, doi:10.4161/psb.24685 (2013).
44 Erni, P., Varagnat, M. & McKinley, G. H. in *AIP Conference Proceedings.* 579-581 (American Institute of Physics).
45 Rost, K. & Schauer, R. Physical and chemical properties of the mucin secreted by Drosera capensis. *Phytochemistry* **16**, 1365-1368 (1977).
46 Ravee, R., Salleh, F. I. M. & Goh, H.-H. Discovery of digestive enzymes in carnivorous plants with focus on proteases. *PeerJ* **6**, e4914 (2018).
47 Butts, C. T., Bierma, J. C. & Martin, R. W. Novel proteases from the genome of the carnivorous plant Drosera capensis: structural prediction and comparative analysis. *Proteins: Structure, Function, and Bioinformatics* **84**, 1517-1533 (2016).
48 Ďurechová, D., Matušíková, I., Moravčíková, J., Jopčík, M. & Libantová, J. ISOLATION AND CHARACTERIZATION OF CHITINASE GENE FROM THE UNTRADITIONAL PLANT SPECIES. *Journal of Microbiology, Biotechnology and Food Sciences* **2021**, 2208-2216 (2021).
49 Matušíková, I. *et al.* Tentacles of in vitro-grown round-leaf sundew (Drosera rotundifolia L.) show induction of chitinase activity upon mimicking the presence of prey. *Planta* **222**, 1020-1027 (2005).

50 Michalko, J. & Matušíková, I. Study on the role of glucanases in digestion of carnivorous plant Drosera rotundifolia L. *Journal of Microbiology, Biotechnology and Food Sciences* **2021**, 671-678 (2021).
51 Tedersoo, L. *et al.* Global diversity and geography of soil fungi. *Science* **346**, 1256688, doi:10.1126/science.1256688 (2014).
52 Kozich, J. J., Westcott, S. L., Baxter, N. T., Highlander, S. K. & Schloss, P. D. Development of a dual-index sequencing strategy and curation pipeline for analyzing amplicon sequence data on the MiSeq Illumina sequencing platform. *Appl Environ Microbiol* **79**, 5112-5120, doi:10.1128/AEM.01043-13 (2013).
53 Edgar, R. C. Search and clustering orders of magnitude faster than BLAST. *Bioinformatics* **26**, 2460-2461, doi:10.1093/bioinformatics/btq461 (2010).
54 Edgar, R. C. UPARSE: highly accurate OTU sequences from microbial amplicon reads. *Nat Methods* **10**, 996-998, doi:10.1038/nmeth.2604 (2013).
55 McMurdie, P. J. & Holmes, S. phyloseq: an R package for reproducible interactive analysis and graphics of microbiome census data. *PLoS One* **8**, e61217, doi:10.1371/journal.pone.0061217 (2013).
56 Edgar, R. C. Accuracy of taxonomy prediction for 16S rRNA and fungal ITS sequences. *PeerJ* **6**, e4652, doi:10.7717/peerj.4652 (2018).
57 Edgar, R. C. SINTAX: a simple non-Bayesian taxonomy classifier for 16S and ITS sequences. *biorxiv*, 074161 (2016).
58 Abarenkov, K. *et al.* The UNITE database for molecular identification of fungi–recent updates and future perspectives. *The New Phytologist* **186**, 281-285 (2010).
59 Davis, N. M., Proctor, D. M., Holmes, S. P., Relman, D. A. & Callahan, B. J. Simple statistical identification and removal of contaminant sequences in marker-gene and metagenomics data. *Microbiome* **6**, 1-14, doi:10.1186/s40168-018-0605-2 (2018).
60 Love, M. I., Huber, W. & Anders, S. Moderated estimation of fold change and dispersion for RNA-seq data with DESeq2. *Genome Biol* **15**, 1-21, doi:10.1186/s13059-014-0550-8 (2014).
61 Leck, A. Preparation of lactophenol cotton blue slide mounts. *Community Eye Health* **12**, 24 (1999).
62 Větrovský, T. *et al.* GlobalFungi, a global database of fungal occurrences from high-throughput-sequencing metabarcoding studies. *Scientific Data* **7**, 1-14 (2020).

63 Coleine, C., Stajich, J. E. & Selbmann, L. Fungi are key players in extreme ecosystems. *Trends in ecology & evolution* (2022).
64 Deb, D., Khan, A. & Dey, N. Phoma diseases: Epidemiology and control. *Plant Pathology* **69**, 1203-1217 (2020).
65 Zhdanova, N. *et al.* Peculiarities of soil mycobiota composition in Chernobyl NPP. *Ukrayins' kij Botanyichnij Zhurnal* **51**, 134-144 (1994).
66 Luque, J., Parladé, J. & Pera, J. Pathogenicity of fungi isolated from Quercus suber in Catalonia (NE Spain). *Forest Pathology* **30**, 247-263 (2000).
67 Tokumasu, S. Mycofloral succession on Pinus densiflora needles on a moder site. *Mycoscience* **37**, 313-321 (1996).
68 Tiscornia, S., Segui, C. & Bettucci, L. Composition and characterization of fungal communities from different composted materials. *Cryptogamie Mycol* **30**, 363-376 (2009).
69 Nagano, Y. *et al.* Comparison of techniques to examine the diversity of fungi in adult patients with cystic fibrosis. *Medical mycology* **48**, 166-176 (2010).
70 Ruibal, C., Platas, G. & Bills, G. High diversity and morphological convergence among melanised fungi from rock formations in the Central Mountain System of Spain. *Persoonia: Molecular Phylogeny and Evolution of Fungi* **21**, 93 (2008).
71 Prabhugaonkar, A. & Pratibha, J. Isolation of Acrodontium crateriforme as a pitcher trap inquiline. *Curr. Res. Environ. Appl. Mycol* **7**, 203-207 (2017).
72 Sa'diyah, W., Hashimoto, A., Okada, G. & Ohkuma, M. Notes on some interesting sporocarp-inhabiting fungi isolated from xylarialean fungi in Japan. *Diversity* **13**, 574 (2021).
73 TAKAHASHI, K., MATSUMOTO, K., NISHII, W., MURAMATSU, M. & KUBOTA, K. DIGESTIVE FLUIDS OF NEPENTHES, CEPHALOTUS, DIONAEA, AND DROSERA.
74 de Hoog, G. S. The genera Beauveria, Isaria, Tritirachium and Acrodontium gen. nov. *Stud. Mycol.* **1**, 1-41 (1972).
75 Vannier, N., Agler, M. & Hacquard, S. Microbiota-mediated disease resistance in plants. *PLoS pathogens* **15**, e1007740 (2019).
76 Grothjan, J. J. & Young, E. B. Bacterial recruitment to carnivorous pitcher plant communities: identifying sources influencing plant microbiome composition and function. *Frontiers in Microbiology* **13**, 791079 (2022).

77 Burns, J. H., Anacker, B. L., Strauss, S. Y. & Burke, D. J. Soil microbial community variation correlates most strongly with plant species identity, followed by soil chemistry, spatial location and plant genus. *AoB plants* **7**, plv030 (2015).

78 Noman, M. *et al.* Plant–Microbiome crosstalk: Dawning from composition and assembly of microbial community to improvement of disease resilience in plants. *International Journal of Molecular Sciences* **22**, 6852 (2021).

79 Chaudhry, V. *et al.* Shaping the leaf microbiota: plant–microbe–microbe interactions. *Journal of Experimental Botany* **72**, 36-56 (2021).

80 Bittleston, L. S. *et al.* Convergence between the microcosms of Southeast Asian and North American pitcher plants. *Elife* **7**, e36741 (2018).

81 Armitage, D. W. Linking the development and functioning of a carnivorous pitcher plant's microbial digestive community. *The ISME journal* **11**, 2439-2451 (2017).

82 Karlsson, P., Nordell, K., Carlsson, B. & Svensson, B. The effect of soil nutrient status on prey utilization in four carnivorous plants. *Oecologia* **86**, 1-7 (1991).

83 Pavlovič, A. & Mithöfer, A. Jasmonate signalling in carnivorous plants: copycat of plant defence mechanisms. *Journal of experimental botany* **70**, 3379-3389 (2019).

84 Renner, T. & Specht, C. D. Inside the trap: gland morphologies, digestive enzymes, and the evolution of plant carnivory in the Caryophyllales. *Current opinion in plant biology* **16**, 436-442 (2013).

85 Pavlovič, A., Vrobel, O. & Tarkowski, P. Water Cannot Activate Traps of the Carnivorous Sundew Plant Drosera capensis: On the Trail of Darwin's 150-Years-Old Mystery. *Plants* **12**, 1820 (2023).

86 True, J. R. & Carroll, S. B. Gene co-option in physiological and morphological evolution. *Annual review of cell and developmental biology* **18**, 53-80 (2002).

87 Mesny, F., Hacquard, S. & Thomma, B. P. Co-evolution within the plant holobiont drives host performance. *EMBO reports* **24**, e57455 (2023).

88 Videira, S. *et al.* Mycosphaerellaceae–chaos or clarity? *Studies in Mycology* **87**, 257-421 (2017).

89 Katoh, K. & Standley, D. M. MAFFT multiple sequence alignment software version 7: improvements in performance and usability. *Mol Biol Evol* **30**, 772-780, doi:10.1093/molbev/mst010 (2013).

90 Capella-Gutierrez, S., Silla-Martinez, J. M. & Gabaldon, T. trimAl: a tool for automated alignment trimming in large-scale phylogenetic analyses. *Bioinformatics* **25**, 1972-1973, doi:10.1093/bioinformatics/btp348 (2009).

91 Nguyen, L. T., Schmidt, H. A., von Haeseler, A. & Minh, B. Q. IQ-TREE: a fast and effective stochastic algorithm for estimating maximum-likelihood phylogenies. *Mol Biol Evol* **32**, 268-274, doi:10.1093/molbev/msu300 (2015).

92 Krolicka, A. *et al.* Antibacterial and antioxidant activity of the secondary metabolites from in vitro cultures of the Alice sundew (Drosera aliciae). *Biotechnol Appl Biochem* **53**, 175-184, doi:10.1042/BA20080088 (2009).

93 Rueden, C. T. *et al.* ImageJ2: ImageJ for the next generation of scientific image data. *BMC bioinformatics* **18**, 1-26 (2017).

94 Koren, S. *et al.* Canu: scalable and accurate long-read assembly via adaptive k-mer weighting and repeat separation. *Genome research* **27**, 722-736 (2017).

95 Vaser, R., Sović, I., Nagarajan, N. & Šikić, M. Fast and accurate de novo genome assembly from long uncorrected reads. *Genome Res* **27**, 737-746, doi:10.1101/gr.214270.116 (2017).

96 Walker, B. J. *et al.* Pilon: an integrated tool for comprehensive microbial variant detection and genome assembly improvement. *PloS one* **9**, e112963 (2014).

97 Dierckxsens, N., Mardulyn, P. & Smits, G. NOVOPlasty: de novo assembly of organelle genomes from whole genome data. *Nucleic acids research* **45**, e18-e18 (2017).

98 Dobin, A. & Gingeras, T. R. Mapping RNA-seq Reads with STAR. *Curr Protoc Bioinformatics* **51**, 11 14 11-11 14 19, doi:10.1002/0471250953.bi1114s51 (2015).

99 Grabherr, M. G. *et al.* Full-length transcriptome assembly from RNA-Seq data without a reference genome. *Nat Biotechnol* **29**, 644-652, doi:10.1038/nbt.1883 (2011).

100 Pertea, M. *et al.* StringTie enables improved reconstruction of a transcriptome from RNA-seq reads. *Nat Biotechnol* **33**, 290-295, doi:10.1038/nbt.3122 (2015).

101 Trapnell, C. *et al.* Differential gene and transcript expression analysis of RNA-seq experiments with TopHat and Cufflinks. *Nat Protoc* **7**, 562-578, doi:10.1038/nprot.2012.016 (2012).

102 Wu, T. D. & Watanabe, C. K. GMAP: a genomic mapping and alignment program for mRNA and EST sequences. *Bioinformatics* **21**, 1859-1875, doi:10.1093/bioinformatics/bti310 (2005).
103 Ter-Hovhannisyan, V., Lomsadze, A., Chernoff, Y. O. & Borodovsky, M. Gene prediction in novel fungal genomes using an ab initio algorithm with unsupervised training. *Genome Res* **18**, 1979-1990, doi:10.1101/gr.081612.108 (2008).
104 Tempel, S. Using and understanding RepeatMasker. *Methods Mol Biol* **859**, 29-51, doi:10.1007/978-1-61779-603-6_2 (2012).
105 Korf, I. Gene finding in novel genomes. *BMC Bioinformatics* **5**, 59, doi:10.1186/1471-2105-5-59 (2004).
106 Venturini, L., Caim, S., Kaithakottil, G. G., Mapleson, D. L. & Swarbreck, D. Leveraging multiple transcriptome assembly methods for improved gene structure annotation. *GigaScience* **7**, doi:10.1093/gigascience/giy093 (2018).
107 Holt, C. & Yandell, M. MAKER2: an annotation pipeline and genome-database management tool for second-generation genome projects. *BMC Bioinformatics* **12**, 491, doi:10.1186/1471-2105-12-491 (2011).
108 Matthew Berriman, A. C., Isheng Jason Tsai Creation of a comprehensive repeat library for a newly sequenced parasitic worm genome. *PROTOCOL (Version 1) available at Protocol Exchange* doi:https://doi.org/10.1038/protex.2018.054 (2018).
109 Smit, A., Hubley, R & Green, P. RepeatMasker Open-4.0. (2013-2015).
110 Emerson, I. A. & Chitluri, K. K. DCMP: database of cancer mutant protein domains. *Database* **2021**, baab066 (2021).
111 Finn, R. D. *et al.* Pfam: the protein families database. *Nucleic acids research* **42**, D222-D230 (2014).
112 Buchfink, B., Xie, C. & Huson, D. H. Fast and sensitive protein alignment using DIAMOND. *Nature methods* **12**, 59-60 (2015).
113 Elbourne, L. D., Tetu, S. G., Hassan, K. A. & Paulsen, I. T. TransportDB 2.0: a database for exploring membrane transporters in sequenced genomes from all domains of life. *Nucleic acids research* **45**, D320-D324 (2017).
114 Yin, Y. *et al.* dbCAN: a web resource for automated carbohydrate-active enzyme annotation. *Nucleic acids research* **40**, W445-W451 (2012).

115 Rawlings, N. D., Barrett, A. J. & Bateman, A. MEROPS: the peptidase database. *Nucleic acids research* **38**, D227-D233 (2010).
116 Blin, K. *et al.* antiSMASH 6.0: improving cluster detection and comparison capabilities. *Nucleic acids research* **49**, W29-W35 (2021).
117 Huerta-Cepas, J. *et al.* eggNOG 5.0: a hierarchical, functionally and phylogenetically annotated orthology resource based on 5090 organisms and 2502 viruses. *Nucleic acids research* **47**, D309-D314 (2019).
118 Ihaka, R. & Gentleman, R. R: a language for data analysis and graphics. *Journal of computational and graphical statistics* **5**, 299-314 (1996).
119 Alexa, A. & Rahnenführer, J. Gene set enrichment analysis with topGO. *Bioconductor Improv* **27**, 1-26 (2009).
120 Kolde, R. & Kolde, M. R. Package 'pheatmap'. *R package* **1**, 790 (2015).
121 Wickham, H. ggplot2. *Wiley interdisciplinary reviews: computational statistics* **3**, 180-185 (2011).
122 Emms, D. M. & Kelly, S. OrthoFinder: phylogenetic orthology inference for comparative genomics. *Genome Biol* **20**, 238, doi:10.1186/s13059-019-1832-y (2019).
123 Zhang, C., Rabiee, M., Sayyari, E. & Mirarab, S. ASTRAL-III: polynomial time species tree reconstruction from partially resolved gene trees. *BMC bioinformatics* **19**, 15-30 (2018).
124 Baum, B. R. (JSTOR, 1989).
125 Chen, S., Zhou, Y., Chen, Y. & Gu, J. fastp: an ultra-fast all-in-one FASTQ preprocessor. *Bioinformatics* **34**, i884-i890 (2018).
126 Liao, Y., Smyth, G. K. & Shi, W. featureCounts: an efficient general purpose program for assigning sequence reads to genomic features. *Bioinformatics* **30**, 923-930 (2014).
127 Chen, Y.-L. *et al.* Quantitative peptidomics study reveals that a wound-induced peptide from PR-1 regulates immune signaling in tomato. *The Plant Cell* **26**, 4135-4148 (2014).
128 Sprague-Piercy, M. A. *et al.* The Droserasin 1 PSI: a membrane-interacting antimicrobial peptide from the carnivorous plant Drosera capensis. *Biomolecules* **10**, 1069 (2020).
129 Buch, F., Kaman, W. E., Bikker, F. J., Yilamujiang, A. & Mithöfer, A. Nepenthesin protease activity indicates digestive fluid dynamics in carnivorous Nepenthes plants. *PLoS One* **10**, e0118853 (2015).

130 Cantarel, B. L. *et al.* MAKER: an easy-to-use annotation pipeline designed for emerging model organism genomes. *Genome research* **18**, 188-196 (2008).
131 Selbmann, L. *et al.* Drought meets acid: three new genera in a dothidealean clade of extremotolerant fungi. *Studies in mycology* **61**, 1-20 (2008).
132 Aylward, J. *et al.* Novel mating-type-associated genes and gene fragments in the genomes of Mycosphaerellaceae and Teratosphaeriaceae fungi. *Molecular Phylogenetics and Evolution* **171**, 107456 (2022).
133 Coleine, C. *et al.* Peculiar genomic traits in the stress-adapted cryptoendolithic Antarctic fungus Friedmanniomyces endolithicus. *Fungal biology* **124**, 458-467 (2020).
134 Romeo, O. *et al.* Whole genome sequencing and comparative genome analysis of the halotolerant deep sea black yeast Hortaea werneckii. *Life* **10**, 229 (2020).
135 Bradley, E. L. *et al.* Secreted glycoside hydrolase proteins as effectors and invasion patterns of plant-associated fungi and oomycetes. *Frontiers in Plant Science* **13**, 853106 (2022).
136 Miyauchi, S. *et al.* Large-scale genome sequencing of mycorrhizal fungi provides insights into the early evolution of symbiotic traits. *Nature communications* **11**, 5125 (2020).
137 Lee, L., Zhang, Y., Ozar, B., Sensen, C. W. & Schriemer, D. C. Carnivorous nutrition in pitcher plants (Nepenthes spp.) via an unusual complement of endogenous enzymes. *Journal of proteome research* **15**, 3108-3117 (2016).
138 Gan, P. *et al.* Subtelomeric regions and a repeat-rich chromosome harbor multicopy effector gene clusters with variable conservation in multiple plant pathogenic Colletotrichum species. *bioRxiv*, 2020.2004. 2028.061093 (2020).
139 Goodwin, S. B. *et al.* Finished genome of the fungal wheat pathogen Mycosphaerella graminicola reveals dispensome structure, chromosome plasticity, and stealth pathogenesis. *PLoS genetics* **7**, e1002070 (2011).
140 Ohm, R. A. *et al.* Diverse lifestyles and strategies of plant pathogenesis encoded in the genomes of eighteen Dothideomycetes fungi. *PLoS pathogens* **8**, e1003037 (2012).

141 Cairns, T. & Meyer, V. In silico prediction and characterization of secondary metabolite biosynthetic gene clusters in the wheat pathogen Zymoseptoria tritici. *BMC genomics* **18**, 1-16 (2017).
142 Haas, B. J., Delcher, A. L., Wortman, J. R. & Salzberg, S. L. DAGchainer: a tool for mining segmental genome duplications and synteny. *Bioinformatics* **20**, 3643-3646 (2004).
143 Krzywinski, M. *et al.* Circos: an information aesthetic for comparative genomics. *Genome research* **19**, 1639-1645 (2009).
144 Pavlovič, A., Jakšová, J. & Novák, O. Triggering a false alarm: wounding mimics prey capture in the carnivorous Venus flytrap (Dionaea muscipula). *New Phytologist* **216**, 927-938 (2017).
145 Chase, M. W., Christenhusz, M. J., Sanders, D. & Fay, M. F. Murderous plants: Victorian Gothic, Darwin and modern insights into vegetable carnivory. *Botanical Journal of the Linnean Society* **161**, 329-356 (2009).
146 Jopcik, M. *et al.* Structural and functional characterisation of a class I endochitinase of the carnivorous sundew (Drosera rotundifolia L.). *Planta* **245**, 313-327 (2017).
147 Hedrich, R. & Fukushima, K. On the origin of carnivory: molecular physiology and evolution of plants on an animal diet. *Annual review of plant biology* **72**, 133-153 (2021).
148 Scherzer, S. *et al.* The Dionaea muscipula ammonium channel DmAMT1 provides NH4+ uptake associated with Venus flytrap's prey digestion. *Current Biology* **23**, 1649-1657 (2013).
149 Bemm, F. *et al.* Venus flytrap carnivorous lifestyle builds on herbivore defense strategies. *Genome Research* **26**, 812-825 (2016).
150 Wong, H.-K., Chan, H.-K., Coruzzi, G. M. & Lam, H.-M. Correlation of ASN2 gene expression with ammonium metabolism in Arabidopsis. *Plant Physiology* **134**, 332-338 (2004).
151 Schulze, W., Frommer, W. B. & Ward, J. M. Transporters for ammonium, amino acids and peptides are expressed in pitchers of the carnivorous plant Nepenthes. *The Plant Journal* **17**, 637-646 (1999).
152 Langfelder, P. & Horvath, S. WGCNA: an R package for weighted correlation network analysis. *BMC bioinformatics* **9**, 1-13 (2008).
153 Reichard, U. *et al.* Sedolisins, a new class of secreted proteases from Aspergillus fumigatus with endoprotease or tripeptidyl-peptidase activity at acidic pHs. *Applied and Environmental Microbiology* **72**, 1739-1748 (2006).

154 Muszewska, A. *et al.* Fungal lifestyle reflected in serine protease repertoire. *Scientific Reports* **7**, 9147 (2017).
155 Pozo, M. J., López-Ráez, J. A., Azcón-Aguilar, C. & García-Garrido, J. M. Phytohormones as integrators of environmental signals in the regulation of mycorrhizal symbioses. *New Phytologist* **205**, 1431-1436 (2015).
156 Jung, S. C., Martinez-Medina, A., Lopez-Raez, J. A. & Pozo, M. J. Mycorrhiza-induced resistance and priming of plant defenses. *Journal of chemical ecology* **38**, 651-664 (2012).
157 Darwin, C. & Darwin, F. *Insectivorous plants*. (J. Murray, 1888).
158 Alcalá, R. E. & Domínguez, C. A. Patterns of prey capture and prey availability among populations of the carnivorous plant Pinguicula moranensis (Lentibulariaceae) along an environmental gradient. *American Journal of Botany* **90**, 1341-1348 (2003).
159 Mauch-Mani, B., Baccelli, I., Luna, E. & Flors, V. Defense priming: an adaptive part of induced resistance. *Annual review of plant biology* **68**, 485-512 (2017).
160 Miller, T. E., Bradshaw, W. E., Holzapfel, C. M., Ellison, A. & Adamec, L. Pitcher-plant communities as model systems for addressing fundamental questions in ecology and evolution. *Carnivorous Plants: Physiology, Ecology, and Evolution*, 333-348 (2018).